Estimation of Time-dependent Reliability of Suspension Bridge Cables

Bin Liang

Submitted in partial fulfillment of the

requirements for the degree

of Doctor of Philosophy

in the Graduate School of Arts and Sciences

COLUMBIA UNIVERSITY

2016

ABSTRACT

Estimation of Time-dependent Reliability of Suspension Bridge Cables

Bin Liang

The reliability of the main cable of a suspension bridge is crucial to the reliability of the entire bridge. Throughout the life of a suspension bridge, its main cables are subject to corrosion due to various factors, and the deterioration of strength is a slowly evolving and dynamic process. The goal of this research is to find the pattern of how the strength of steel wires inside a suspension bridge cable changes with time. Two methodologies are proposed based on the analysis of five data sets which were collected by testing pristine wires, artificially corroded wires, and wires taken from three suspension bridges: Severn Bridge, Forth Road Bridge and Williamsburg Bridge.

The first methodology is to model wire strength as a random process in space whose marginal probability distribution and power spectral density evolve with time. Both the marginal distribution and the power spectral density are parameterized with time-dependent parameters. This enables the use of Monte Carlo methods to estimate the failure probability of wires at any given time. An often encountered problem – the incompatibility between the non-Gaussian marginal probability distribution and prescribed power spectral density – which arises when simulating non-Gaussian random processes using translational field theory, is also studied. It is shown by copula theory that the selected marginal distribution imposes restrictions on the selection of

power spectral density function.

The second methodology is to model the deterioration rate of wire strength as a stochastic process in time, under Ito's stochastic calculus framework. The deterioration rate process is identified as a mean-reversion stochastic process taking non-negative values. It is proposed that the actual deterioration of wire strength depends on the deterioration rate, and may also depend on the state of the wire strength itself. The probability distribution of wire strength at any given time can be obtained by integrating the deterioration rate process. The model parameters are calibrated from the available data sets by matching moments or minimizing differences between probability distributions.

Table of Contents

List of Figures

List of Tables

Acknowledgments

I would like to express my deep and sincere gratitude to my research advisor Professor George Deodatis for his guidance and inspirations throughout the course of my Ph.D. study. Especially his patience and encouragement on innovative work is the key to the completion of this thesis.

I am also very grateful to Professor Raimondo Betti for his support of my research. He provided precious experimental data and valuable discussions at various stages of this research.

My gratitude also extends to Adrian Brugger and Liming Li for their kindly help with experimental work I conducted in the Carleton Lab for collecting data from the artificially corroded wires.

I would also like to thank Jason Lambert at Weidlinger Associates Inc. for providing additional wire testing data.

I am very grateful to Professor Maria Feng, Professor Ioannis Kougioumtzoglou, and Professor Paul Duby for their willingness to form part of the defense committee.

I gratefully acknowledge the support of the National Science Foundation under grant No. CMMI-0928129.

Finally, I would express my love to my wife Sijia. This work could not be done without her support.

To my beautiful wife Sijia, and my beloved parents.

Chapter 1

Introduction

1.1 Reliability of suspension bridge cables

A suspension bridge is a structural type of bridge where the roadway is supported by hanging on the suspension cables. The key components of a suspension bridge are suspension cable, bridge towers, cable anchors, vertical suspenders and deck. The cables, which are the most iconic component of a suspension bridge, are suspended between bridge towers, and anchored on both ends of the bridge. The traffic load and the self-weight of the deck is transferred to the suspension cable through vertical suspenders. Such design makes the bridge light-weighted and strong, able to span far longer than any other kind of bridges. Modern suspension bridges have been built all over the world since late 19th century. As shown in Figure 1.1, the George Washington Bridge is a typical suspension bridge, which connects New York City and New Jersey.

Figure 1.1: Aerial look of George Washington Bridge. By Gryffindor (Own work) [CC BY-SA 3.0 (http://creativecommons.org/licenses/by-sa/3.0) or GFDL (http://www.gnu.org/copyleft/fdl.html)], via Wikimedia Commons

The suspension cables are subject to huge tensile force, which is eventually transferred to the towers and the anchors. The suspension cable can be considered as the most critical structural component to a suspension bridge as it connects all other load-bearing components. Over the years of service, the suspension bridge cable is subject to environmental degradation and intensive loads, which reduce its load-bearing capacity. The deterioration of the main suspension cable is the major concern in practice, and studying the reliability of the suspension cable is of great importance to assessing the safety of the entire bridge.

The suspension bridge cable is made of thousands of small-diameter high-strength steel wires. For example, the main cable of George Washington Bridge is made of 26,474 steel wires, each of about 5 mm in diameter. It has been observed in past inspections that the strength of the wires deteriorates over time to different extends, and it is possible to find wires in pristine condition and broken wires within the same cross-section[Shi *et al.*, 2007]. This is because many contributing factors to deterioration, including environmental conditions and dynamic loads, have inherent uncertainties. This prompts for probabilistic models for studying the deterioration process, and for capturing the statistical characteristics of the entire population of wires in a suspension cable.

1.2 Literature review

The quantification of uncertainty of wire strength are usually achieved from two aspects. One is to directly study wire samples and the other is to study the randomness of the deterioration process. This section briefly reviews researches in both approaches, as well as challenges and unsolved problems.

1.2.1 Random wire strength

The strength of a steel wire of a certain length is usually referred to as the minimum strength along its length direction. This is based based on the weakest link model, which states that the minimum strength along its length determines the strength of the entire wire, as the wire is mostly likely to fail at its weakest point under tensile loads.

Methods for quantifying the uncertainty of wire strength can be further categorized into two types. Methods of the first type model the strength of each unit-length segment of the wire of prescribed length as discrete random variables, while methods of the second type model strength of the entire wire as a continuous random process. Both types of methods aim to establish the probability distribution of the strength of a wire of prescribed length. To achieve this goal the probability distribution of the strength of wire segments of unit length must be established first. In the following context we call it *unit-length distribution* for short.

In practice the unit-length distribution is established by extracting and testing wires from real bridge cables or experimental devices, following the common steps listed below:

1. Select a number of wire within the cable's cross-section to form a representative pool of all wires;

2. Remove selected wires of a length of 6-12 m (20-40 ft) from the cable;

3. Cut wires into a series of segments with unit length, usually 1 30.48 cm (1 ft) long, and the location of the each segment in the cable is also recorded;

4. Conduct tensile testing on each unit-length segment to obtain samples of tensile strengths.

The unit-length distribution is established from these samples.

1.2.1.1 Random variable approach

Suppose the wire of prescribed length is discretized into n segments of unit length:

$$n = \frac{\text{prescribed length}}{\text{unit length}} \tag{1.1}$$

Methods based on random variables consider the strengths of n unit-length wire segments as n random variables, and the overall strength of the wire is determined by the minimum of the n random variables. It is implicitly assumed that the strengths of wire segments are independent of each other, which is a good assumption for brittle materials, but not necessarily a good one for ductile materials like steel. However, the validity of this assumption improves as wire deteriorate and become more brittle[Camo, 2003]. Once the unit-length distribution is determined, the distribution of the strength of the entire wire can be estimated numerically by Monte Carlo simulation, or approximated analytically as Type I or Type III extreme value distributions (EVD).

In the technical resort of cable investigation program of Williamsburg Bridge[Steinman *et al.*, 1988], the strength of unit-length wire segments was assumed to follow Gaussian distribution. The Monte Carlo simulation for estimating the distribution of the entire wire takes the following steps. First, realizations are generated for the n random variables representing the n wire segments. Then, by taking the minimum of these n realizations, one realization of the strength of the entire wire is obtained. Finally, repeat these two steps to obtain many realizations of wire strength and estimate its distribution. Strictly speaking, Gaussian distribution may not be suitable for modeling strength as it allows strength to take negative values, however, it is often

found to match the unit-length distribution well. [Camo, 2003] also used Gaussian distribution for modeling strength of unit-length wire segments based on Ben Franklin Bridge and Bear Mountain Bridge testing data.

As the number of wire segments n becomes large, the distribution of the strength of the entire wire converges to extreme value distribution (EVD). When the strength of unit-length segments has exponential tails, e.g., Gaussian distribution, the strength of the entire wire follows Type I EVD; when the strength of unit-length segments has exponential tails and also a lower bound, the strength of the entire wire follows Type III EVD (Weibull distribution). [Matteo, 1994] used Type I EVD based on the same data and Gaussian distribution assumption as in [Steinman *et al.*, 1988], and compared results with Monte Carlo simulations. [Haight *et al.*, 1997] further applied Type I EVD estimate the reliability of four suspension bridges: Williamsburg Bridge, Bear Mountain Bridge, Triborough Bridge and Golden State Bridge. [Perry, 1998] proposed using Type III EVD based on Williamsburg Bridge data.

1.2.1.2 Random process approach

The methods based on random process recognize the correlation among the strength of wire segments and eventually model the wire strength as a continuous random process. A framework of suspension cable reliability assessment was established in [Shi, 2006], based on modeling the variation of the strength of a single wire along its length direction as a random process. To estimate the strength of the entire wire, realizations of the random process must be generated by Monte Carlo simulation. Since the marginal distribution of the wire strength is not Gaussian by nature, techniques for simulating non-Gaussian random processes were developed such as [Grigoriu, 1998]. To estimate the strength of the suspension cable, the correlation of strength among adjacent parallel wires must also be considered. [Montoya, 2012] studied the variation

of mean of such random processes across the cross-section of a cable.

1.2.2 Simulation of random processes

Various methods have been proposed for simulating random processes, among which the Spectral Representation Method (SRM) is the most widely used one. Besides, also available in the literatures are ARMA methods[Gersch and Yonemoto, 1977] and methods based on K-L decomposition [Karhunen, 1947][Loeve, 1978]. Aforementioned random process simulation methods used for simulating wire strength are all based on SRM.

The spectral representation method was first introduced in [Shinozuka and Jan, 1972] for simulating homogeneous multivariate processes in civil engineering with various applications such as wind field and material properties. Given the marginal distribution and the spectral density function of a random process, SRM synthesizes realizations of the random process by summing up trigonometric basis functions with random phases and weights specified by the spectral density function. The SRM was extended to simulating non-stationary multivariate random processes with application in earthquake engineering[Deodatis, 1996a]. The SRM was also extended to simulating non-Gaussian random processes based on translation process theory[Yamazaki and Shinozuka, 1988][Grigoriu, 1995] which maps the underlying Gaussian random process to the desired non-Gaussian process. A challenging issue is the "incompatibility" between the marginal distribution and the spectral density function of the non-Gaussian process, as they can be prescribed arbitrarily. Efforts have been made to remedy this issue, such as [Deodatis and Micaletti, 2001a][Shi *et al.*, 2007][Shields *et al.*, 2011][Benowitz, 2013]. A comprehensive review of non-Gaussian random process simulation techniques can be found in [Bocchini and Deodatis, 2008].

1.2.3 Random deterioration process

The uncertainty of wire strength can also be quantified by studying the wire deterioration process. This also needs to be combined with knowledge of initial wire strength. The deterioration of wires includes two important aspects: corrosion and hydrogen embrittle, both of which are subject to many environmental factors such as temperature, moisture and pH level[Betti *et al.*, 2005][Barton *et al.*, 2000], which makes the deterioration process of the wires difficult to model. In order to observe the effect of each factor a nondestructive corrosion monitoring system was developed at Columbia University[Deeble Sloane *et al.*, 2012]. The device was a full-scale suspension bridge cable model placed inside an environmental chamber which was able to simulate cyclic changes in temperature, relative humidity and pH level. Corrosion rate sensor placed at different locations revealed that corrosion rate may be different at different depths within the cable.

Since the deterioration rate has inherent fluctuation over time and the resulting wire strength has uncertainty among the population, the deterioration rate is also modeled as stochastic process in time. The deterioration process is treated as a gamma process, whose increments are independent and follow gamma distribution [Heutink *et al.*, 2004], A comprehensive of review of the properties of gamma process and its applications can be found in [van Noortwijk, 2009].

1.3 Research scope and objectives

The two key components to uncertainty quantification of random wire strength as random process, i.e., the marginal distribution and the power spectral density function, are studied first. The objective is to demonstrate a procedure for estimating the two from wire testing data. First, the marginal distribution as the best fit to the

data is selected by various criteria such log-likelihood, Bayesian information criterion (BIC), Akaike information criterion (AIC). Then power spectral density function is constructed using Clough-Penzien spectrum with five parameters. Finally, both the marginal distribution and the spectral density function are extended to be time-dependent.

The incompatibility issue between the prescribed marginal distribution and power spectral density function which arises when simulating non-Gaussian random processes is also addressed in the dissertation. The objective is to alleviate, if not completely avoid this issue in the first place – by selecting an appropriate marginal distribution and power spectral density function for the random processes when processing data. It can be shown that based on copula theory the selected marginal distribution actually imposes limitation on the selection of autocorrelation function and spectral density function.

This research also aims to establish an innovative framework for modeling the deterioration rate process using Ito's stochastic calculus. Under this framework only minimum assumptions must be made regarding the actual deterioration process, which are non-negativity and mean-reversion. Once the dynamics of the deterioration rate process is determined, then its statistical properties can then be derived analytically. In addition to the stochastic deterioration rate, the actual deterioration of wire strength may also depend on the state of the wire. Model calibration methods based on moment matching are also proposed and demonstrated using the observed probability distribution of wire strengths.

1.4 Outline of the dissertation

The dissertation is organized in the following way. Chapter 2 briefly introduce the sources of data used throughout the dissertation. A total of five data sets are used. Laboratory testing methods for accessing wire conditions are briefly introduced. The sampling method for selecting wire samples is also introduced.

Chapter 3 aims to establish the pattern of evolution for the key statistical properties of wire strength based on the five data set. Descriptive statistics of the five data sets of wire strength are shown first. A method for selecting the proper distribution is developed based on criteria. Parameters of the selected distribution are then estimated and made into functions of time. The wire strength is also modeled as random fields, where consistent change of spectral density functions in time was observed, including rising peak values and increasing areas under the curve. The parameters of the PSD are also modeled as functions of time. This chapter finishes with an attempt to provided a theoretical explanation to the incompatibility issue between the marginal distribution and the PSD, which may arise when applying translation process theory for simulating non-Gaussian process.

Chapter 4 establishes a theoretical framework for modeling the deterioration process as a stochastic process defined under Ito's stochastic calculus theory. The square-root process is suggested for modeling the deterioration rate, which has nice properties such as mean-reversion and non-negative (under certain conditions) that fit the physical law of deterioration well. The probability distribution of the deterioration rate at any given time can be obtained by solving the Kolmogorov forward equation or by Monte Carlo methods. Simulation methods of squared-root process are reviewed. The deterioration of wire strength is a function of the deterioration rate and optionally the wire strength itself. Methods for calibrating the model are developed, based

on matching moments or matching the distribution function.

Chapter 5 discusses a few loose topics. The first is about quantitatively estimating the equivalent age of artificially corroded wires. The second is a comparative study between methods developed Chapter 3 and Chapter 4, where both are able to predict the distribution of wire strength at any given time. The third is an extension of the stochastic deterioration model developed in Chapter 4, to account for spatial correlation. This chapter also summarize the contributions and suggests future works.

Chapter 2

Tensile testing of suspension bridge cables

2.1 Chapter summary

This chapter mainly focuses on the collection of five data sets of wire strength that are used in this research from real bridges and from experimental devices. The past suspension bridge cable inspection programs are first reviewed, during which three data sets were collected from real bridges, which are Severn Bridge and Forth Road Bridge in the United Kingdom, and Williamsburg Bridge in the City of New York. The other two data sets were collected in the Carleton Lab at Columbia University: one of them was from pristine wires, which serves as a baseline; the other one was from a full-scale suspension cable model which was subject to artificial corrosion.

2.2 Testing of cable wires

Various laboratory testings can be conducted on wire samples to collect necessary information to study its strength and degree of corrosion. These testings include visual inspection, tensile testing, zinc coating testing, and chemical analysis.

2.2.1 Visual inspection

The visual inspection must be performed ahead of all other tests, which includes assessing the condition of the wire, taking measurements of dimensions, such as length and diameter. The condition of a wire sample can be categorized into the following four stages of corrosion:

Stage 1 - spots of zinc oxidation on the wires;

Stage 2 - Zinc oxidation on the whole wire surface;

Stage 3 - spots of brown rust covering up to 30% of the surface of a 3 to 6 inch length of the wire;

Stage 4 - brown rust covering more than 30% of the surface of a 3 to 6 inch length of wire.

2.2.2 Zinc coating test

Wire samples of Stage 1 and 2 are first selected and then tested following 1) Preece test according to ASTM A239, which finds the thinnest spot of zinc coating; and/or 2) Weight of zinc coating test according to ASTM A-90, which is then compared with specification requirements. The samples selected for zinc coating tests should be spreaded over the length of the sample wire. Note that the zinc coating tested samples is destroyed after each testing.

2.2.3 Chemical analysis

A chemical analysis is usually performed on selected samples to measure the percentages of C, Si, Mn, P, S, Cu, Ni, Cr and Al. The result may be used for analyzing the cause of corrosion.

2.2.4 Tensile testing

Tensile tests are in accordance with ASTM A586 and ASTM A370 to include yield strength (0.2% offset method), stress at 2.5% strain, tensile strength, reduction of area, and modulus of elasticity. Each cut specimen will have a length of 18 inches, and the zinc coating is removed using hydrochloric acid on both ends around the gripping area to avoid slipping.

2.3 Suspension bridge cable inspection programs

2.3.1 Williams Bridge

In 1988, an assessment for evaluating the strength of the main cable of Williamsburg Bridge was conducted by the Williamsburg Bridge Cable Investigation group, which was form by engineering firms of Steinman, Boynton, Gronquist, and Birdsall in association with Columbia University. The main cable was opened by wedging and a total of 32 cable samples were extracted. These 32 samples are symmetrically distributed across the cross-section area, and the sample have length ranging from 22.5ft to 36ft. Each sample was cut into 18-inch segments and tensile testing were performed for each segment. At the end testing results of a total of 330 segments were recorded. At the time of the testing, the bridge had been in service for 85 years.

2.3.2 Severn Bridge

In 2010, AECOM (as Faber Maunsell) in association with Weidlinger Associates Inc. conducted inspection for the main cables of Severn Bridge [Cocksedge *et al.*, 2010][Fisher and Lambert, 2011]. A total of 1029 segments of wire samples were extracted and tested. At the time of the testing, the bridge had been in service for 41 years.

2.3.3 Forth Road Bridge

In 2003 Faber Maunsell of London in association with Weidlinger Associates Inc. recommended and carried out the first internal inspection of the main cables of Forth Road Bridge [Mahmoud, 2006]. A total of 620 segments of wires were extracted and tested. At the time of the testing, the bridge had been in service for 44 years.

2.4 Wire testing in Carleton Lab

As part of this research, tensile testings of pristine wires and artificially corroded wires were performed in the Carleton Lab at Columbia University. A total of 65 pristine wire samples and a total of 1209 artificially corroded wire samples were tested, and the results are presented in Appendix A.

Each wire was 20 foot long and cut into thirteen 18 inch samples for tensile testing and one 6 inch sample for chemical component testing. The samples were required to have 18 inches to allow for the grip length (3 inch on each end) and the strain gauge length (10 inch). The zinc coating was removed around the gripping area to avoid slipping. Measurements of wire diameter were taken at areas with and without zinc coating (which are referred to as gross and net diameters in the results), as well as at the necking area. Photos were taken for all tested samples before and after testing, as shown in Figure 2.1.

Both the stress-strain curve and the loading curve of each sample were recorded. As an example, Figure 2.2 shows a typical stress-strain curve of a tested wire sample. The straight line between the two "X" markers was used to estimate Young's modulus. Since the wire is made of hard steel so that the stress-strain curve does not show obvious yielding point. The yield stress was calculated using the 0.2% offset method, shown as the "o" marker in the figure. The stress at 2.5% strain is also shown in the figure as an triangle marker, beyond which the strain measurement is considered not accurate since necking might occur outside the wire segment that the strain gauge measures.

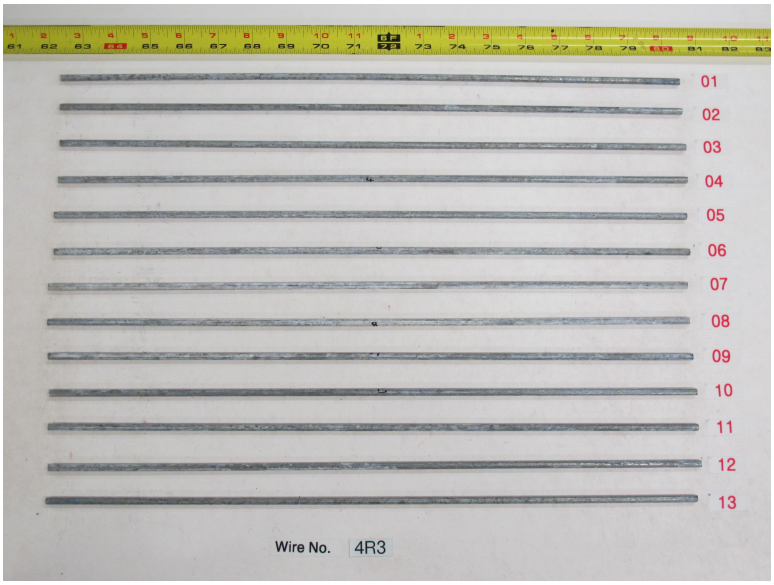

(a) Before testing.

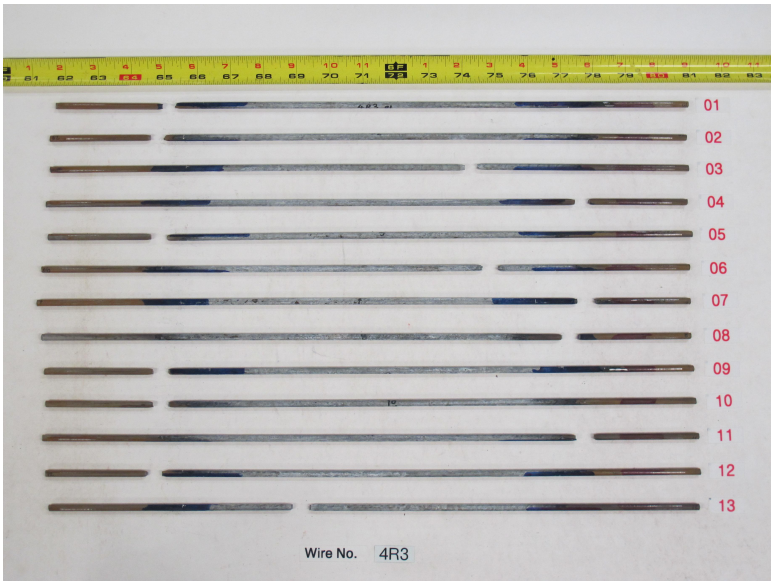

(b) After testing.

Figure 2.1: Thirteen samples from one of the wires extracted from artificially corroded cable.

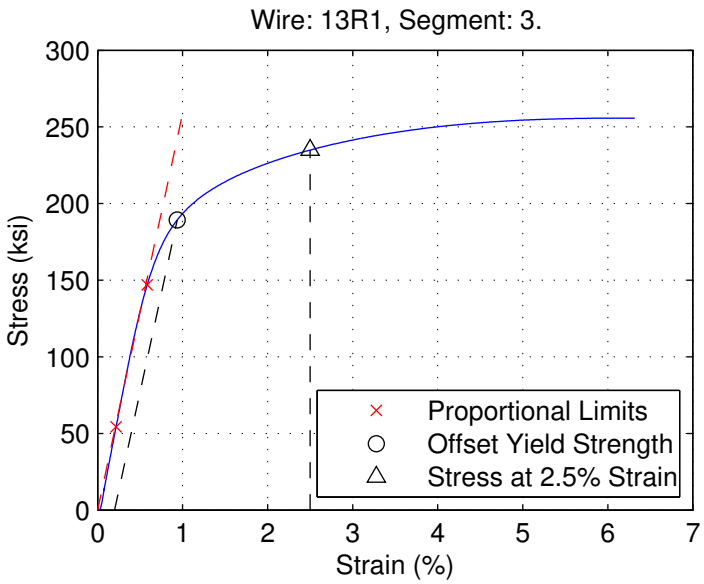

Figure 2.2: Typical stress-strain plot of a sample wire from tensile testing.

2.4.1 Pristine wires

A total 65 samples from 5 pristine wires were tested to serve as a baseline.

2.4.2 Artificially corroded cable

To study the deterioration of suspension bridge cable subject to weather conditions, researchers in the Carleton lab at Columbia University placed a full-scale cable specimen in an accelerated corrosion chamber [Deeble Sloane *et al.*, 2013] and exposed the cable to simulated environment for a period of approximately two years. The corrosion chamber was able to simulated various weather conditions, with different temperature, humidity and pH level. These conditions were cycled multiple times per day, so as to accelerate the deterioration speed. These wires are estimated to have an equivalent age of 10 years base on observing their corrosion stages. This estimation is used as given in Chapter 3 and Chapter 4, but in Chapter 5 a quantitative method

is developed for better estimating the equivalent age.

2.4.2.1 Sampling of wires

The entire cable consists of 61 hexagonal wire strands, as well as loose wires filling the gap to make the cross section a full circle. In order to re-use the cable after the testing, each hexagonal strands must be preserved, so that the cable can be re-assembled afterwards. To achieve this goal, only wires in the middle of each side of each strand should be extracted for testing.

A space-filling design of experiment (DOE) based on maximizing the minimum distance between samples[Santner *et al.*, 2013] was applied to draw samples from the strands of the cable. Let $\mathcal{X}$ be the entires pool of accessible wires and $\mathcal{D}$ be the desired samples. Then $\mathcal{D}$ is selected by solving the following optimization problem:

$$\max_{\mathcal{D}\subset\mathcal{X}} \min_{\boldsymbol{x}_1,\boldsymbol{x}_2\in\mathcal{D}} \|\boldsymbol{x}_1 - \boldsymbol{x}_2\| \tag{2.1}$$

where $||\cdot||$ is a measure of distance. Using this method, 81 wires were selected among all stranded wires. Besides, 12 wires were selected on the surface of the cable, making the total number 93. The locations of all accessible wires and selected wires are shown in Figure 2.3.

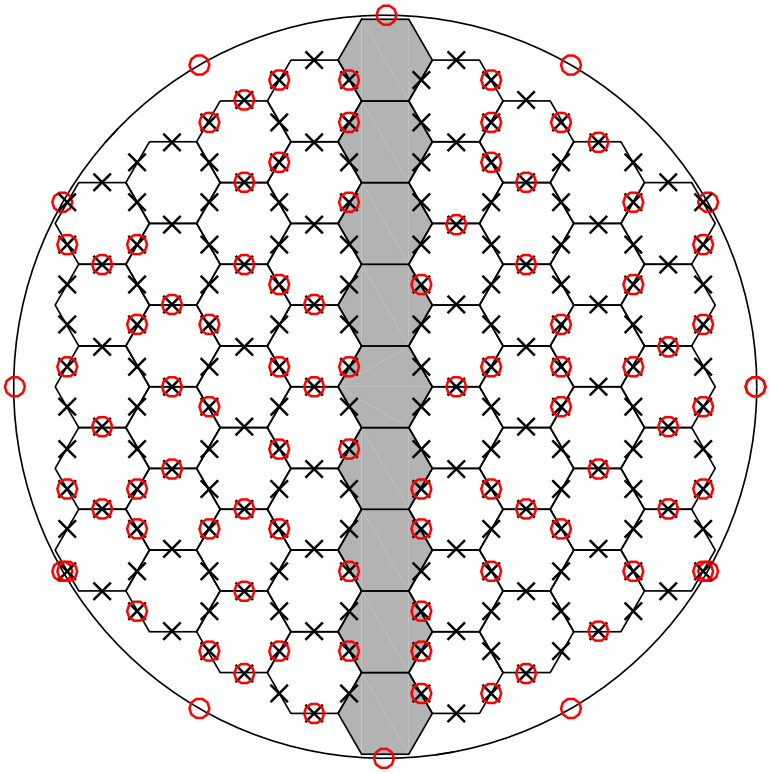

Figure 2.3: Locations of accessible and selected wires. X: accessible wires; O: selected wires.

Chapter 3

Time-dependent statistical models of wire strength

3.1 Chapter summary

In this chapter statistical analysis is performed on tensile testing data obtained from wires of different ages and conditions. The statistical analysis includes fitting various probability distributions to wire strength data and selecting the best fits, and fitting autocorrelation functions and power spectral functions. First, descriptive statistics such as moments and histograms are presented for all five data sets which were collected from three suspension bridges including Williams Bridge, Severn Bridge, Forth Road Bridge, as well as pristine wires and artificially corroded wires.

This chapter is organized in the following order. First, the mathematical definitions of random variable and random process are given, as well as their various properties. Then the copula theory is also introduced in order to explain puzzle of the incompatibility between marginal distribution and power spectral density function which arises in the simulation of non-Gaussian random processes using translation field theory. The foundation of this section is the measure theory and probability theory, interested reader can refer to [Kolmogorov and Fomin, 1975] for a good introduction.

The main contribution of this chapter is the recognition of time-dependency of probably distribution and power spectral density function of cable wires as the corrosion and deterioration is a constantly evolving process. This is done by fitting simple analytical functions to the model parameters by regression analysis. Another major contribution is to demonstrate that the aforementioned incompatibility issue which arises in the simulation of non-Gaussian processes can be partially avoided by fitting appropriate marginal distribution and power spectral density function to the data.

3.2 Wire strength as random variables

We start our statistical analysis by modeling the tensile strength of wires as random variables. This section first covers the definition of a random variable as well as its various properties, especially the distribution functions. Then the discussion continues with how to select the appropriate distribution for tensile testing data and how to estimate the parameters of selected distribution. Finally this section finishes with the proposed evolutionary distribution functions.

3.2.1 Definition of random variable

To define a random variable we need to first define the probability space. The probability space is defined by a triple $(\Omega, \mathcal{F}, \mathbb{P})$, in which each component in the triple is given below:

1. Sample space Ω: it is a given set of all possible outcomes;
2. σ-algebra $\mathcal{F}$: it is a σ-algebra define on Ω. Each element of $\mathcal{F}$ is a subset of Ω, which are called events;
3. Probability measure $\mathbb{P}$: it defines a measure over $\mathcal{F}$, which maps each $B \in \mathcal{F}$ to $[0, 1]$. And the mapping is countably additive.

A random variable is a (real-valued) measurable function $X : \Omega \to \mathbb{R}$ such that for any $B \in \mathcal{B}$, which is a Borel set of $\mathbb{R}$, we have

$$\{\omega \in \Omega : X(\omega) \in B\} \in \mathcal{F} \tag{3.1}$$

Then for any $B \in \mathbb{R}$ we can define the probability measure $\mu_X(B)$ in terms of the measure $\mathbb{P}$ in Ω:

$$\mu_X(B) = \mathbb{P}(X^{-1}(B)) \tag{3.2}$$

In practice we often "forget" about the probability space which is used to define X and only concern about the probabilities that X taking certain values in $\mathbb{R}$. Formally such probabilities can always be represented by the *cumulative distribution function* $F_X(x)$ of X:

$$F_X(x) = P(X \leq x) = \int_B \mu_X(x)\,\mathrm{d}x \tag{3.3}$$

Furthermore we define the derivative of $F_X(x)$ with respect to x as the *probability density function*:

$$f_X(x) = \frac{\partial}{\partial x} F_X(x) \tag{3.4}$$

In theory all real-valued continuous random variable can be uniquely defined by its probability density function.

3.2.2 Statistical Moments

Moments are quantitative measures of the distribution of a random variable. A random variable X is often characterized by its first and second moments, known as the *mean* and *variance*. The mean denoted as μ_X, is the average value that X takes. It is defined as

$$\mu_X = E[X] = \int_{\mathbb{R}} x f_X(x)\,\mathrm{d}x \tag{3.5}$$

And the variance of X, denoted as σ_X, is the degree that X may vary around its mean value. It is defined as

$$\sigma_X = \mathrm{Var}[X] = \mathrm{E}[(X - \mathrm{E}[X])^2] = \int_{\mathbb{R}} (x - \mu_X)^2 f_X(x)\,\mathrm{d}x \tag{3.6}$$

In practice if we had observed n realizations $x_1, x_2, \ldots, x_n$ of a random variable X, then we can also estimate its mean and variance of the following

$$\bar{\mu}_X = \frac{1}{n}\sum_{i}^{n} x_i \tag{3.7}$$

$$\bar{\sigma}_X = \frac{1}{n-1}\sum_{i}^{n}(x_i - \mu_X)^2 \tag{3.8}$$

Here $\bar{\mu}_X$ and $\bar{\sigma}_X$ are called *unbiased estimator* of μ_X and σ_X since we have

$$\lim_{n\to\infty} \bar{\mu}_X = \mu_X, \quad \lim_{n\to\infty} \bar{\sigma}_X = \sigma_X \tag{3.9}$$

In addition, we may also be interested in the third and fourth moments in order to describe the random variable in greater details. To be more precise, the moments here are all referred to as the central moments, i.e., centered at its mean value. The third moment, also known as the *skewness*, is a measure of asymmetry of a probability distribution function about its mean. It is defined as

$$s_X = \text{skew}(X) = \text{E}\left[\left(\frac{X - \mu_X}{\sigma_X}\right)^3\right] \tag{3.10}$$

General speaking, a unimodal distribution with a longer or fatter left tail would have negative skew, and that with a longer or fatter right tail would have positive skew. This is illustrated in Figure.3.1.

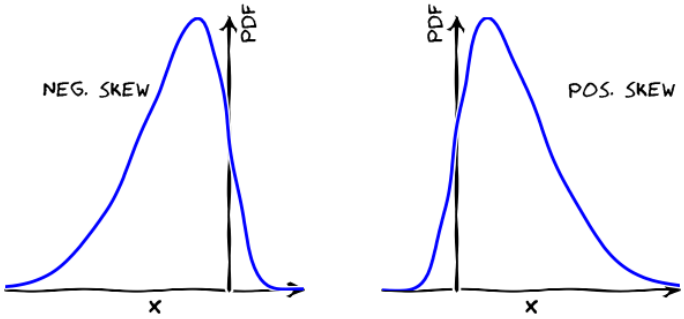

(a) Negative skew (b) Positive skew

Figure 3.1: Probability distributions with negative skew (left) and positive skew (right).

Unlike mean and variance, the estimators for sample skewness are biased in general[Doane and Seward, 2011]. A commonly used estimator is the adjusted Fisher-Pearson standardized moment coefficient G_1, which is computed as

$$G_1 = \frac{n^2}{(n-1)(n-2)} \frac{m_3}{\bar{\sigma}_X^3} \tag{3.11}$$

where $m_3 = \frac{1}{n}\sum_{i=1}^{n}(x_i - \bar{\mu}_X)^3$. Or equivalently

$$G_1 = \frac{\sqrt{n(n-1)}}{n-2} \left[\frac{\frac{1}{n}\sum_{i=1}^{n}(x_i - \bar{\mu}_X)^3}{\left(\frac{1}{n}\sum_{i=1}^{n}(x_i - \bar{\mu}_X)^2\right)^{3/2}} \right] \tag{3.12}$$

Finally, the *Kurtosis*, which is derived from the fourth moment, is a measure of the peakedness of the shape of a probability distribution function. The kurtosis is commonly defined as the fourth standardized moment minus 3,

$$\gamma_2 = \frac{\mathrm{E}[(X - \mu_X)^4]}{\sigma_X^4} - 3 \tag{3.13}$$

The "minus 3" sets the kurtosis of the normal distribution to be zeros (since the fourth standardized moment of the normal distribution is always 3), and therefore

it is also referred to as *excess kurtosis*. Compared to the normal distribution, a distribution with a positive kurtosis (leptokurtic) has a higher peak and fatter tails, while a distribution with a negative kurtosis (platykurtic) is has a flatter peak and thinner tail. A commonly used estimator of sample kurtosis is defined as

$$G_2 = \frac{(n+1)n(n-1)}{(n-2)(n-3)} \frac{\sum_{i=1}^{n}(x_i - \bar{\mu}_X)^4}{(\sum_{i=1}^{n}(x_i - \bar{\mu}_X)^2)^2} - 3\frac{(n-1)^2}{(n-2)(n-3)} \tag{3.14}$$

Like the estimator of sample skewness G_1, this estimator of sample kurtosis is also biased in general.

3.2.3 Commonly used probability distributions

Several probability distributions are extensively used in the rest of this dissertation. A brief introduction to each of these probability distributions is given below.

1. **Uniform distribution**. It has two parameter a and b which specify the bounds between which the random variable is distributed uniformly. Its PDF is given by

$$f_X(x) = \frac{1}{b-a}, \quad (x \in [a, b]) \tag{3.15}$$

   A random variable X following uniform distribution is denoted as X $U(a, b)$. Especially, $U(0, 1)$ is often used as a bridge for transforming random variable from one distribution to another.

2. **Gaussian distribution**. Also named **normal distribution**, it is another important distribution is statistics. It has two parameters μ and σ, which specify its mean and standard deviation. It PDF is given by

$$f_X = \frac{1}{\sqrt{2\pi}\sigma} e^{-\frac{1}{2}\left(\frac{x-\mu}{\sigma}\right)^2} \tag{3.16}$$

3. **Weibull distribution**, also known as the Type III extreme value distribution, has the following PDF

$$f_X(x;,a,b) = \frac{b}{a}\left(\frac{x}{a}\right)^{b-1} e^{-(x/a)^b}, \quad (x>0, a>0, b>0) \tag{3.17}$$

where a is the scale parameter and b is the shape parameter. And its CDF is given by

$$F_X(x;a,b) = 1 - e^{-(x/a)^b}, \quad (x>0, a>0, b>0) \tag{3.18}$$

The mean and variance of a Weibull random variable X is given by

$$\mathrm{E}[X] = a\Gamma\left(1+\frac{1}{b}\right) \tag{3.19}$$

and

$$\mathrm{Var}[X] = a^2\left[\Gamma\left(1+\frac{2}{b}\right) - \left(\Gamma\left(1+\frac{1}{b}\right)\right)^2\right] \tag{3.20}$$

where $\Gamma(\cdot)$ is the gamma function.

3.2.3.1 Connection with uniform random variables

A random variable of any distribution can be mapped and from to a uniform random variable through its cumulative distribution function and its inversion function. Let X be a random variable whose cumulative distribution function is $F_X(x)$. Let $Y = F_X(X)$ then we have $Y \sim U[0,1]$. Such mapping of a random variable of an arbitrary distribution to a random variable of uniform distribution is called *probability integral transform*. Conversely, the mapping a uniform random variable to a random variable of an arbitrary distribution is called *inverse transform sampling*: let $Y \sim U[0,1]$, then $X = F_X^{-1}(Y)$, has cumulative distribution function $F_X(x)$. This connection between

any random variable and a uniform random variable plays an important role in the copula theory, as we may see in the following chapters.

3.2.4 Wire tensile testing data

Preliminary statistical analysis are perform on the wire strength data including computing statistical moments and plotting histograms. Table 3.1 lists the first four moments for each of the five data sets, as well as sample sizes and ages. Figure 3.2 plots the histogram of wire strength of the five data sets. Here the number of bins in each histogram is computed by the Freeman-Diaconis Rule.

Table 3.1: Statistical moments of wire tensile testing data

	Age	Sample Size	Mean	Variance	Skewness	Kurtosis
New Wires	0	65	254.62	3.82	-0.29	-0.28
Carleton Lab	10	1209	251.45	18.94	-4.25	43.62
Severn Bridge	41	1029	247.99	54.16	-1.12	3.93
Forth Road Bridge	44	620	245.62	84.58	-2.34	18.57
Williamsburg Bridge	85	330	216.53	149.18	-0.68	-0.00

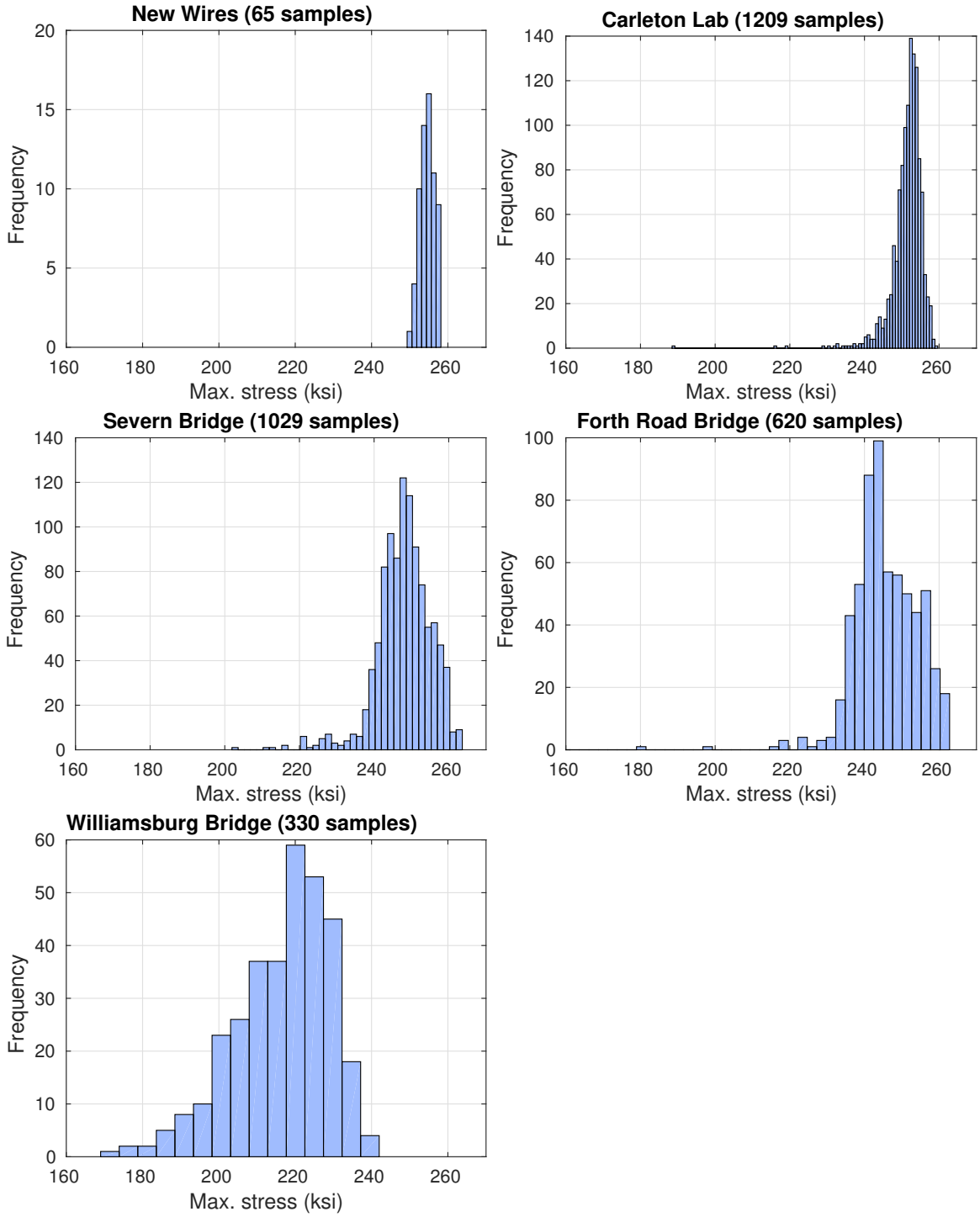

Figure 3.2: Histograms of wire strength of five data sets: new wires, Carleton Lab arificially corroded wires, Forth Road Bridge wires, Severn Bridge wires, Williamsburg Bridge wires.

3.2.5 Distribution fitting

With the presence of negative skew and/or non-zero kurtosis, the sample of wire strength are unlikely to follow normal distribution. Two hypothesis test for normality, i.e., skew test and kurtosis test, both give extremely small p-values for each data set, which further suggest that the data does not strictly follow normal distribution. The same exercise can be conducted for logarithm of the data to test if the data follows lognormal distribution. Again, it turns out that the data are unlikely to follow lognormal distribution either.

Therefore, a proper distribution must be found for wire strength, as it determines the statistical properties of the data set. A good fitted distribution must be faithfully representing the nature of the data and yet mathematically convenient. A large sameple size of the data set is desired, as many of the statistical properties, especially the subtle ones such as excess kurtosis, tail behavior will become more apparent as sample size gets larger. Fitting a proper probability distribution to a given data set can be achieved in two steps: first is to choose the best type of distribution, and second is to estimate the parameters of the chosen distribution. In the following sections the second step is discussed first.

3.2.5.1 Maximum likelihood estimation

Suppose a distribution with PDF $f_X(x; \boldsymbol{p})$ is selected to represent a data set of n samples $x_1, x_2, \ldots, x_n$, where $\boldsymbol{p} = \{p_1, p_2, \ldots, p_m\}$ are the parameters of the distribution to be determined. For distributions whose parameters are closely related to statistical moments, the *method of moments* can be used to estimate the distribution parameters. For example, the two parameters μ and σ of normal distribution can be estimate using the first two moments of the data. However, if the relationship

between distribution parameters and its moments is not straight-forward, another commonly used method for estimating these parameters is the *maximum likelihood method*. Generally speaking, the likelihood is a measure of probability that the data samples are produced by the given distribution. The parameters of the distribution are so chosen that the likelihood is maximized.

Assuming the samples are independent to each other. Since the likelihood of observing a sample x_i is proportional to its PDF $f_X(x_i; \boldsymbol{p})$, and the PDF's are multiplicable by its nature, the likelihood function of the data set is defined as

$$L(x_1, x_2, \ldots, x_n; \boldsymbol{p}) = f_X(x_1; \boldsymbol{p}) f_X(x_2; \boldsymbol{p}) \ldots f_X(x_n; \boldsymbol{p}) \tag{3.21}$$

The parameters $\boldsymbol{p}$ which are found by maximizing the likelihood function are called the maximum likelihood estimator (MLE) $\hat{\boldsymbol{p}}$. Formally it can be formulated as an optimization problem:

$$\hat{\boldsymbol{p}} \subseteq \arg\max_{p} L(\boldsymbol{x}; \boldsymbol{p}) \tag{3.22}$$

In practise, the likelihood function is replaced by the log-likelihood function

$$l(x_1, x_2, \ldots, x_n; \boldsymbol{p}) = \ln L(x_1, x_2, \ldots, x_n; \boldsymbol{p}) = \sum_{i=1}^{n} \ln f_X(x_i; \boldsymbol{p}) \tag{3.23}$$

which turns the multiplication into a summation, making the problem much easier to tackle numerically. The solution obtained by maximizing the log-likelihood function also maximizes the origin likelihood function since logarithm is a strictly monotonically increasing function. In practise the solution is often unique, and therefore they can be estimated by equating the first order derivative of l with respect to $\boldsymbol{p}$ to zeros,

which is equivalent to solving the following system of equations

$$\frac{\partial}{\partial p_j} l(x_1, x_2, \ldots, x_n; \boldsymbol{p}) = 0, \quad j = 1, 2, \ldots, m \tag{3.24}$$

3.2.6 Distribution selection

Determining the best distribution for a given data set is often achieved by trying out a series of different distributions. Each of the candidate distribution is first fitted to the data set either by method of moments or maximum-likelihood method, and then the best distribution is selected according to a certain measure of goodness of fit. Three commonly used measures are negative log-likelihood (NlogL), Bayesian information criterion (BIC) and Akaike information criteron (AIC). These three measures are defined as the following:

1. **Negative log-likelihood (NlogL)**. Smaller value indicates a bigger likelihood and hence a better fit.

2. **Bayesian information criterion (BIC)**. It is based on likelihood, and it is given by

$$\mathrm{BIC} = -2 \ln L + k \ln n \tag{3.25}$$

   where n is the sample size and k is the number of parameters in the distribution. For example $k = 2$ for normal distribution. Increasing number of model parameters may increase likelihood but may also result in overfitting, and hence the second term is added to penalize for the number of parameters in the model. Like NlogL, a smaller BIC indicates a better fit.

3. **Akaike information criterion (AIC)**. Similar to BIC, but the penalty is

smaller. It is given by

$$\mathrm{AIC} = 2k - 2\ln L \tag{3.26}$$

The AIC is derived based on information theory. It is the Kullback-Leibler divergence between the assumed "true distribution" and the fitted distribution with k model parameters. The K-L divergence can be considered as the information loss for using the fitted model to represent the true model. A detailed introduction to KL divergence in given in Sec. 4.5.2.1. Since the true distribution is not known, the AIC is only valid in a relative sense, i.e., it can only be used for comparing two fitted distributions. Again, a smaller AIC indicates a better fit.

A pool of 14 commonly used probability distributions are fitted to the data sets except for the new wires. These candidates are beta distribution, exponential distribution, extreme value distribution, gamma distribution, generalized extreme value distribution, generalized Pareto distribution, inversegaussian distribution, logistic distribution, log-logistic distribution, lognormal distribution, normal distribution, Rayleigh distribution, t location-scale distribution and Weibull distribution. Table 3.2, 3.4, 3.3 and 3.5 list the the first four distributions of best fits, ranked by NlogL measure. In the tables also listed are BIC and AIC measures. These two measures both concur with NlogL regarding the goodness of fit in all cases. The results show that the Weibull distribution is the only distribution included in the top four best fit distributions for each date set. Therefore in the following context Weibull distribution is chosen for all data sets, including for the new wires. The fitted parameters of Weibull distribution for all five data sets are summarized in Tabel 3.6.

Table 3.2: Distribution selections for Carleton Lab

	Distr 1	Distr 2	Distr 3	Distr 4
Distr Name	extreme value	Weibull	t location-scale	logistic
# params	2	2	3	2
NlogL	3187.0248	3192.5564	3219.9858	3279.3044
BIC	6388.2447	6399.3079	6461.2643	6572.804
AIC	6378.0496	6389.1128	6445.9716	6562.6089

Table 3.3: Distribution selections for Severn Bridge

	Distr 1	Distr 2	Distr 3	Distr 4
Distr Name	Weibull	t location-scale	extreme value	logistic
# params	2	3	2	2
NlogL	3456.1187	3453.406	3459.9624	3460.5418
BIC	6926.1102	6927.621	6933.7976	6934.9564
AIC	6916.2375	6912.812	6923.9249	6925.0837

Table 3.4: Distribution selections for Forth Road Bridge

	Distr 1	Distr 2	Distr 3	Distr 4
Distr Name	t location-scale	logistic	log-logistic	Weibull
# params	3	2	2	2
NlogL	2189.4337	2198.7343	2205.9773	2206.1689
BIC	4398.1565	4410.3281	4424.8139	4425.1973
AIC	4384.8673	4401.4687	4415.9545	4416.3378

Table 3.5: Distribution selections for Williamsburg Bridge

	Distr 1	Distr 2	Distr 3	Distr 4
Distr Name	Weibull	extreme value	generalized extreme value	normal
# params	2	2	3	2
NlogL	1286.3252	1286.6686	1289.1133	1305.7358
BIC	2584.2487	2584.9353	2595.6238	2623.0698
AIC	2576.6505	2577.3372	2584.2265	2615.4716

Table 3.6: Parameters of fitted Weibull distribution

Data Set	Age	a (scale)	b (shape)
New wires	0	255.567	145.455
Carleton Lab	10	253.1128	88.37854
Severn Bridge	41	251.2461	40.70697
Forth Road Bridge	44	249.5643	32.93703
Williamsburg Bridge	85	222.0711	21.35886

3.2.6.1 Probability plot

A probability plot can be used to visually assess how well a given data set follows the specified probability distribution. A probability plot is constructed such that a reference line which represents the specified distribution as a straight line. If the data closely follows the specified distribution, then it falls on this reference line on the probability plot. There are two types of probability plot: the Q-Q plot which plots the quentiles[1] of the data against that of the specified distribution; and the P-P plot

[1]By a quantile, we mean the fraction (or percent) of points below the given value. That is, the 0.3 (or 30%) quantile is the point at which 30% percent of the data fall below and 70% fall above that value.

which plots the cumulative densities. The P-P plot has good resolution in the center but less in the tails, and vice versa for the Q-Q plot. In the following context the probability plots are referred to as the P-P plots.

The scales of the axes of a probability plot can be set up such that the CDF of the specified distribution becomes a straight line. However, in general there isn't a universal procedure that works for all distributions, as all probability plots customized for each distribution, although there are commonly used techniques such as shifting, scaling and take log scale. As an example Weibull probability plots are constructed for the five data sets. Recall the Weibull CDF in Eq. (3.18), which can be rewritten as

$$\ln\ln\left(\frac{1}{1-F_X(x)}\right) = b\ln x - b\ln a \tag{3.27}$$

Let $y' = \ln\left(\frac{1}{1-F_X(x)}\right)$, then y' is in linear with respect to x if plotted in log-log scale.

All five data sets are plotted on the Weibull probability plots, as shown in Figure 3.3. Visual inspection suggests that Weibull distribution fits all data sets well, except for the behavior of the left tails of Carleton Lab, Severn Bridge and Forth Road Bridge can not be fully explained by Weibull distrution. The left tails of these three data sets are all arced above the reference lines, which indicates that they have more skewness than Weibull distribution.

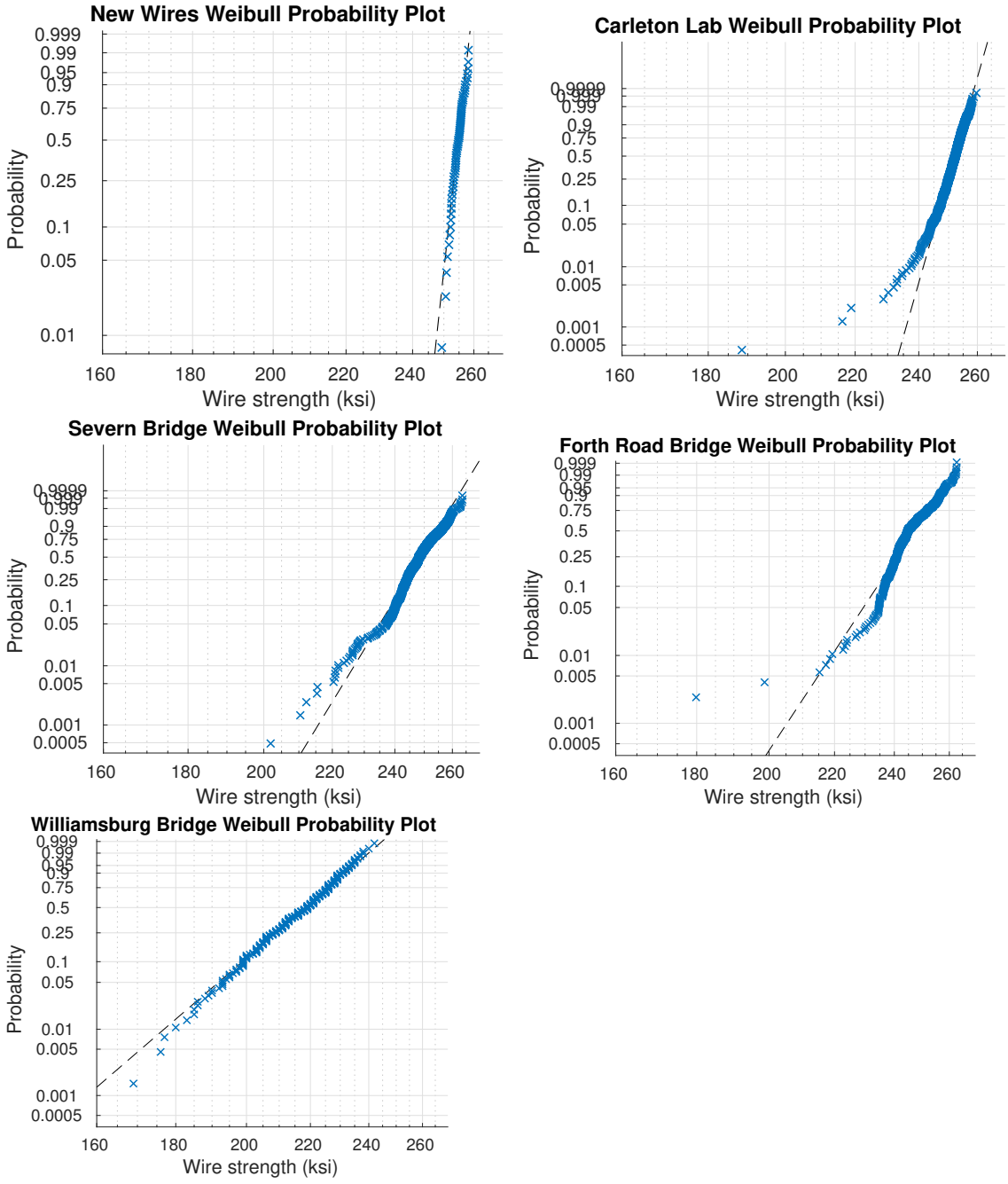

Figure 3.3: Weibull probability plots of wire strength of five data sets: new wires, Carleton Lab artificially corroded wires, Forth Road Bridge wires, Severn Bridge wires, Williamsburg Bridge wires.

3.2.7 Evolutionary distribution

The deterioration of wire strength is a constantly but slowly evolving process over time. As a result the probability distribution of wire strength also evolves in time. In order to capture the pattern of such change, an *evolutionary distribution* is proposed, where the parameters of the distribution are assumed to be functions of time.

Suppose data is available for the same set of wires across different periods of time. After the best fit of distribution is determined and the distribution parameters are estimated for data of each period, then by observing the pattern that each parameter varies over time, a function of time, preferably simple analytical function, is fitted to each parameter. Note the fitted function must meet the requirements as a suitable distribution parameter when extrapolating into reasonable future. For example, a function for the standard deviation of normal distribution $\sigma(t)$ must be strictly positive.

As a demonstration of concept, an evolutionary distribution is created for the five available data sets, although strictly speaking their evolution in time **may not** follow the same pattern, as the wires in these five data set were taken from different bridges or experimental devices and were subject to different environments. Moreover, wires in each data set have different initial strength. To make the five data sets comparable as much as possible, they are normalized by dividing wire strength by their nominal initial strength which are taken as a rounded number of maximum strength in each data set, as listed in Table 3.7.

Table 3.7: Nominal initial wire strength of the five data sets.

Data Set	Age	Nominal initial strength (ksi)
New wires	0	261
Carleton Lab	10	261
Severn Bridge	41	265
Forth Road Bridge	44	265
Williamsburg Bridge	85	258

Weibull distributions are then fitted to the normalized data sets, and the parameters are listed in Table 3.8. Compared to the parameter in Table 3.6, the shape parameters b stay the same.

Table 3.8: Parameters of Weibull distribution fitted to normalized data.

Data Set	Age	a (scale)	b (shape)
New wires	0	0.97919	145.455
Carleton Lab	10	0.96978	88.37854
Severn Bridge	41	0.94810	40.70697
Forth Road Bridge	44	0.94175	32.93703
Williamsburg Bridge	85	0.86074	21.35886

Analytical functions of time are then fitted to Weibull parameter a and b, which are estimated from normalized data. The candidates for such analytical function are:

1. Polynomial functions of order k:

$$p(t) = c_0 + c_1 t + c_2 t^2 + \ldots + c_k t^k \tag{3.28}$$

2. Exponential of polynomial of order k:

$$p(t) = e^{c_0 + c_1 t + c_2 t^2 + \ldots + c_k t^k} \tag{3.29}$$

3. Shifted exponential of polynomial of order k:

$$p(t) = c_{-1} + e^{c_0 + c_1 t + c_2 t^2 + \ldots + c_k t^k} \tag{3.30}$$

4. Logistic function:

$$p(t) = \frac{1}{1 + e^{-(c_0 + c_1 t)}} \tag{3.31}$$

Weibull parameter a and b are plotted against the ages of the data sets in Figure 3.4. By observing the pattern that each parameters changes over time, a second order polynomial function is selected for fitting parameter a, and an exponential function of first order polynomial is selected for fitting parameter b. The fitted functions are given by

$$a(t) = 0.976666 - 1.690447 \times 10^{-4} t - 1.401448 \times 10^{-5} t^2 \tag{3.32}$$

and

$$b(t) = 115.115300 e^{-0.022254 t} \tag{3.33}$$

Combining the Weibull distribution PDF in Eq. (3.17) and the time-dependent parameters in Eq. (3.32) and Eq. (3.33), a time-dependent Weibull distribution is established. We call such probability distribution with time-dependent parameters an *evolutionary distribution*. As a comparison Table 3.9 show the statistics of the five data sets and of the fitted evolutionary Weibull distribution. Figure 3.5 plots the PDF's of the fitted evolutionary Weibull distribution, evaluated at the ages of the five data sets. It shows a clear trend that as time passes the mean value of strength shifts towards lower values, while the variance increases.

An important feature of the evolutionary distribution is that it can be extrap-

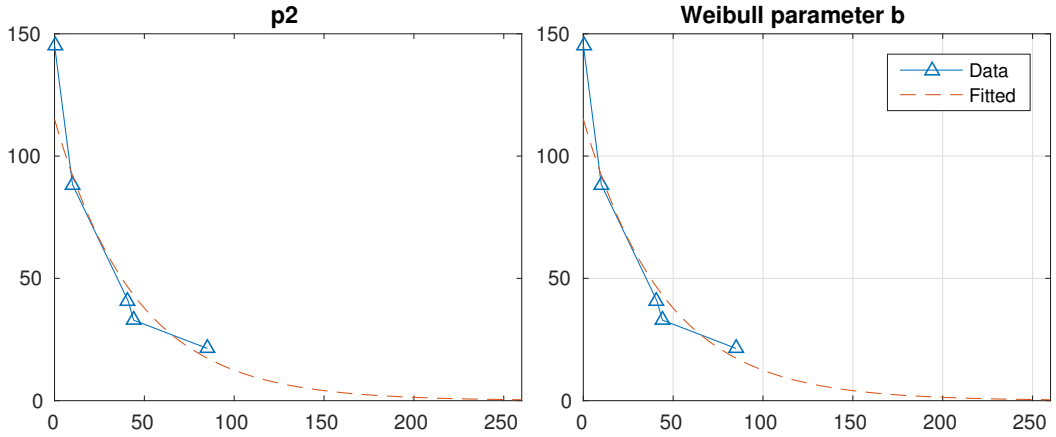

(a) a (b) b

Figure 3.4: Weibull distribution parameters as functions of time.

Table 3.9: Statistics of the data and fitted evolutionary Weibull distribution.

Data Set	Mean		Median		Std. Dev.	
	Data	Fitted	Data	Fitted	Data	Fitted
New Wires	0.97534	0.97184	0.97672	0.97356	0.00856	0.01076
Carleton Lab	0.96357	0.96759	0.96577	0.96971	0.01387	0.01336
Severn Bridge	0.93521	0.93479	0.93960	0.93870	0.02896	0.02554
Forth Road Bridge	0.92608	0.93001	0.93133	0.93414	0.03530	0.02714
Williamsburg Bridge	0.83927	0.83510	0.84610	0.84306	0.04880	0.05933

olated into the future, which is useful in reliability engineering. Two issues must be paid attention to when performing the extrapolation. The first issue is that the time-dependent parameters must remain eligible as parameters of the distribution. For example, both parameters for Weibull distribution must be greater than zero. In the above case $b(t) > 0$ for all t, but $a(t) > 0$ only for $t < 258.02$yr. As a result the evolutionary Weibull distribution is only valid in this range. The second issue is that it is preferred that the fitted evolutionary distribution preserves the observed monotonicity of the key statistics over time. In the above case it is observed in Table. 3.9 that the mean of the normalized wire strength decreases in time while the variance increases. Let $m(t)$ and $v(t)$ be the mean and variance of the fitting evolu-

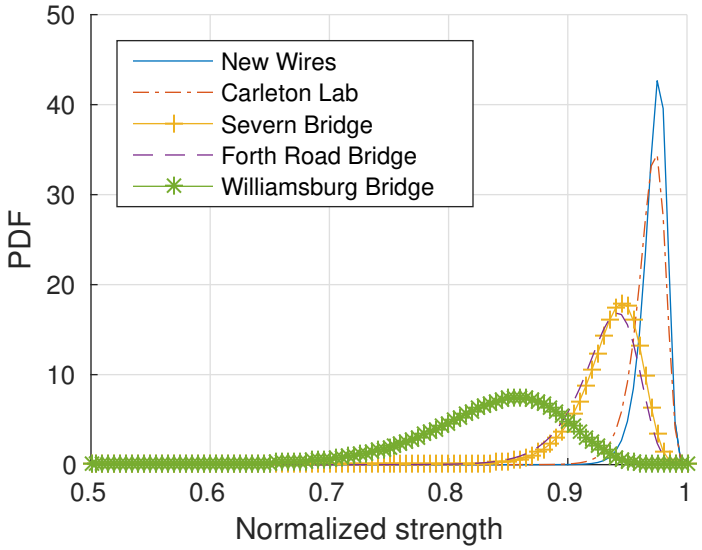

Figure 3.5: PDF's of the fitted evolutionary Weibull distribution evaluated at the ages of the five data sets.

tionary Weibull distribution, respectively, which can be computed using Eq. (3.19) and Eq. (3.20). Taking derivative with respect to time t of the mean $m(t)$ yields

$$\begin{aligned} m'(t) &= \frac{\partial m}{\partial a} a'(t) + \frac{\partial m}{\partial b} b'(t) \\ &= \Gamma\left(1+\frac{1}{b}\right) a'(t) - \frac{a}{b^2}\Gamma'\left(1+\frac{1}{b}\right) b'(t) \end{aligned} \tag{3.34}$$

where $\Gamma'(\cdot)$ is the polygamma function. For $0 \leq t < 258.02$, we have $a > 0$, $b > 0$, $\Gamma(1+1/b) > 0$ and $\Gamma'(1+1/b) < 0$. From Eq. (3.32) and Eq. (3.33) we have $a' < 0$ and $b' < 0$. Therefore we have $m'(t) < 0$, indicating the mean of the fitted evolutionary Weibull distribution monotonically decreases over time, which fits observation. The monotonicity of the variance $v(t)$ is hard to see analytically. It can be found numerically that $v(t)$ monotonically increases for $t < 240$yr (approximately). Therefore we take the valid range of the fitted evolutionary Weibull distribution as $[0, 240]$yr. Figures 3.6a and 3.6b show the mean and variance as functions of time over this range, respectively.

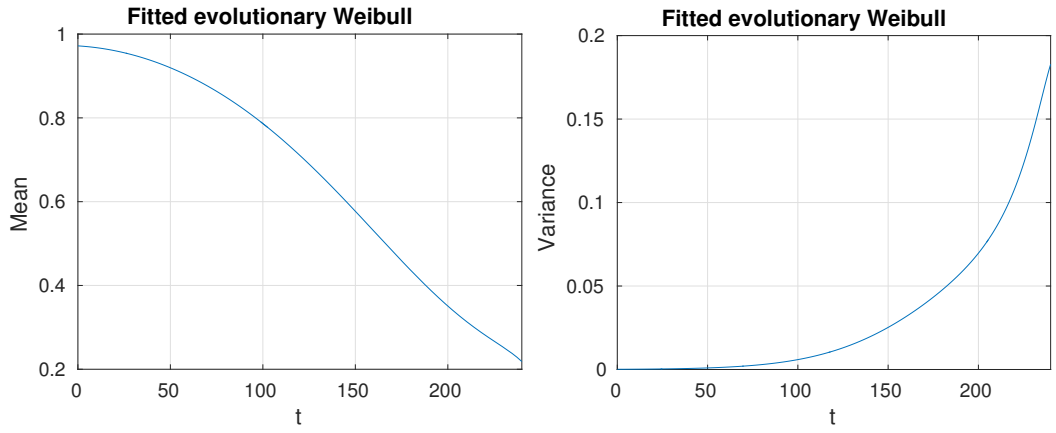

(a) Mean (b) Variance

Figure 3.6: Mean and variance of fitted evolutionary Weibull distribution as functions of time.

Beyond this range, both the mean and variance quickly drop to zero simutaneously, which indicates that the PDF eventually degenerates into a delta function centered at zero when the strength of all wires become zero. Note that the breaks of wires are not explicitly considered here, if it was, the distribition of wire strength would evolve more abruptly especially when the wire strength is low.

3.3 Correlation and Copula

Let X and Y be two random variables defined on the same probability space $(\Omega, \mathcal{F}, P)$. Then we would like to know the probability that they both taking certain values, and this is given by their joint cumulative distribution function, defined as

$$F_{XY}(x, y) = P(X \leq x, Y \leq y) \tag{3.35}$$

Similarly, taking derivatives on F_{XY} twice with respect to x and y yields the joint probability density function

$$f_{XY}(x, y) = \frac{\partial^2}{\partial x \partial y} F_{XY}(x, y) \tag{3.36}$$

Based on the joint probability density function we can define the covariance $\mathrm{Cov}[X, Y]$ of X and Y, which measures how much Y varies in response to the change in X, and vice versa. In general if X and Y tend to take their biggest values and smallest values at the same time, the their covariance is positive; otherwise their covariance is negative. It is defined as

$$\mathrm{Cov}[X, Y] = \mathrm{E}[(X - \mathrm{E}[X])(Y - \mathrm{E}[Y])] \tag{3.37}$$

Alternatively, after expanding it and collecting terms, we have

$$\mathrm{Cov}[X, Y] = \mathrm{E}[XY] - \mathrm{E}[X]\mathrm{E}[Y] \tag{3.38}$$

where the $E[XY]$ term is computed by integrating over their joint probability density

function

$$\mathrm{E}[XY] = \int_{\mathbb{R}^2} xy f_{XY}(x, y)\,\mathrm{d}x\,\mathrm{d}y \tag{3.39}$$

If the value that random variable X takes does not depend on the value that random variable Y takes and vice versa, then we say that X and Y are indenpendent. Mathematically X and Y are indenpendent if and only if their joint cumulative distribution function is separable

$$F_{XY}(x, y) = F_X(x)F_Y(y) \tag{3.40}$$

or alternatively, their probability density function is separable

$$f_{XY}(x, y) = f_X(x)f_Y(y) \tag{3.41}$$

As a result the expectation of their product can be expressed in terms of the product of their expectations:

$$\begin{aligned}\mathrm{E}[XY] &= \int xy f_{XY}(x, y)\,\mathrm{d}x\,\mathrm{d}y \\ &= \int x f_X(x)\,\mathrm{d}x \cdot \int y f_Y(y)\,\mathrm{d}y \\ &= \mathrm{E}[X]\mathrm{E}[Y]\end{aligned} \tag{3.42}$$

Apparently that if X and Y are independent of each other then their covariance is zero

$$\mathrm{Cov}[X, Y] = 0, \quad \text{if } X \text{ and } Y \text{ are independent.} \tag{3.43}$$

Closely related to covariance is the *Pearson's correlation coefficient*, defined as a

normalized quantity:

$$\rho_{X,Y} = \frac{\mathrm{Cov}[X,Y]}{\sigma_X \sigma_Y} \tag{3.44}$$

And it can be shown that $-1 \leq \rho_{X,Y} \leq 1$ due to normalization. It measures the linear correlation between two random variables, and being -1 or 1 indicates the data points of X and Y fall exactly a line. The Pearson's correlation coefficient is symmetric, i.e., $\rho_{X,Y} = \rho_{Y,X}$ and is invariant to affine transformation to each X or Y, or both.

3.3.1 Copula and correlation bounds

The drawback of both covariance and Pearson's correlation coefficient as measures of correlation between two random variables is that they only measure the correlation with a single number, which might not provide enough resolution on the entire correlation structure which is defined by the joint distribution function. However, the joint distribution function is often too cumbersome to work with, and it is hard to directly observe the correlation structure from it. To overcome this drawback, we briefly introduce a more powerful tool for describing the correlation structure, which is called *copula*. The beauty of it is that by using the probability integral transformation (see 3.2.3.1), a copula is capable of stripping the correlation structure out of the original joint distribution function, and representing it in an universal way.

By definition, a copula is a multivariate probability distribution with the marginal distribution of each random variable being uniform distribution. For simplicity, in the following context we restrict our discussion to copulas on two random variables. Let X_1, X_2 be two random variables with marginal CDF $F_{X_1}(x)$, $F_{X_2}(x)$, respectively, and joint CDF $F_{X_1X_2}(x_1, x_2)$. Applying probability integral transformation on X_1 and X_2 gives

$$U_1 = F_{X_1}(X_1), \quad U_2 = F_{X_2}(X_2) \tag{3.45}$$

where $U_1 \sim U[0,1]$ and $U_2 \sim U[0,1]$. Then a copula of X_1 and X_2 is defined as the joint CDF of U_1 and U_2:

$$C(u_1, u_2) = F_{U_1U_2}(u_1, u_2) \tag{3.46}$$

The *Sklar's Theorem* guarantees that $F_{U_1U_2}(u_1, u_2)$ always exists for the given $F_{X_1X_2}(x_1, x_2)$ and the marginal CDF $F_{X_1}(x)$, $F_{X_2}(x)$, and hence the copula $C(u_1, u_2)$ of X_1 and X_2 always exists. $F_{X_1X_2}(x_1, x_2)$ is directly linked to the copula through the marginal CDF's:

$$F_{X_1X_2}(x_1, x_2) = C(F_{X_1}(x_1), F_{X_2}(x_2)) \tag{3.47}$$

In this way the information regarding the marginal distribution is filtered out, while the information regarding the correlation structure remains. Universal methods can then be developed to study the copula itself, yet literally such methods can be applied to any marginal distribution.

An important property of copula is that it can be bounded. The *Fréchet-Hoeffding Theorem* states that in the bivariate case

$$\max(u + v - 1, 0) = W(u, v) \leq C(u, v) \leq M(u, v) = \min(u, v) \tag{3.48}$$

where the lower and upper bounds are denoted as $W(u, v)$ and $M(u, v)$, respectively. Note that the lower bound may not be generalized to multivariate cases. When the Fréchet upper bound is achieved, the random variables X_1 and X_2 are called *comonotoic*, referred to as the perfect positive dependence between the two variables, where the Pearson's correlation coefficient reaches its maximum $\rho_{\max}$. When the Fréchet lower bound is achieved, the random variables X_1 and X_2 are called *countermonotoic*, referred to as the perfect negative dependence between the two variables, where the Pearson's correlation coefficient reaches its minimum $\rho_{\min}$. $\rho_{\min}$ and $\rho_{\max}$ to-

gether give the *attainable correlation bounds* on the Pearson's correlation coefficient for a specific distribution.

One of the commonly used copula is the Gaussian copula, which is given by

$$C_G(u, v) = \Phi(\Phi^{-1}(u), \Phi^{-1}(v); \rho) \tag{3.49}$$

which is parameterized by the parameter ρ in the CDF of joint standard Gaussian distribution. It can be verified that Gaussian copula achieves Fréchet upper bound if and only if $\rho = 1$, and it achieves Fréchet lower bound if and only if $\rho = -1$.

3.3.2 Bounds of Pearson's correlation coefficient

The standard definition of the Pearson's correlation coefficient in Eq. (3.44) can be used to find $\rho_{\min}$ and $\rho_{\max}$. In this section we study the attainable correlation bounds of two random variable X_1 and X_2 with the same marginal CDF $F_X(x)$, and hence the same mean μ_X and standard deviation σ_X. Let their joint CDF be $F_{X_1X_2}(x_1, x_2)$. Then we have

$$\rho_{X_1X_2} = \frac{\mathrm{E}[X_1X_2] - \mu_X^2}{\sigma_X^2} \tag{3.50}$$

The problem is reduced to finding the maximum and minimum values of $\mathrm{E}[X_1X_2]$, which can be computed in terms of copula:

$$\mathrm{E}[X_1X_2] = \int_{\mathbb{R}^2} X_1X_2 \,\mathrm{d}F_{X_1X_2}(x_1, x_2) \tag{3.51}$$

$$= \int_0^1 \int_0^1 F_X^{-1}(u_1)F_X^{-1}(u_2) \,\mathrm{d}C(u_1, u_2) \tag{3.52}$$

When the copula $C(u_1, u_2)$ achieves the Fréchet upper bound, we have

$$\begin{aligned}
\mathrm{E}[X_1X_2]_{\max} &= \int_0^1 \int_0^1 F_X^{-1}(u_1)F_X^{-1}(u_2)\,\mathrm{d}\min(u_1,u_2) && (3.53)\\
&= \int_0^1 \int_0^1 F_X^{-1}(u_1)F_X^{-1}(u_2)\delta(u_1-u_2)\,\mathrm{d}u_1\,\mathrm{d}u_2 && (3.54)\\
&= \int_0^1 F_X^{-1}(u)F_X^{-1}(u)\,\mathrm{d}u && (3.55)\\
&= \int_{\mathbb{R}} X^2\,\mathrm{d}F_X(x) && (3.56)
\end{aligned}$$

Therefore if X_1 and X_2 have the same marginal CDF then $\rho_{\max} = 1$. When the copula achieves the Fréchet lower bound, we have

$$\begin{aligned}
\mathrm{E}[X_1X_2]_{\min} &= \int_0^1 \int_0^1 F_X^{-1}(u_1)F_X^{-1}(u_2)\,\mathrm{d}\max(u_1+u_2-1,0) && (3.57)\\
&= \int_0^1 \int_0^1 F_X^{-1}(u_1)F_X^{-1}(u_2)\delta(u_1+u_2-1)\,\mathrm{d}u_1\,\mathrm{d}u_2 && (3.58)\\
&= \int_0^1 F_X^{-1}(u)F_X^{-1}(1-u)\,\mathrm{d}u && (3.59)
\end{aligned}$$

However, the minimum value is not immediate available as it depends on the marginal CDF. In particular we are interested in finding it for standard normal distribution and Weibull distribution.

Standard normal distribution

For standard normal distribution, due to its symmetry we have $F_X^{-1}(x) = -F_X^{-1}(x)$, and therefore

$$\begin{aligned}
\mathrm{E}[X_1X_2]_{\min} &= \int_0^1 -F_X^{-1}(u)F_X^{-1}(u)\,\mathrm{d}u && (3.60)\\
&= -\int_{\mathbb{R}} X^2\,\mathrm{d}F_X(x)a && (3.61)\\
&= -1 && (3.62)
\end{aligned}$$

which indicates that $\rho_{\min} = -1$ for standard normal distribution.

Weibull distribution

For Weibull distribution with parameter a and b, we have

$$F_X^{-1}(x) = a\left(\ln\frac{1}{1-x}\right)^{\frac{1}{b}} \tag{3.63}$$

and

$$\mathrm{E}[X_1X_2]_{\min} = \int_0^1 a^2[\ln u \ln(1-u)]^{\frac{1}{b}}\,\mathrm{d}u \tag{3.64}$$

The result depends on a and b, and it can be evaluated numerically. The minimum correlation coefficient is computed for all five data sets, assuming the data follows the fitted Weibull distribution with parameters in Table 3.6. The results are listed in Table 3.10. This indicates that the selection of probability distribution for the data also imposes bounds on the data itself.

Table 3.10: Minimum correlation coefficient of the fitted Weibull distributions (see Table 3.6 for fitted parameters) for the five data sets.

Data Set	Age	Min. ρ
New wires	0	-0.8919
Carleton Lab	10	-0.8956
Severn Bridge	41	-0.9064
Forth Road Bridge	44	-0.9109
Williamsburg Bridge	85	-0.9230

3.4 Wire strength as random processes

When testing the wire samples for tensile strength, their spatial coordinates were also recorded. Using this information the wire strength along the wire length direction can be modelled as a random process with marginal distribution being the Weibull distribution as identified previously. This section gives the formal definition of a random process, followed by concepts such as stationarity and second moment properties. Then evolutionary correlation function and power spectral density function are introduced to capture how the nature of the random process that represents wire strength changes over time.

3.4.1 Definition of a random process

A random process is a parameterized collection of random variable

$$\{X_\xi\}_{\xi\in\Xi} \tag{3.65}$$

defined on a probability space $(\Omega, \mathcal{F}, P)$ and taking values in $\mathbb{R}^n$. Ξ is the parameter space. The parameter can be either time or spatial coordinate. If the parameter is time, the parameter space is usually the half line $[0, \infty)$. Random process in time is often also referred to as *stochastic process* in many literatures. In the next chapter the deterioration rate will be modelled as a stochastic process. If the paramter is spatial coordinate, the parameter space is often a subset of $\mathbb{R}^n$ for $n \geq 1$, and such process is often also referred to as a *random field*, which has extensive applications in engineering. In this chapter the wire strength at a specified time is modelled as a random process, with the parameter being the spatial coordinate along the wire length direction.

For each fixed $\xi \in \Xi$ we have a random variable

$$\omega \to X_\xi(\omega), \quad \omega \in \Omega \tag{3.66}$$

On the other hand, fixing $\omega \in \Omega$ gives us a function

$$\xi \to X_\xi(\omega), \quad \xi \in \Xi \tag{3.67}$$

which is called a *path* of X_ξ for a stochastic process or a *realization*, or a *sample* for a random field.

If the parameter space $\Xi = \mathbb{R}$, i.e., the random process is one-dimensional, a finite dimensional distribution of order k of such process X_ξ, $\xi \in \mathbb{R}$ is defined as the joint probability disiribution of a set $X_{\xi_1}, X_{\xi_2}, \ldots, X_{\xi_k}$:

$$F_{\xi_1,\xi_2,\ldots,\xi_k}(x_1, x_2, \ldots, x_k) = P(X_{\xi_1} \leq x_1, X_{\xi_2} \leq x_2, \ldots, X_{\xi_k} \leq x_k) \tag{3.68}$$

Especially when $k = 1$, it is called the *marginal distribution* of the process. When $k > 1$, the finite dimensional distribution contain information regarding the correlation structure of the process.

3.4.2 Second moment properties

The first two moments of a random process are of great importance as many of the properties of a random process are related to or defined based on them. For a real-valued, one-dimensional, and square integrable random process $X(t)$, the following second moment properties can be defined

1. Mean function: $\mu(t) = \mathrm{E}[X(t)]$

2. Correlation function: $R(t,s) = \mathrm{E}[X(t)X(s)]$

3. Covariance function: $C(t,s) = \mathrm{E}[(X(t) - \mu(t))(X(s) - \mu(s))]$

The correlation function and covariance function defined on a single random process are also be called autocorrelation function [2] and autocovariance function, respectively. Both functions are positive semidefinite. The second moment properties of a random process are given by the pair of mean function and either one of the correlation function or the covariance function.

3.4.3 Stationary process

A random process is said to be *strictly stationary* if its finite dimensional distribution is invariate to time shift:

$$\begin{aligned} &P\{X(t_1) \le x_1, X(t_2) \le x_2, \ldots, X(t_k) \le x_k\} \\ &= P\{X(t_1+\tau) \le x_1, X(t_2+\tau) \le x_2, \ldots, X(t_k+\tau) \le x_k\}, \quad \text{for all } \tau \end{aligned} \tag{3.70}$$

As a result, the mean function is constant, and both the correlation function and covariance function depend only on the time lag $\tau = t - s$:

1. $\mu(t) = \mu$, constant (3.71)

2. $R(t,s) = R(t-s) = R(\tau)$ (3.72)

3. $C(t,s) = C(t-s) = C(\tau)$ (3.73)

[2] In some applications the autocorrelation function is defined in terms of the normalized covariance function:

$$R(t,s) = \frac{\mathrm{E}[(X(t) - \mu(t))(X(s) - \mu(s))]}{\sqrt{\mathrm{Var}[X(t)]}\sqrt{\mathrm{Var}[X(s)]}} \tag{3.69}$$

In practice the condition on finite-dimensional distribution often turns out to be too strong and therefore has limited applications. Instead, a random process is said to be *weakly stationary* or stationary in a wide sense if its mean, correlation, and covariance satisfy Eq. (3.71) Eq. (3.73), regardless of the finite dimensional distribution. For a weakly station random process, both $R(\tau)$ and $C(\tau)$ are even functions, and satisfy

$$R(\tau) \leq R(0),\ C(\tau) \leq C(0) \tag{3.74}$$

3.4.4 Power spectral density

For a weakly stationary random process, the power spectral density (PSD) function is defined as the expectation of direct Fourier tranform of the random process:

$$S(\omega) = \lim_{T\to\infty} \mathrm{E}\left[|\hat{X}_T(\omega)|^2\right] \tag{3.75}$$

where the subscript T indicates that the Fourier transform $X(\omega)$ is computed using realizations of $X(t)$ over the interval $[0, T]$. The power spectral density function is symmetric, and it describes the distribution of power over different frequencies. The *Wiener-Khintchin Theorem* states that correlation function and power spectral density function of a weakly stationary random process form a Fourier pair:

$$R(\tau) = \int_{-\infty}^{\infty} S(\omega) e^{i\tau\omega}\,\mathrm{d}\omega \tag{3.76}$$

and

$$S(\omega) = \frac{1}{2\pi}\int_{-\infty}^{\infty} R(\tau) e^{-i\omega\tau}\,\mathrm{d}\tau \tag{3.77}$$

The power spectral density function contains all information of both the mean and the correlation funciton. If the mean of the random process is not zero, the power

spectral density function contains a delta function at origin $\mu^2\delta(0)$. Therefore the power spetral density function provides an alternative way for specifying the second moment properties for weakly stationary processes.

For zero-mean weakly stationary random processes, the one-sided spetral density is often used in engineering, which is defined as

$$S^{\text{one-sided}}(\omega) = 2S(\omega), \quad \omega \geq 0 \tag{3.78}$$

The one-sided power spectral density function is used throughout this chapter. Furthermore, it can be shown that the following relationship holds:

$$\text{Var}[X(t)] = R(0) = \int_0^\infty S^{\text{one-sided}}(\omega)\,\mathrm{d}\omega \tag{3.79}$$

3.4.5 Estimating spectral density and correlation from data

Suppose that wire strength can be modelled as weakly stationary random process. This section seeks to estimate the power spectral density function and correlation function of wire strength from the five available data sets. In practise the spectral density function is estimated first since it is easier to construct than the correlation function. This is because it is hard to guarantee the correlation function be positive semidefinite when estimated it from data, but it is easier to require the estimated power spectral be non-negative.

The power spectral density function can not be directly estimated using its definition as given in Eq. (3.75) as the result may suffer from severe frequency leakage due to finite T. Instead the Welch method[Stoica and Moses, 2005] with Hamming window and without overlapping is used. The window length is selected by trying different values. For each data set the overall mean is subtracted from all wire

strength samples. The estimated one-sided power spectral density functions are plotted in Figure 3.7a. Then the correlation functions are obtained by Wiener-Khinchin transformation Eq. (3.76), as shown in Figure 3.8a.

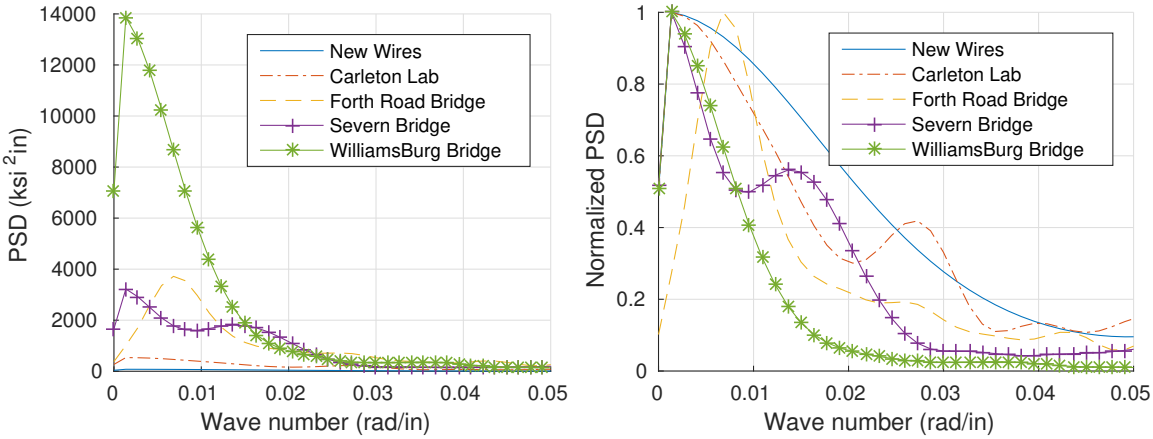

(a) Power spectral density (b) Normalized power spectral density

Figure 3.7: Power spectral density functions estimated from all five data sets.

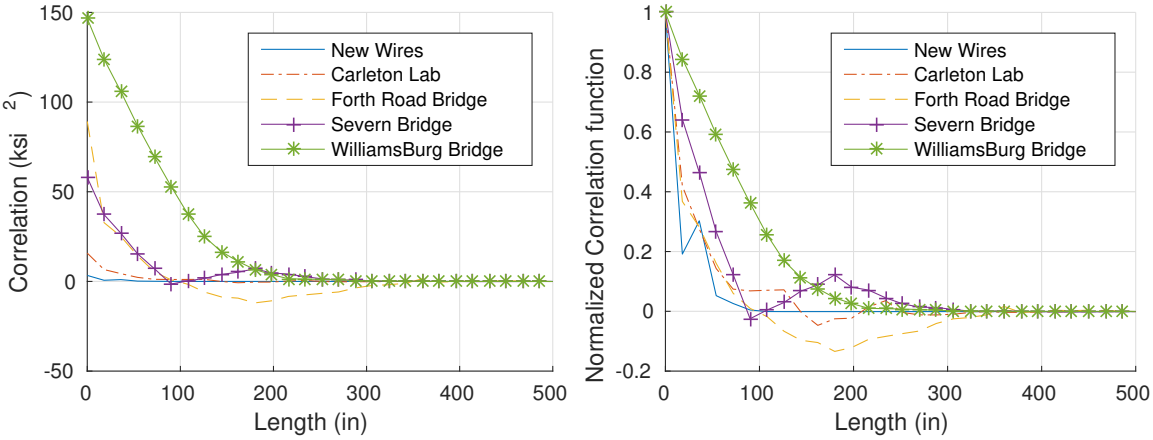

(a) Correlation (b) Normalized correlation

Figure 3.8: Correlation functions estimated from all five data sets.

To make the the power spectral density functions comparable, they are normalized such that their maximum value is equal to 1, as shown in Figure 3.7b. The spectral density of new wires has the widest spread over frequency while the spectral density

of Williamsburg bridge wires, which is the most aged, has the narrowest spread. The spectral densities of the other three data sets lie in between. The similar phenomenon can also be observed on the correlation functions which are normalized by dividing $R(0)$, as shows in Figure 3.8b. Both observation suggests that the second moment properties of the random process of wire strength may follow a certain pattern of evolution in time.

3.4.6 Evolutionary power spectral density and correlation

This section studies the pattern of how power spectral density function evolves as wire deteoriates. As a demonstration of concept, the pattern is established using the five available data sets, although strictly speaking, as mentioned in Sec. 3.2.7, the evolution of each set of wires may not follow the same pattern.

The Clough-Penzien spectrum with five parameters is chosen to fit the power spectral density functions of each data set, which is given by

$$S(\omega) = \frac{\omega_g^4 + (2\zeta_g\omega_g\omega)^2}{(\omega_g^2 - \omega^2)^2 + (2\zeta_g\omega_g\omega)^2} \cdot \frac{\omega^4}{(\omega_f^2 - \omega^2)^2 + (2\zeta_f\omega_f\omega)^2} \cdot \frac{S_0}{2\pi} \tag{3.80}$$

where the first term is the Kanai-Tajimi spectrum, and the second term is a high-pass filter. This is a two sided spectrum. The parameters ω_g and ζ_g determine the peak and spread of the Kanai-Tajimi spectrum, while parameters ω_f and ζ_f determine the cut-off frequency and convergence speed of the high-pass filter. Parameter S_0 is a scaling factor[3] such that the area under $S(\omega)$ is equal to the variance of the wire strength samples. The correlation function corresponding to Clough-Penzien spectrum is also available in analytical form. The derivation can be found in [Kung and Pecknold,

[3]The original Clough-Penzien spectrum was resulted from filtering a white noise vibration whose spectral density is constant S_0.

1982]. Following the notations as in [Fu, 1995], the correlation function $R(\tau)$ is given by

$$R(\tau) = \frac{S_0}{4\zeta_g\omega_g} e^{-\zeta_g\omega_g|\tau|}\left[(C_{a1}+C_{b1})\cos\omega_g^d|\tau| + \frac{\zeta_g\omega_g}{\omega_g^d}(C_{a1}-C_{b1})\sin\omega_g^d|\tau|\right] + \frac{S_0}{4\zeta_f\omega_f} e^{-\zeta_f\omega_f|\tau|}\left[(C_{a2}+C_{b2})\cos\omega_f^d|\tau| + \frac{\zeta_f\omega_f}{\omega_f^d}(C_{a2}-C_{b2})\sin\omega_f^d|\tau|\right] \quad (3.81)$$

where

$$\omega_g^d = \sqrt{1-\zeta_g^2}\omega_g \quad (3.82)$$

$$\omega_f^d = \sqrt{1-\zeta_f^2}\omega_f \quad (3.83)$$

And C_{a1}, C_{a2}, C_{b1} and C_{b2} are given in Appendix C.

The cut-off frequency ω_f of the high-pass filter is chosen to be 0.0014, to account for finite sample size. The damping ratio ζ_f of the high-pass filter is chosen to be 0.7, to avoid sharp peak in the spectrum. The remaining three parameters ω_g, ζ_g and S_0 are estimated separately for each data set by simutaneously minimizing the maximum absolute errors on the spectral density functions and the correlation functions. Figure 3.9 compares the fitted Clough-Penzien spectrum to the target spectral density functions estimated from data, as well as the fitted Clough-Penzier correlation function to the targets. The estimated values of the parameters ω_g, ζ_g and S_0 are summarized in Table 3.11.

The parameters ω_g, ζ_g and S_0 are then modelled as functions of time. Candidates of analytical function forms are given by Eq. (3.28)∼Eq. (3.31). By plotting their values in Figure 3.10 and observing their behaviors, exponential functions are fitted to both ω_f and ζ_f, and a quadratic function is fitted to S_0. However, from Figure 3.10a and Figure 3.10b it is suspected that the Forth Road Bridge data is an outlier, as

it significantly deviates fromt the pattern which is followed by the other four data sets. Therefore the analytical functions are fitted again excluding the Forth Road Bridge data set. The fitted analytical functions are given by Eq. (3.84), Eq. (3.85) and Eq. (3.86).

Table 3.11: Estimation of parameters of Clough-Penzien spectrum for all five data sets.

	Age	ω_g	ζ_g	S_0
New wires	0	4.538×10^{-3}	2.741	3.144×10^{2}
Carleton Lab	10	3.832×10^{-3}	2.337	2.138×10^{3}
Severn Bridge	41	2.353×10^{-3}	1.944	1.231×10^{4}
Forth Road Bridge	44	8.714×10^{-3}	1.185	7.261×10^{3}
Williamsburg Bridge	85	1.689×10^{-3}	1.782	5.883×10^{4}

$$\omega_g(t) = 0.0043e^{-0.0116t} \tag{3.84}$$

$$\zeta_g(t) = 2.5454e^{-0.0047t} \tag{3.85}$$

$$S_0(t) = 1006.9 - 80.01t + 8.9323t^2 \tag{3.86}$$

By now the evolutionary power spectral density function is constructed as the Clough-Penzien spectrum with time-dependent parameters. It is plotted in Figure 3.11a from 0 years to 120 years with 30-year increments. The peaks of the spectral density functions get higher in time as the variance of wire strength increases. By fixing $S_0 = 1$, the normalized spectral density functions are plotted in Figure 3.11b. As the age of the wires increases, the location of the peak of the spectral density shifts towards zero, while the spread of the spectral density becomes narrower. The corresponding correlation functions and their normalized versions are plotted in Fig-

ures 3.12a and 3.12b, respectively. As the spread of the spectral density becomes narrower, the corresponding effect is that the correlation function decays slower. The correlation functions are guaranteed to decay towards zero due to the presence of the exponential functions in Eq. (3.81).

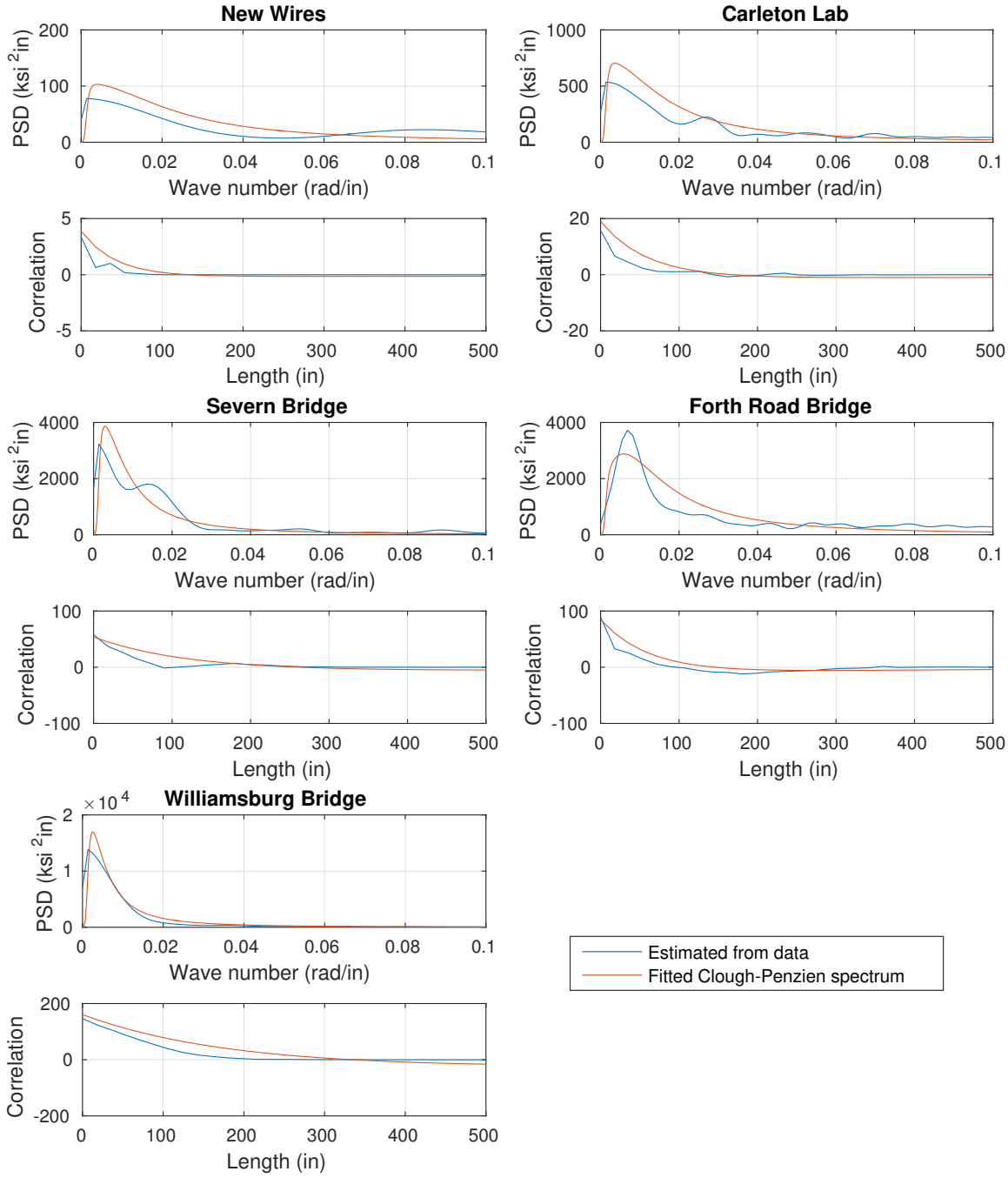

Figure 3.9: Comparison between fitted Clough-Penzien spectrum and correlation with the targets estimated from data.

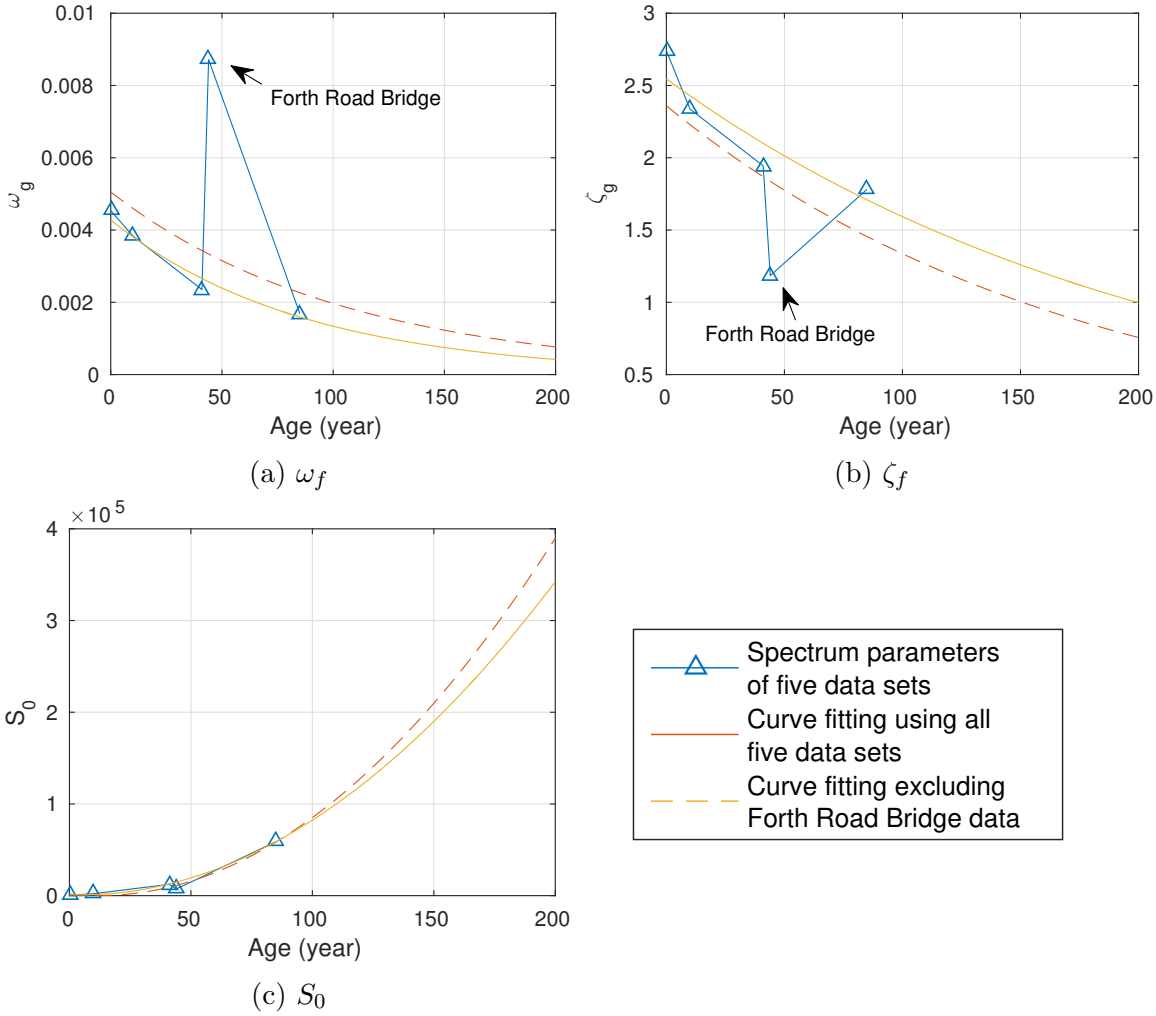

(a) ω_f

(b) ζ_f

(c) S_0

Figure 3.10: Fitting analytical function to time-dependent parameters of Clough-Penzien spectrum.

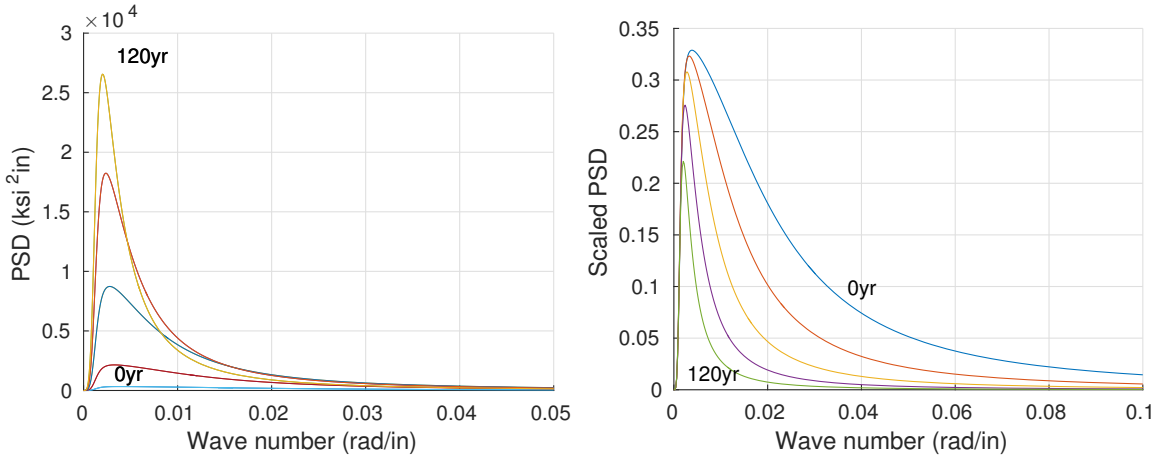

(a) Power spectral density (b) Scaled power spectral density

Figure 3.11: Clough-Penzien spectrum with time-dependent parameters at 0, 30, 60, 90 and 120 years.

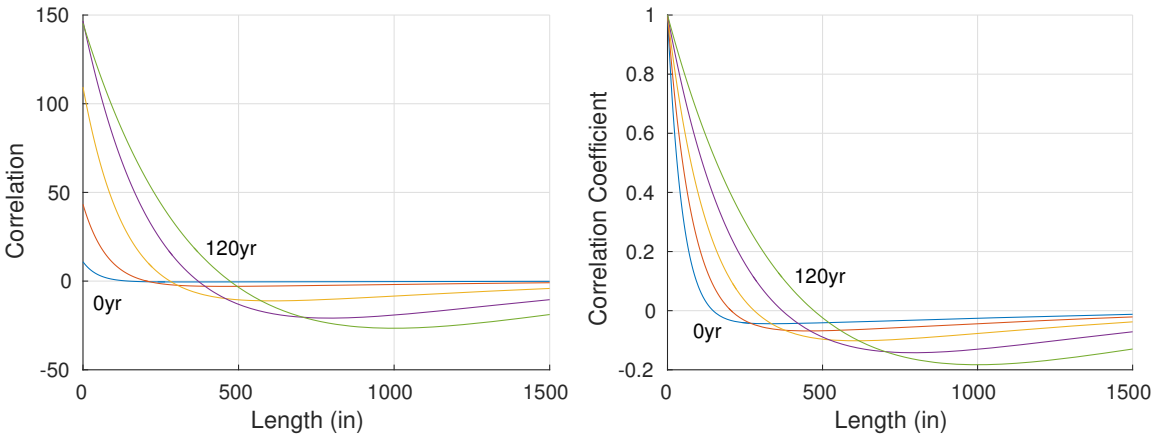

(a) Correlation (b) Scaled correlation coefficient

Figure 3.12: Correlation functions corresponding to Clough-Penzien spectrum with time-dependent parameters at 0, 30, 60, 90 and 120 years.

3.5 Simulation of non-Gaussian process

Using the evolutionary distribution developed in Sec.3.2.7 as the marginal distribution, and the evolutionary spectral density developed in Sec.3.4.6, realizations of random process of wire strength can be generated. With the realizations and a care-

fully selected failure criterion, the failure probability of the suspension bridge cable can be estimated for any given time. This section reviews the simulation method for non-Gaussian random process and discusses the often encountered incompatibility issues.

3.5.1 Simulation by translation process

Simulation of a non-Gaussian process $X(t)$ with prescribed marginal distribution $F_{NG}(x)$ and prescribed spectral density function $S^T_{NG}(\omega)$ (or equivalently, prescribed correlation function $R^T_{NG}(\tau)$) can be achieved by using the translation process theory[Grigoriu, 2002]. It takes the following steps. Let $Y(t)$ be a stationary process with standard Gaussian distribution as its marginal distribution and normalized correlation function $\rho(\tau)$. Realizations of $Y(t)$ are first generated using spectral respresentation method[Deodatis, 1996b]. Then the realizations of $Y(t)$ go through a memoryless mapping $g(\cdot)$ to tranform into realizations of the desired non-Gaussian process $X(t)$:

$$X(t) = g[Y(t)] = F^{-1}_{NG}\{\Phi[Y(t)]\} \tag{3.87}$$

The resulting process $X(t)$ will still be stationary and have $F_{NG}(\cdot)$ as marignal distribution. The correlation function of $Y(t)$ obtained by this transformation can be related to the correlation function $\rho(\tau)$ of the underlying Gaussian process through the following mapping:

$$R_{NG}(\tau) = h(\rho(\tau)) = \int_{-\infty}^{\infty}\int_{-\infty}^{\infty} g(y_1)g(y_2)\phi[y_1, y_2; \rho(\tau)]\,\mathrm{d}y_1\,\mathrm{d}y_2 \tag{3.88}$$

where $\phi(y_1, y_2; \rho(\tau))$ is the joint PDF of bivariate normal distribution with correlation $\rho(\tau)$. In order that the transformation works, the correlation function $\rho(\tau)$ must

be carefully selected such that $R_{NG}(\tau)$ matches the prescribe correlation function $R^T_{NG}(\tau)$.

3.5.2 The incompatibility issue

In most cases a valid correlation function $\rho(\tau)$ of the underlying Gaussian random process $Y(t)$ can be found by solving the inverse problem in Eq. (3.88). However, in some cases there is no solution of $\rho(\tau)$ exists for a given $R^T_{NG}(\tau)$. When this occurs, we say the prescribed correlation function $R_{NG}(\tau)$ is incompatible with the prescribed marginal distribution $F_{NG}(x)$. There are two types of incompatibility issues. The first type arises when given a value of $R_{NG}(\tau)$ the corresponding $\rho(\tau)$ does not exist, or its value is outside of $[-1, 1]$. In some rare cases, although $\rho(\tau)$ exists point-wise for all τ and its values are all within $[-1, 1]$, the second type of incompability issue may arise when $\rho(\tau)$ itself is not positive semi-definite, making it ineligible as an correlation function. Both types of incompatible issues are due to the fact that the marginal distribution $F_{NG}(x)$ and correlation function $R_{NG}(\tau)$ can be prescribed separately and arbitrarily.

Here we claim that *if $R^T_{NG}(\tau)$ conforms with its attainable correlation $[R_*, R^*]$ specified by the marginal CDF $F_{NG}(\cdot)$, and the function $g = F^{-1}_{NG} \circ \Phi$ has two-sided Laplace transformation, then the solution $\rho(\tau)$ to the inverse problem in Eq.* (3.88) *exists.* In other words, the incompatibility issue of the first type will not occur in this case. A sketchy proof is given below.

Suppose $X(t)$ has finite dimensional distribution $F^{(\tau)}_{NG}(x_1, x_2)$, which is parameterized by τ. Then $R_{NG}(\tau)$ can be computed as

$$R_{NG}(\tau) = \int_{-\infty}^{\infty}\int_{-\infty}^{\infty} x_1 x_2 \, \mathrm{d}F^{(\tau)}_{NG}(x_1, x_2) \tag{3.89}$$

By Sklar's theorem it can be rewritten in term of its copula:

$$R_{NG}(\tau) = \int_0^1 \int_0^1 F_{NG}^{-1}(u_1) F_{NG}^{-1}(u_2)\, \mathrm{d}C_{NG}^{(\tau)}(u_1, u_2) \tag{3.90}$$

Again the copula is also parameterized by τ. The attainable correlation R_* and R^* can be found by substituting the copula with its Fréchet-Hoeffding lower and upper bounds given by Eq. (3.48).

$$R_* = \int_0^1 \int_0^1 F_{NG}^{-1}(u_1) F_{NG}^{-1}(u_2)\, \mathrm{d}W(u_1, u_2) \tag{3.91}$$

$$R^* = \int_0^1 \int_0^1 F_{NG}^{-1}(u_1) F_{NG}^{-1}(u_2)\, \mathrm{d}M(u_1, u_2) \tag{3.92}$$

On the other hand, rewriting Eq. (3.88) gives

$$h[\rho(\tau)] = \int_{-\infty}^{\infty} \int_{-\infty}^{\infty} F_{NG}^{-1}[\Phi(y_1)] F_{NG}^{-1}[\Phi(y_2)]\, \mathrm{d}\Phi[y_1, y_2; \rho(\tau)] \tag{3.93}$$

$$= \int_0^1 \int_0^1 F_{NG}^{-1}(u_1) F_{NG}^{-1}(u_2)\, \mathrm{d}C_G^{\rho(\tau)}(u_1, u_2) \tag{3.94}$$

where $C_G^{\rho(\tau)}(u_1, u_2)$ is the Gaussian copula parameterized by $\rho(\tau)$. Since the Gaussian copula achieves Fréchet-Hoeffding lower and upper bounds when $\rho(\tau)$ takes -1 and 1, respectively, by comparing Eq. (3.94) with Eq. (3.92) we see that

$$h(-1) = R_*, \quad h(1) = R^* \tag{3.95}$$

Therefore if h is continuous on $[-1, 1]$, then by Intermediate Value Theorem for any $R \in [R_*, R^*]$ there must exists a $\rho \in [-1, 1]$ such that $h(\rho) = R$. Actually the continuity is implied by the *Price's Theorem*[Price, 1958] which states that if g admits

Laplace transform then the derivative of h is given by

$$\frac{\partial h(\rho)}{\partial \rho} = \mathrm{E}\left[\frac{\partial g(y_1)}{\partial y_1}\frac{\partial g(y_2)}{\partial y_2}\right] \tag{3.96}$$

Furthermore if F_{NG}^{-1} is strictly increasing (e.g. Weibull distsribution) then g is also strictly increasing and hence $\partial h/\partial \rho > 0$. This indicates that $h : [-1, 1] \to [R_*, R^*]$ is one-to-one and it has an inverse function h^{-1} which can be used to find ρ directly for given R_{NG}.

However, so far there is not an effective way to avoid the compatibility issue of the second type. Even if the $R_{NG}(\tau)$ is positive semi-definite and the correponding $\rho(\tau)$ can be found for all τ, $\rho(\tau)$ may not necessarily be positive semi-definite. A iterative method was proposed[Deodatis and Micaletti, 2001b] to remedy this issue by adaptively altering the power spectral density function corresponding to $\rho(\tau)$ such that the correlation function of the realizations simulated by translation process approximates the prescribed target. A mathematically explanation behind such method was given by [Grigoriu, 2009].

3.6 Procedures for estimating reliability by simulation

Due to the restriction imposed by the attainable correlation bounds, the following guidelines are proposed for establishing probability distribution and power spectral density function to a target data set, and eventually estimating the failure probaiblity by simulation. By following this guideline the resulting marginal probability distribution will be compatible with the power spectral density function. Suppose wire strength data is available for different ages.

1. Select the probability distribution according to either log-likelihood, BIC or AIC;

2. Compute attainable correlation bounds imposed by the selected and fitted probability distribution using Eq. (3.59) based on copula theory;

3. Estimate power spectral density function directly from data by Welch method, and compute correlation function using Wiener-Khinchin transform. These two results are called target power spectral density $S^{\mathrm{T}}(\omega)$ and target correlation $R^{\mathrm{T}}(\tau)$, respectively;

4. Select a parameterized function form $S(\omega;\boldsymbol{p})$ for the power spectral density function, which should have enough flexibility for fitting to target PSD, for example, the Clough-Penzien spectrum;

5. Estimate the parameters $\boldsymbol{p}$ of the selected power spectral density function $S^{\mathrm{T}}(\omega)$, by simulaneous minimizing the error between $S(\omega;\boldsymbol{p})$ and $S^{\mathrm{T}}(\omega)$, as well as the error between $R(\tau;\boldsymbol{p})$ and $R^{\mathrm{T}}(\tau)$, where $R(\tau;\boldsymbol{p})$ is the Wiener-Kninchin transformation of $S(\omega;\boldsymbol{p})$;

6. Check if the resulting correlation function $R(\tau;\boldsymbol{p})$ is within attainable correlation bounds, if not, impose penalties in the optimization problem in the previous step.

7. Generate realizations of random process of wire strength, and estimate failure probability using selected failure criterion.

Chapter 4

Stochastic deterioration model of wire strength

4.1 Chapter summary

In this chapter a stochastic deterioration model of wire strength is proposed, based on Ito's stochastic calculus. The goal of the proposed model is to quantitatively study the evolution of the probability distribution of wire strength by studying the deterioration rate.

In the previous chapter the probability distribution functions of wire strength were plotted on Weibull probability papers and it was observed that heavy tails exist on corroded wires for some data sets but not for the other. Besides, some data sets are more skewed or have higher kurtosis than the other, let alone the mean and variance of each data set is different. The proposed stochastic deterioration model aims offer the flexibility to incorporate the various characteristics exhibited by the data sets.

In the proposed model, the deterioration rate of wire strength will be considered as a stochastic process with respect to time under Ito's stochastic calculus, and the wire strength is a function of the deterioration rate. This chapter is organized as the following. First, a simple and heuristic example is used to give the intuition behind such model. Then a brief introduction is given to the fundamentals of Ito calculus, followed by the proposed stochastic deterioration rate model. Lastly, methods are developed for estimating model parameters using wire strength data.

4.2 Overview of proposed model

4.2.1 Need for a probabilistic model

A model that directly captures the nature of deterioration rate of wire strength is of great interest, such that one can estimate the wire strength at any time given the initial wire strength at installation. The actual deterioration rate of wire strength

is highly uncertain, as it is subject to many contributing factors, each of which has inherent uncertainty. For example, factors like temperature, humidity and acid level are subject to weather and climate change; live load on the wire is subject to daily and seasonal change; the quality of installation and protection of wires are subject to human uncertainty. A good model must be capable of incorporating all sources of uncertainties.

However, it is in general very difficult to directly establish the law that the deterioration rate follows due to the following reasons. First, to observe a credible deterioration rate of wire strength, a virtual-reality environment is needed, in which all aforementioned factors can be controlled. An example of such device is the corrosion chamber built in the Carleton Lab at Columbia University[Deeble Sloane *et al.*, 2013], which was used for testing sensors that measure various factors as well as the corrosion rate. Such devices are often costly to build and maintain. Second, the deterioration of wire strength is a very slow process, whose time scale is measured in decades, or even centuries. Although such environmental chamber may accelerate the deterioration process by applying rapid cycles of selected factors, extrapolating the results into long term future, for example 100 years, is prone to error.

To overcome the aforementioned difficulties, a stochastic deterioration model of wire strength is proposed in the chapter. The proposed model has two assumptions, one being the form of the stochastic deterioration rate process, and the other being law of deterioration, i.e., wire strength as a function of deterioration rate. Instead of explicitly modeling the uncertainty in each contributing factor, the proposed model only considers the overall effect. This gives the model an advantage that it can be calibrated using only a single snapshot of the wire conditions. In addition, the model is based on well-established Ito's stochastic calculus, which makes it mathematically tractable. Last but not least, few assumptions about the laws of physics are needed,

yet the model is still flexible enough to match observed data.

4.2.2 Review of gamma process model

Before introducing the proposed model, it must be noted that there is a popular probabilistic model in reliability analysis, called the gamma process model. It is widely used in modeling the process of stochastic deterioration which is monotonically accumulating over time. A comprehensive review of the theoretical background and applications of gamma process model is available in [Nicolai *et al.*, 2007] and in [Frangopol *et al.*, 2004].

The gamma process model was first proposed in [Abdel-Hameed, 1975] to model the life distribution of a device subject to random deterioration. The gamma process model was also applied to modeling deterioration of steel coating [Heutink *et al.*, 2004] [van Noortwijk, 2009]. Especially, in [Nicolai *et al.*, 2007] the author suggested that deterioration models can be categorized into the following three types, which concurs with the arguments in the previous section:

1. Black-box statistical model, which is purely based on descriptive statistics;
2. Gray-box model, which specifically models a measurable quantity related to time-dependent deterioration;
3. White-box model, which explicitly models the physics of deterioration.

The gamma process model and our proposed model are both gray-box models. The main idea is to model the deterioration, measured by either the reduction of strength, or loss of mass or dimension, as a random process in time. And the amount of deterioration accumulated over each time interval is modeled as a random variable.

Recall that a gamma distribution has two parameters, which can be specified in two different ways, either by shape parameter k and scaling factor θ, or by shape parameter α and rate parameter β. In the following context the second flavor is used. A random variable $X \sim \text{Gamma}(\alpha, \beta)$ has the following PDF

$$f_X(x) = \frac{\beta^\alpha}{\Gamma(\alpha)} x^{\alpha-1} e^{-\beta x}, \quad x > 0,\ \alpha > 0,\ \beta > 0. \tag{4.1}$$

By definition, a gamma process $X(t)$ has independent, non-negative increments that follow gamma distribution with an identical shape parameter β. For a non-stationary gamma process, the shape parameter must be a non-decreasing function of time $\alpha(t)$. Therefore $X(t)$ have the following characteristics:

1. $X(0) = 0$;
2. $X(t+\tau) - X(t) \sim \text{Gamma}(\alpha(t+\tau) - \alpha(t), \beta)$;
3. $X(t)$ has independent increments.

Due to the fact that the sum of gamma random variables still follows gamma distribution, these three characteristics result in $X(t) \sim \text{Gamma}(\alpha(t), \beta)$. And the mean and variance of $X(t)$ are given by

$$\text{E}[X(t)] = \frac{\alpha(t)}{\beta} \tag{4.2}$$

$$\text{Var}[X(t)] = \frac{\alpha(t)}{\beta^2} \tag{4.3}$$

A stationary gamma process requires $\alpha(t)$ to be proportional to time t. However, empirical studies show that by allowing gamma process to be non-stationary offers more flexibility on fitting observed data. It was shown that $\alpha(t)$ instead of being

linear in time, it is ofter proportional to a power law:

$$\mathrm{E}[X(t)] = \frac{ct^b}{\beta} \propto t^b, \quad c > 0,\, b > 0 \tag{4.4}$$

According to a few examples summarized in [van Noortwijk, 2009], the constant b varies for different applications. For example, b may take different values between 0 and 2 for degradation of concrete, due to the cause of degradation, e.g., corrosion of reinforcement, sulphate attack, creeping, etc. The parameters can be estimated from observation data either by method of moments or by Bayesian methods.

If a failure criterion is defined as the resistance $R(t) = r_0 - X(t)$ dropping below a critical stress level s, then the distribution time to failure, or lifetime T is given by

$$F_T(t) = \Pr[T \le t] = \Pr[X(t) \ge r_0 - s] \tag{4.5}$$

$$= \int_{r_0-s}^{\infty} f_{X(t)}(x)\,\mathrm{d}x \tag{4.6}$$

$$= \frac{\Gamma[\alpha(t), \beta(r_0 - s)]}{\Gamma(\alpha(t))} \tag{4.7}$$

where $\Gamma(\cdot,\,\cdot)$ and $\Gamma(\cdot)$ are incomplete gamma function and gamma function, respectively. The analytical tractability of the lifetime as well as the time-dependent mean and variance help people in developing theories in optimal maintenance and lifetime management, as well as inspection schedules.

4.2.3 The proposed model

The proposed model consists of two parts. The first part is the stochastic deterioration rate model. The deterioration rate is treated as a stochastic process in time, which is developed under Ito's stochastic calculus framework. This gives the proposed model a rigorous mathematical foundation. Compared to the gamma process

model, the proposed model is no longer solely based on descriptive statistics. Instead, we seek to explore the essential physics that governs the wire strength deterioration process. As we may see later the fact that the deterioration rate following a gamma distribution becomes a natural conclusion under certain intuitive assumptions about the deterioration rate process.

The second part is the deterioration of wire strength as a function of deterioration rate. Both state-independent model and state-dependent model are proposed. In the state-independent model the reduction of wire strength is simply the cumulation of deterioration rate, while in the state-dependent model the reduction of wire strength may also depend on the wire strength itself. The intuition is that corroded may be prone to further corrosion. The state-dependent model has more flexibility in matching tails of the wire strength distribution.

4.3 Basics of stochastic calculus

This section gives a brief introduction to Ito's stochastic calculus, based on which the proposed stochastic deterioration model is developed. Note that the stochastic processes discussed in this chapter are indexed by time.

4.3.1 Wiener process and Ito integral

The most fundamental stochatic process is the Wiener process, also know as the Brownian motion. It is often used as a building block of other stochastic processes. A stochastic process $W(t)$ is a Wiener process if it satisfies the following conditions:

1. $W(0) = 0$;

2. $W(t)$ has independent increments;

3. Each increment follows Gaussian distribution:

$$W(t) - W(s) \sim N(0, t-s) \tag{4.8}$$

4. $W(t)$ is continuous.

Consider an increment $\Delta W(t) = W(t) - W(s)$ from s to t, $s < t$. One of the most important findings of Ito's calculus is that when pushing $\Delta t \to 0$, formally we can write

$$[\,\mathrm{d}W(t)]^2 = \mathrm{d}t \tag{4.9}$$

as if the square of an increment of $W(t)$ over an infinitesimal time $\mathrm{d}t$ become "deterministic", and its magnitude is comparable with $\mathrm{d}t$. A rigorous proof can be referred to [Øksendal, 2003], but intuitively, consider the following. Due to the above properties, $\Delta W(t)$ follows Gaussian distribution with zero mean and variance Δt. Therefore we have

$$\mathrm{E}[\Delta W] = 0 \tag{4.10}$$

$$\mathrm{E}[(\Delta W)^2] = \Delta t \tag{4.11}$$

$$\mathrm{Var}[(\Delta W)^2] = 2(\Delta t)^2 \tag{4.12}$$

As $\Delta t \to 0$ the variance of $\Delta W(t)$ is of higher order than the mean, making its randomness is negligible.

Now consider a stochastic process $X(t)$ which satisfies the following difference equation:

$$X(t+\Delta t) - X(t) = \mu(t, X(t))\Delta t + \sigma(t, X(t))\Delta W(t) \tag{4.13}$$

Then $X(t)$ has a locally deterministic drift $\mu(t, X(t))$ and a Gaussian random fluc-

tuation term $\Delta W(t)$ which is amplified by the diffusion coefficient $\sigma(t, X(t))$. In the follow context $\mu(t, X(t))$ and $\sigma(t, X(t))$ are also denoted as μ and σ, respectively, for convenience. Besides, $X(t)$ is sometimes also denoted as X_t, and the two notations are interchangeable.

Pushing $\Delta t \to 0$ in Eq. (4.13) yields the canonical form of the stochastic differential equation that $X(t)$ follows

$$\mathrm{d}X_t = \mu(t, X_t)\,\mathrm{d}t + \sigma(t, X_t)\,\mathrm{d}W_t \tag{4.14}$$

$$X(0) = x_0 \tag{4.15}$$

whose solution is given by

$$X_t = x_0 + \int_0^t \mu(s, X_s)\,\mathrm{d}s + \int_0^t \sigma(s, X_s)\,\mathrm{d}X_s \tag{4.16}$$

Note that the second term can be evaluated using Riemann-Stieltjes integral, but the third term cannot. In Ito calculus the third term is defined as an *Ito integral* of the form

$$\int_a^b g(s)\,\mathrm{d}W_s \tag{4.17}$$

in which $g(s)$ is a process satisfying the following conditions:

1. $\int_0^t \mathrm{E}[g^2(s)]\,\mathrm{d}s < \infty$
2. $g(s)$ is $\mathcal{F}_t^W$-adapted

Note that a process $g(s)$ being $\mathcal{F}_t^W$-adapted means when given the a trajectory of $W(s)$ on $[0, t]$ then the trajectory of $g(s)$ is also known up to t. Clearly $W(t)$ is

$\mathcal{F}_t^W$-adapted, and therefore we have

$$\mathrm{E}[W(t)|\mathcal{F}(t)] = W(t) \tag{4.18}$$

where $W(t)$ is a known quantity since $\mathcal{F}(t)$ contains information of it. Refer to [Björk, 2009] for more rigorous definitions and further details. For an Ito integral, the following also holds:

$$\mathrm{E}\left[\int_0^t g(s)\,\mathrm{d}W_s\right] = 0 \tag{4.19}$$

$$\mathrm{E}\left[\left(\int_0^t g(s)\,\mathrm{d}W_s\right)^2\right] = \int_0^t \mathrm{E}\left[g^2(s)\right]\,\mathrm{d}s. \quad (\textbf{Ito isometry}) \tag{4.20}$$

Eq. (4.19) indicates that the Ito integral is a *martingale*, whose definition will be given in the next section.

4.3.2 Martingale and Markov property

By definition, a $\mathcal{F}(t)$-adapted stochastic process $X(t)$ is called a *martingale* if

$$\mathrm{E}[X(t)|\mathcal{F}(s)] = X(s), \text{ for } 0 \le s \le t \tag{4.21}$$

This indicates that $X(t)$ has no drift, and therefore maintains a constant mean. Actually, letting the drift term $\mu(t, X_t) = 0$ makes $X(t)$ defined in Eq. (4.14) a martingale.

More generally, a stochastic process $X(t)$ is a *Markov process* if for all non-negative function f, there exists another function g such that

$$\mathrm{E}[f(X(t))|\mathcal{F}(s)] = g(X(s)), \text{ for } 0 \le s \le t \tag{4.22}$$

For a Markov process $X(t)$, we may define its transitional probability $p(s, y; t, x)$[1], and then g can then be written as a functional of p:

$$g(y) = \int_{-\infty}^{\infty} f(x)p(s, y; t, x)\,\mathrm{d}x \tag{4.23}$$

In later sections the Markov property is particularly useful for numerically generating paths of a stochastic process.

Example 4.3.1. Consider a standard Brownian motion $W(t)$, then $W(t)$ is a martingale since for $0 \leq s \leq t$ we have

$$\begin{aligned} \mathrm{E}[W(t)|\mathcal{F}(s)] &= \mathrm{E}[W(t) - W(s)|\mathcal{F}(s)] + E[W(s)|\mathcal{F}(s)] \\ &= W(s) \end{aligned} \tag{4.24}$$

where the increment $W(t) - W(s)$ has zero mean and $W(s)$ is known given $\mathcal{F}(s)$. Furthermore, $W(t)$ is also a Markov process. To see this, for a given non-negative function f, we have

$$\mathrm{E}[f(W(t))|\mathcal{F}(s)] = \mathrm{E}[f([W(t) - W(s)] + W(s)]|\mathcal{F}(s)] \tag{4.25}$$

where $W(s)$ is a known quantity while $W(t) - W(s) \sim N(0, t - s)$. Therefore the transitional probability is given by

$$p(s, y; t, x) = \frac{1}{\sqrt{2\pi(t-s)}} e^{-\frac{(x-y)^2}{2(t-s)}} \tag{4.26}$$

[1] $p(s, y; t, x)$ reads the joint probability density of $X(s) = y$, and $X(t) = x$.

And we find such function g that satisfies the Markov property as

$$g(y) = \int_{-\infty}^{\infty} f(x) \frac{1}{\sqrt{2\pi(t-s)}} e^{-\frac{(x-y)^2}{2(t-s)}} \, \mathrm{d}x \tag{4.27}$$

4.3.3 Ito's lemma

Suppose process $X(t)$ satisfies the stochastic differential equation given by

$$\mathrm{d}X_t = \mu \, \mathrm{d}t + \sigma \, \mathrm{d}W_t \tag{4.28}$$

Consider a function $f(t, X_t)$, then *Ito's Lemma* states that f has a stochastic differential given by

$$\mathrm{d}f(t, X_t) = \frac{\partial f}{\partial t} \, \mathrm{d}t + \frac{\partial f}{\partial x} \, \mathrm{d}X_t + \frac{1}{2} \frac{\partial^2 f}{\partial x^2} \, (\, \mathrm{d}X_t)^2 \tag{4.29}$$

Or substituting Eq. (4.28) into Eq. (4.29) yields

$$\mathrm{d}f(t, X_t) = \left(\frac{\partial f}{\partial t} + \mu \frac{\partial f}{\partial x} + \frac{1}{2} \sigma^2 \frac{\partial^2 f}{\partial x^2} \right) \, \mathrm{d}t + \sigma \frac{\partial f}{\partial x} \, \mathrm{d}W_t \tag{4.30}$$

where we used the following implications

$$\mathrm{d}t \cdot \mathrm{d}W_t = 0 \tag{4.31}$$

$$(\, \mathrm{d}t)^2 = 0 \tag{4.32}$$

$$(\, \mathrm{d}W_t)^2 = \, \mathrm{d}t \tag{4.33}$$

Again, a rigorous proof can be found in [Øksendal, 2003]. Ito's Lemma serves as the counterpart of the chain rule in stochastic calculus.

4.3.4 Kolmogorov forward and backward equations

In Eq. (4.30) we notice that if we make the drift term equals zero then $f(t, X_t)$ is effectively a martingale, where we have

$$F(t,x) = \mathrm{E}_{t,x}[F(T, X_T)], \quad \forall (t,x), \text{ and } t \leq T \tag{4.34}$$

The subscripts of the expectation operator means X_t is equal to x at time t. If we know that at time $T \geq t$, $F(T, X_T) = \Phi(X_T)$ where $\Phi(X_T)$ is a deterministic function of X_T, then putting together we reach the *Kolmogorov backward equation*:

$$\frac{\partial F}{\partial t} + \mu(t,x)\frac{\partial F}{\partial x} + \frac{1}{2}\sigma^2(t,x)\frac{\partial^2 F}{\partial x^2} = 0 \tag{4.35}$$

$$F(T,x) = \Phi(x) \tag{4.36}$$

This result is known as the *Feynman-Kac Theorem*. As a special case, if we let $\Phi(X_T) = I_B(X_T)$, which is an indicator function over a set B, and let

$$P(s,y) = \mathrm{E}_{s,y}[I_B(X_T)] = P(X_T \in B | X_s = y) \tag{4.37}$$

In this case $P(s, y; T, B)$ is the transitional probability of X_t starting from a point $X_s = y$ and ends up in a set B at time T. By Feynman-Kac we can immediately write down the PDE that $P(s, y)$ follows, and this PDE is usually known Kolmogorov backward equation

$$\frac{\partial P}{\partial s} + \mu(s,y)\frac{\partial P}{\partial y} + \frac{1}{2}\sigma^2(s,y)\frac{\partial^2 P}{\partial y^2} = 0 \tag{4.38}$$

$$P(T, y; T, B) = I_B(y) \tag{4.39}$$

As a result the density function $p(s, y; t, x)$ of the probability measure $P(s, y; t, \mathrm{d}x)$ follows another form of the Kolmogorov backward equation

$$\frac{\partial p}{\partial s} + \mu(s, y)\frac{\partial p}{\partial y} + \frac{1}{2}\sigma^2(s, y)\frac{\partial^2 p}{\partial y^2} = 0 \tag{4.40}$$

$$p(s, y; t, x) \to \delta_x, \text{ as } s \to t \tag{4.41}$$

These two equations are called "backwards" as they must be solved backwards in time, i.e., from t to s if $s \leq t$. This is because the diffusion term has the same sign as the time differential term. Kolmogorov backward equation tells us that for a stochastic process X_s starting with arbitrarily given (s, y), the probability that it reaches a certain position at time $t \geq s$.

In the contrast, there is Kolmogorov forward equation for the density of transitional probability.

$$\frac{\partial}{\partial t}p(s, y; t, x) = -\frac{\partial}{\partial x}[\mu(t, x)p(t, x)] + \frac{1}{2}\frac{\partial^2}{\partial x^2}[\sigma^2(t, x)p(t, x)] \tag{4.42}$$

$$p(s, y; t, x) \to \delta_y, \text{ as } s \downarrow t \tag{4.43}$$

The Fokker-Planck equation can also be extended to multi-dimensional cases to depict the joint distribution of a d-dimensional vector-valued stochastic process $\boldsymbol{X}_t$, whose dynamics is given by

$$\mathrm{d}\boldsymbol{X}_t = \boldsymbol{\mu}(t, \boldsymbol{X}_t)\,\mathrm{d}t + \boldsymbol{\sigma}(t, \boldsymbol{X}_t)\,\mathrm{d}W_t \tag{4.44}$$

where $\boldsymbol{X}_t$ and $\boldsymbol{\mu}(t, \boldsymbol{X}_t)$ are d-dimensional random vectors, $\boldsymbol{\sigma}(t, \boldsymbol{X}_t)$ is a $d \times n$ matrix and $\boldsymbol{W}_t$ is an n-dimensional standard Wiener process whose components are independent of each other. We can further define the covariance matrix, also known as the

diffusion tensor $\boldsymbol{D}$ of $\boldsymbol{X}_t$, which is a $d \times d$ matrix given by

$$[\boldsymbol{D}(t, \boldsymbol{x})]_{d\times d} = \boldsymbol{\sigma}(t, \boldsymbol{x})\boldsymbol{\sigma}(t, \boldsymbol{x})^{\boldsymbol{T}} \tag{4.45}$$

with each components given by

$$D_{ij}(t, \boldsymbol{x}) = \sum_{i=1}^{n} \sigma_{i,k}(t, \boldsymbol{x})\sigma_{j,k}(t, \boldsymbol{x}) \tag{4.46}$$

Then the joint probability density function $p(t, X_t)$ follows the multi-dimensional Fokker-Planck equation:

$$\frac{\partial p(t, \boldsymbol{x})}{\partial t} = -\sum_{i=1}^{d} \frac{\partial}{\partial x_i}[\mu_i(t, \boldsymbol{x})p(t, \boldsymbol{x})] + \frac{1}{2}\sum_{i,j=1}^{d} \frac{\partial^2}{\partial x_i \partial x_j}[D_{ij}(t, \boldsymbol{x})p(t, \boldsymbol{x})] \tag{4.47}$$

The the solution of Fokker-Planck equation of often defined on the entire $\mathbb{R}^d$. In order that $p(s, y; t, x)$ be a legitimate probability density function, it must satisfy the following boundary conditions[Grigoriu, 2002]:

$$\lim_{x_i\to\pm\infty} \mu_i(t, \boldsymbol{x})p(t, x) = 0, \quad i = 1, \ldots, d, \tag{4.48}$$

$$\lim_{x_i\to\pm\infty} D_{ij}(t, \boldsymbol{x})p(t, \boldsymbol{x}) = 0, \quad i, j = 1, \ldots, d, \tag{4.49}$$

$$\lim_{x_i\to\pm\infty} \frac{\partial^2}{\partial x_i \partial x_j}[D_{ij}(t, \boldsymbol{x})p(t, \boldsymbol{x})] = 0, \quad i, j = 1, \ldots, d. \tag{4.50}$$

4.3.5 Numerical solution to SDE

In this section three widely used numerical schemes for solving SDE's are introduced. In other words, these methods can be used as an essential part of Monte Carlo simulation for generating paths of SDE's . Consider a SDE in canonical form as Eq. (4.14), with initial condition $X(0) = 0$. Suppose the solution on the interval $[0, T]$ is of

interest. The first step of all three schemes is to partition the interval into n equal size subintervals as

$$0 = t_0 < t_1 < \ldots < t_n = T \tag{4.51}$$

with the size of each interval being $\Delta t = T/n$. Let X_k denotes the value of the stochastic process X_t at time t_k. The performance of a scheme is measured by the strong order of convergence γ. A scheme is of strong order γ if for any $t_k > 0$ there exist constants $\delta > 0$ and $C > 0$ such that as the partition refines we have

$$\mathrm{E}[X_k - X_{t_k}] \leq C\Delta t^{\gamma}, \quad \forall \Delta t < \delta \tag{4.52}$$

The three schemes are all recursive schemes, which are summarized as the following:

1. *Euler-Maruyama scheme.* This scheme is also known as the Euler scheme. It is a simple generalization of Euler method of ordinary differential equations to SDE's. The recursive formula is given by

$$X_{k+1} = X_k + \mu(t_k, X_k)\Delta t + \sigma(t_k, X_k)\Delta W_k \tag{4.53}$$

   where $\Delta W_k = W_{k+1} - W_k$, $k = 0, 1, \ldots, n$ are independent increments of a Wiener process, and thus $\Delta W_k \sim i.i.d.N(0, \Delta t)$. Apparently the Euler scheme is an explicit scheme. The Euler scheme has strong convergence order of $1/2$.

2. *Milstein scheme.* The Milstein scheme has an additional term compared to the Euler scheme, which serves a correction term for the discretization error so as

to achieve a higher accuracy. The recursive formula is given by

$$X_{k+1} = X_k + \mu(t_k, X_k)\Delta t + \sigma(t_k, X_k)\Delta W_k + \frac{1}{2}\sigma(t_k, X_t)\sigma_x(t, X_t)\left[(\Delta W_k)^2 - \Delta t\right] \tag{4.54}$$

where $\sigma_x(t, x)$ is the partial derivative of σ with respect to x. The Milstein scheme has strong convergence order of 1, which is better than the Euler scheme. If σ does not depend on X_t then the Milstein scheme is the same as Euler scheme, and this is a special case where the Euler scheme achieves convergence of 1. It is worth mentioning that one may further push the Milstein scheme to second order convergence by taking the second order partial derivative σ_{xx} into account.

3. *Exact transitional probability method.* For some special stochastic processes whose transitional probability is readily available in analytical form, one may use a random number generator to draw a sample of the next step X_{k+1} given the previous step X_k. This may be consider as an exact schemes, whose performance is mainly determined by the quality of the random number generated. However, in practice its performance is also impacted by the partition size Δ.

By using schemes, one may find the probability distribution of X_t at any given time $t > 0$ by Monte Carlo simulation. Alternatively, such probability distribution can also be found by solving the Fokker-Planck equation, which is discussed in the next section.

4.3.6 Numerical solution Fokker-Planck equation

In general it is very difficult to find analytical solution to Fokker-Planck equation, unless the coefficients are all constants. In PDE theory, the Fokker-Planck equation is

an advection-diffusion equation, or more generally a second-order parabolic equation. The numerical solution is sought on a bounded domain $\Omega \subset \mathbb{R}^d$, with initial condition $X_0 \in \Omega$ and appropriate boundary conditions. These boundary conditions are set up based on conservation of probability mass. First we re-write Eq. (4.47) in vector form

$$\frac{\partial p}{\partial t} = -\nabla \cdot [\boldsymbol{\mu} p] + \frac{1}{2}\nabla \cdot [\nabla(\boldsymbol{D} p)] \tag{4.55}$$

Note the here $\boldsymbol{D}$ is a second order tensor. Then it can be further written as the following two equations:

$$\frac{\partial p}{\partial t} = -\nabla \cdot \boldsymbol{\lambda}(t, \boldsymbol{x}), \tag{4.56}$$

$$\boldsymbol{\lambda}(t, \boldsymbol{x}) = \boldsymbol{\mu} p - \frac{1}{2}\nabla(\boldsymbol{D} p) \tag{4.57}$$

where $\boldsymbol{\lambda}(t, \boldsymbol{x}) \in \mathbb{R}^d$ is the probability current. As we shrink the original unbounded domain $\mathbb{R}^d$ into a bounded domain Ω, the probability current is of great importance as the conservation of probability is defined in term of this quantity. Let

$$P_\Omega(t) = \int_\Omega p(t, \boldsymbol{x}) \, \mathrm{d}\Omega \tag{4.58}$$

be the probability that $X_t \in \Omega$ at time t. Then the rate of $P_\Omega(t)$ changes over time is given by

$$\frac{\partial P_\Omega}{\partial t} = \int_\Omega \frac{\partial p(t, \boldsymbol{x})}{\partial t} \, \mathrm{d}\Omega \tag{4.59}$$

Substituting Eq. (4.56) into the above equation and apply divergence theorem gives

$$\begin{aligned}\frac{\partial P_\Omega}{\partial t} &= -\int_\Omega \nabla \cdot \boldsymbol{\lambda}(t,\boldsymbol{x})\,\mathrm{d}\Omega \\ &= -\oint_{\partial\Omega} \boldsymbol{\lambda}(t,\boldsymbol{x})\cdot\boldsymbol{n}\,\mathrm{d}s, \quad \text{(divergence theorem)}\end{aligned} \tag{4.60}$$

where $\boldsymbol{n}(\boldsymbol{x})$ is the unit normal vector at $\boldsymbol{x}$ on the boundary. This gives the local conservation law of probability over the domain Ω, which states that change of total probability over Ω is equal to the probability current flowing in or out on the boundary $\partial\Omega$. The boundary conditions that may be used in our applications are of the following three types:

1. *Reflecting boundary*, where the probability flow must not cross the boundary, and thus the probability current along the normal direction is zero:

$$\boldsymbol{n}\cdot\boldsymbol{\lambda}(t,\boldsymbol{x}) = 0 \tag{4.61}$$

2. *Absorbing boundary*, where any probability flow hitting this boundary must vanish, i.e., the probability becomes zero on this boundary:

$$p(t,x) = 0 \tag{4.62}$$

3. *Continuity boundary*, where the probability flow moves freely across the boundary. Thus the probability density and the probability current are both continuous on this boundary:

$$\boldsymbol{n}\cdot\boldsymbol{\lambda}(t,\boldsymbol{x})|_{\partial\Omega^+} = \boldsymbol{n}\cdot\boldsymbol{\lambda}(t,\boldsymbol{x})|_{\partial\Omega^-} \tag{4.63}$$

$$p(t,\boldsymbol{x})|_{\partial\Omega^+} = p(t,\boldsymbol{x})|_{\partial\Omega^-} \tag{4.64}$$

where the superscripts $\pm$ on $\partial\Omega$ indicates both sides of the boundary.

Once the boundary conditions are fixed, numerical solution to the Fokker-Planck equation can be obtained by finite difference method or finite element method.

4.4 Stochastic deterioration rate model

4.4.1 Desired properties

A novel stochastic deterioration rate model is proposed in this section. The desired properties of a stochastic model on the deterioration rate include the following:

1. Steady mean, or in other words, mean-reversion;
2. Fluctuation with constant or time-dependent variance;
3. Non-negative, since the wire strength will not automatically recover;
4. Stationary distribution in the long term, since the deterioration process of material is an intrinsic process.

As we will see later in this section, a special kind of stochastic process named the squared-root process possesses all these properties, and is therefore chosen to model the deterioration rate.

4.4.2 Simple mean-reversion process

We first consider simple a mean-reversion stochastic process for the deterioration rate, which is the Ornstein-Uhlenbeck process (O-U process). Denote the deterioration rate as r_t, then it satisfies the following SDE:

$$\mathrm{d}r_t = b(a - r_t)\,\mathrm{d}t + \sigma\,\mathrm{d}W_t \tag{4.65}$$

where W_t is a standard Brownian motion, a, b and σ are assumed to be constant throughout the following discussion, although they may be generalized to be functions of time. Such process is mean-reversion due the form of it drift term: when r_t is below a the drift is positive which drives r_t up, and vice versa. The O-U process is widely used in engineering and social science due a few nice properties that it possesses. First of all it is simple enough to have an analytical solution, which is given by

$$r_t = r_0 e^{-bt} + a(1 - e^{-bt}) + \sigma e^{-bt} \int_0^t e^{bu} \, \mathrm{d}W_u \tag{4.66}$$

The validity of this solution can be easily verified by applying Ito's lemma on it. From this solution we know that the random variable r_t follows a normal distribution for all $t > 0$, with mean and variance which can be obtained as

$$\begin{aligned} \mathrm{E}[r_t] &= \mathrm{E}\left[r_0 e^{-bt} + a(1 - e^{-bt})\right] + \mathrm{E}\left[\sigma \int_0^t e^{-b(t-u)} \, \mathrm{d}W_u\right] \\ &= r_0 e^{-bt} + a(1 - e^{-bt}) \end{aligned} \tag{4.67}$$

and

$$\begin{aligned} \mathrm{Var}[r_t] &= \mathrm{Var}\left[\sigma \int_0^t e^{-b(t-u)} \, \mathrm{d}W_u\right] \\ &= \sigma^2 \int_0^t \left[e^{-b(t-u)}\right]^2 \mathrm{d}u, \quad \text{(Ito isometry)} \\ &= \frac{\sigma^2}{2b}(1 - e^{-2bt}) \end{aligned} \tag{4.68}$$

Apparently both mean and variance have transient terms e^{-bt} which will be dampened out as t becomes large (with $b > 0$). Therefore the mean and variance converges to constants a and $\frac{\sigma^2}{2b}$, respectively, regardless of the starting point r_0. Asymptotically r_t admits a stationary normal distribution $N(a, \frac{\sigma^2}{2b})$. And the speed that r_t converges

to its equilibrium state is controlled by b.

A major disadvantage of the O-U process based model is that it may take negative value due to its Gaussianity. However, if normal distribution fits observed deterioration rate well and it standard deviation is very small compared to it mean, the O-U process may still be considered as a handy approximation.

4.4.3 Square-root process

A slight variation can be introduced to the O-U process to overcome its disadvantage that it may take negative value. The resulting stochastic process is known as the squared-root process, which satisfies the following SDE:

$$\mathrm{d}r_t = b(a - r_t)\,\mathrm{d}t + \sqrt{r_t}\sigma\,\mathrm{d}W_t, a, b > 0 \tag{4.69}$$

It is named from the presence of the squared-root term $\sqrt{r_t}$, but it is actually derived from the square of an O-U process[2]. The solution to the SDE Eq. (4.69) of the squared-root process is given by

$$r_t = a + (r_0 - a)e^{-bt} + \sigma e^{-bt}\int_0^t e^{bu}\sqrt{r_u}\,\mathrm{d}W_u \tag{4.72}$$

---

[2]Let q_t be an O-U process of the form as in Eq. (4.65), but with zero mean, i.e., $a = 0$. And let

$$r_t = q_t^2 \tag{4.70}$$

Applying Ito's lemma yields

$$\begin{aligned}\mathrm{d}r_t &= 0\cdot\,\mathrm{d}t + 2q_t(\,\mathrm{d}q_t) + \frac{1}{2}\cdot 2\cdot(\,\mathrm{d}q_t)^2\\ &= 2q_t(-bq_t\,\mathrm{d}t + \sigma\,\mathrm{d}W_t) + \sigma^2\,\mathrm{d}t\\ &= (\sigma^2 - 2bq_t^2)\,\mathrm{d}t + 2q_t\sigma\,\mathrm{d}W_t\\ &= (\sigma^2 - 2br_t)\,\mathrm{d}t + 2\sqrt{r_t}\sigma\,\mathrm{d}W_t\end{aligned} \tag{4.71}$$

which is of the form as Eq. (4.69) after matching the constant terms.

The mean of the squared-root process can be easily obtained as

$$\mathrm{E}[r_t] = r_0 e^{-bt} + a(1 - e^{-bt}) \tag{4.73}$$

Then, to obtain the variance it is not straight-forward, but still doable:

$$\begin{aligned}
\mathrm{Var}[r_t] &= \mathrm{E}\left[\left(\sigma e^{-bt}\int_0^t e^{bu}\sqrt{r_u}\,\mathrm{d}W_u\right)^2\right] \\
&= \sigma^2 e^{-2bt}\mathrm{E}\left[\int_0^t e^{2bu} r_u\,\mathrm{d}u\right], \quad \text{(Ito isometry)} \\
&= \sigma^2 e^{-2bt}\int_0^t e^{2bu}\mathrm{E}[r_u]\,\mathrm{d}u, \quad \text{(Stochastic Fubini)}
\end{aligned} \tag{4.74}$$

Substituting Eq. (4.73) into Eq. (4.74) finally yields

$$\mathrm{Var}[r_t] = r_0\frac{\sigma^2}{b}(e^{-bt} - e^{-2bt}) + \frac{a\sigma^2}{2b}(1 - e^{-bt}) \tag{4.75}$$

As we may see that the mean and variance of the squared-root process also converges to constants a and $\frac{a\sigma^2}{2b}$, respectively. The squared-root process not only preserves the mean-reversion feature since it contains the same drift term as the O-U process, but also ensures its value stays strictly positive as long as the *Feller's condition*

$$2ab > \sigma^2 \tag{4.76}$$

is met and $r_0 > 0$. If the Feller's is not met, the squared-root process is non-negative, and it may be zero occasionally.

The Feller's condition can be concluded by imposing an absorbing condition on the left boundary of the Fokker-Planck equation of the probability density function of r_t. Intuitively we may consider that this feature is attributed to the volatility being

modulated by the square-root of the rate itself. As a result, whenever r_t approaches zero, the stochastic part is weakened while the drift drives r_t back towards the mean.

4.4.3.1 Distribution of deterioration rate

Let $p(t, r_t) = p(0, r_0; t, r_t)$ be the probability density function of r_t at any future time t, given that r_t starts from r_0 at $t = 0$. Then $p(t, r_t)$ satisfies the Fokker-Planck equation:

$$\frac{\partial}{\partial t}p(t, r_t) = -\frac{\partial}{\partial r_t}\left[b(a - r_t)p(t, r_t)\right] + \frac{1}{2}\frac{\partial^2}{\partial r_t^2}[\sigma^2 r_t p(t, r_t)] \tag{4.77}$$

$$p(0, x) = \delta(x - r_0) \tag{4.78}$$

This PDE has an exact analytical solution [Albanese and Campolieti, 2006] given by

$$p(t, r_t) = ce^{-u-v}\left(\frac{v}{u}\right)^{q/2} - I_q(2\sqrt{uv}) \tag{4.79}$$

where $c = \frac{2b}{(1-e^{-bt})\sigma^2}$, $q = \frac{2ab}{\sigma^2} - 1$, $u = cr_0e^{-bt}$, $v = cr_t$, and $I_q(\cdot)$ is the modified Bessel function of the first kind of order q. Actually for a fixed time t, the random variable r_t can be written as

$$r_t = \frac{Y}{2c} \tag{4.80}$$

where Y is a random variable of non-central Chi-squared distribution with $\frac{4ab}{\sigma^2}$ degree of freedom and non-centrality parameter $2cr_0e^{-bt}$.

In the long run as $t \to \infty$ the squared-root process follows a stationary distribution, and the probability density function for r_∞ can be solved for from the above Fokker-Planck equation by letting $\frac{\partial p}{\partial t} = 0$. The stationary distribution turns out to

be a gamma distribution whose probability density function is given by

$$p(r_\infty) = \frac{\omega^\nu}{\Gamma(\nu)} r_\infty^{\nu-1} e^{-\omega r_\infty} \tag{4.81}$$

where $\omega = \frac{2b}{\sigma^2}$ and $\nu = \frac{2ab}{\sigma^2}$. The speed that the distribution of r_t converges to gamma distribution is again controlled by parameter b, which appears in the exponential decaying term. This property makes the squared-root process suitable for modeling the deterioration rate. Moreover, compared to the conventional gamma process model, the squared-root process offers more flexibility for fitting to real data as it takes into account the transition of from an observed initial deterioration rate towards a gamma distribution. Significantly, after the process reaches its stationary state, the autocorrelation function is given by [Tankov, 2003]

$$\rho(\tau) = e^{-b\tau} \tag{4.82}$$

This equation as well as Eq. (4.79) indicates that increment of r_t may depend on its state, while r_t itself follows a gamma distribution. This is a major difference between the squared-root process and the traditional gamma process model.

Example 4.4.1. Consider a squared-root process with ultimate mean $a = 0.5$, convergence speed parameter $b = 0.15$, and volatility $\sigma = 0.1$. This example illustrates the convergence of the distribution of a squared-root process towards its stationary distribution – gamma distribution, with different starting point $r_0 = 0.3$ in Fig. 4.1a and $r_0 = a = 0.5$ in Fig. 4.1b. Apparently besides parameter b, the starting point of the squared-root process r_0 also has impact on the time needed for convergence. By comparing the two figures, it is clear that the closer the starting point is to the mean a, the quicker the process converges.

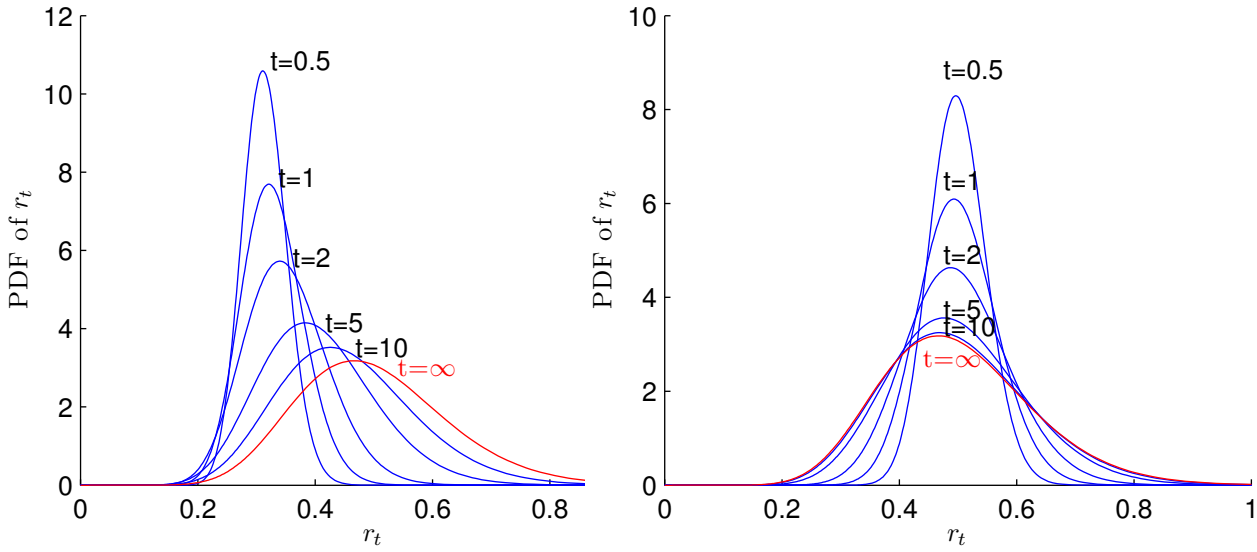

(a) $r_0 = 0.3, a = 0.5$ (b) $r_0 = a = 0.5$

Figure 4.1: Convergence of probability distribution of squared-root process towards its stationary distribution.

In the rest of this chapter we will focus on using the squared-root process for modeling the deterioration rate of wire strength.

4.4.3.2 Simulation of squared-root process

To simulate a path of a squared-root process, one may apply the numerical discretization schemes, e.g., the Euler scheme as in Eq. (4.53), or the Milstein scheme as in Eq. (4.54). Besides, since the transitional probability distribution of squared-process is available in analytical form in Eq. (4.79), one may also apply the exact transitional probability method. Specifically, to simulate paths of a squared-root process, the detailed procedures are summarized as the following. Suppose the time interval Δt is fixed.

1. *Euler method.* Combining the definition of squared-root process in Eq. (4.69)

and the Euler scheme in Eq. (4.53) gives the following recursive equation:

$$r_{k+1} = r_k + b(a - r_k)\Delta t + \sigma\sqrt{r_k}\Delta W_k \tag{4.83}$$

where $\Delta W_k \sim (0, \Delta t)$. A realization of r_{k+1} is obtained by generating a random number of ΔW_k.

2. *Milstein method.* The Milstein method contains the partial derivative of the volatility coefficient with respect to the state variable. For squared-root process, its volatility coefficient is $\sigma\sqrt{r_t}$, in which σ is a constant, and taking partial derivative of this term gives $\frac{\sigma}{2\sqrt{r_t}}$. Finally, combining Eq. (4.69) and Eq. (4.54) gives the recursive equation:

$$r_{k+1} = r_k + b(a - r_k)\Delta t + \sigma\sqrt{r_k}\Delta W_k + \frac{1}{2}\sigma^2[(\Delta W_k)^2 - \Delta t] \tag{4.84}$$

where $\Delta W_k \sim (0, \Delta t)$. A realization of r_{k+1} is obtained by generating a random number of ΔW_k.

3. *Exact transitional probability method.* The transitional probability density function in Eq. (4.79) is for time 0 to t. However, it also holds for time t_k to t_{k+1} by simply substituting r_{k+1} for r_t, r_k for r_0 and Δt for t in Eq. (4.79). Or one may obtain r_{k+1} by generating random number of Y in Eq. (4.80) which is a random variable of non-central Chi-squared distribution with $\frac{4ab}{\sigma^2}$ degree of freedom and non-centrality parameter $2cr_k e^{-b\Delta t}$[3].

Example 4.4.2. Let $a = 0.5$, $b = 0.3$, $\sigma = 0.4$. Fig. 4.2 shows simulated squared-root process for $t \in [0, 30]$ with starting point 0.01, 0.5, and 2.0, respectively. From the

[3]For example in Matlab® the function for generating random variable of non-central Chi-squared distribution is `nxc2rnd()`.

figures we may observe the trend that all paths converge to their ultimate common mean 0.5 and fluctuate around the mean afterwards.

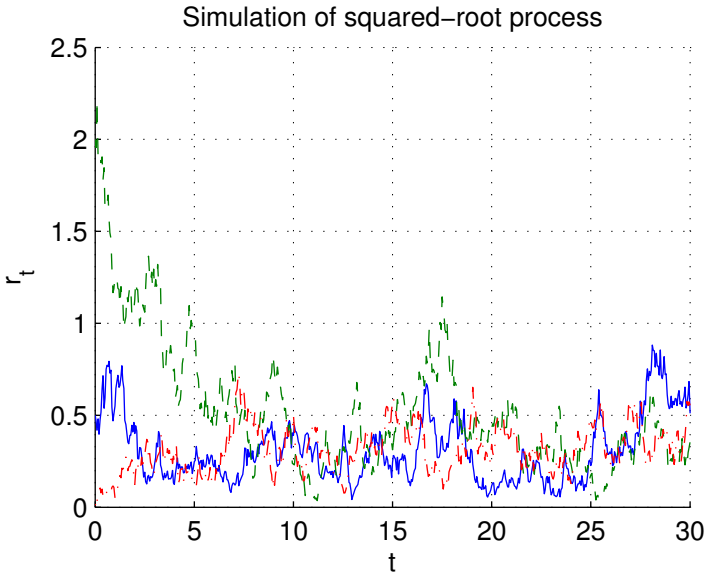

Figure 4.2: Simulation of squared-root process with different initial values.

Example 4.4.3. Let $a = 0.5$, $\sigma = 0.4$, $r_0 = 2.0$. Fig. 4.3 shows the emsemble average of 100 paths and its corresponding theoretical mean for $t \in [0, 30]$ with the convergence speed b equals to 0.1, 0.3 and 0.6, respectively. It shows that the mean of the simulated paths converges to its theoretical value on average, while the theoretical mean itself converges to the ultimate mean over time.

4.5 Deterioration of wire strength

In this section two models for the deterioration of wire strength are developed assuming the deterioration rate is stochastic. Let $g(t, r_t, S_t)$ be the actual deterioration rate of wire strength, then the change of wire strength over time can be formally defined as

$$\mathrm{d}S_t = -g(t, r_t, S_t)\,\mathrm{d}t \tag{4.85}$$

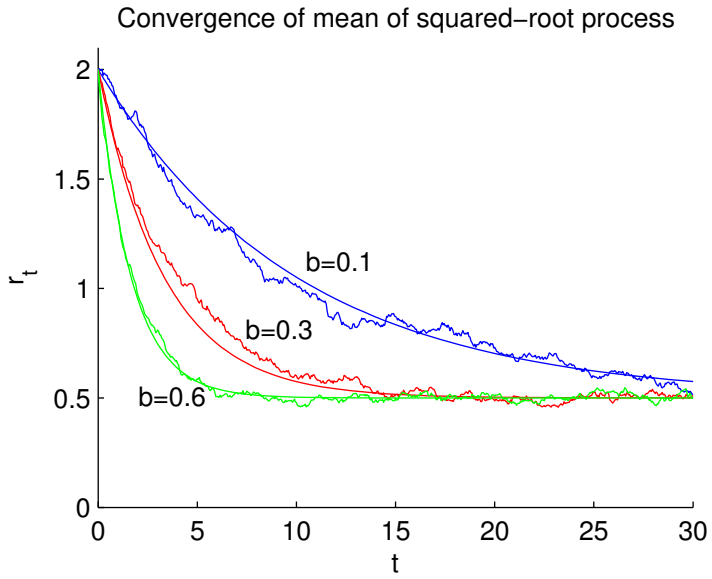

Figure 4.3: Convergence of mean of a squared-root process towards its ultimate mean, with different convergence speed shown.

Here $g(t, r_t, S_t)$ is called the *effective deterioration rate*, while r_t which was studied in the previous section is the *base deterioration rate*. The effective deterioration rate can be a function of both the base deterioration rate r_t and the current wire strength S_t. The general solution to the above equation is given as

$$S_t = S_0 - \int_0^t g(u, r_u, S_u)\,\mathrm{d}u \tag{4.86}$$

where S_0 is the initial wire strength. Since r_t is a stochastic process this integral is an Ito integral, and S_t is a random variable. Two deterioration models, distinguished by whether the effective deterioration rate depends on the current wire strength, are proposed, which are

1. State-independent model: $g(t, r_t, S_t) = r_t$;
2. State-dependent model: $g(t, r_t, S_t) = r_t \left(\dfrac{S_0}{S_t}\right)^p$;

In the following context the statistical properties of both model are first studies. And

then both models are applied to strength data. Calibration methods for both models are also developed.

4.5.1 State-independent model

Under the state-independent model, the effective deterioration rate is simply the base deterioration rate, independent of the current wire strength. In this case we have

$$\mathrm{d}S_t = -r_t \,\mathrm{d}t \tag{4.87}$$

which has the solution

$$S_t = S_0 - \int_0^t r_u \,\mathrm{d}u \tag{4.88}$$

If the deterioration rate r_t is an O-U process then apparently S_t follows a normal distribution, which doesn't fit our previous observations well. Instead, the squared-root process appears to be a better choice for r_t due to its non-negativity and mean-reversion properties. In the following context, we will assume r_t to be a squared-root process as defined in Eq. (4.69).

It is more convenient to define the *loss of strength* L_t as:

$$L_t = S_0 - S_t \tag{4.89}$$

And thus L_t satisfies the

$$\mathrm{d}L_t = r_t \,\mathrm{d}t \tag{4.90}$$

In general we have $L_0 = 0$, and therefore the solution to the above equation is given by

$$L_t = \int_0^t r_u \,\mathrm{d}u \tag{4.91}$$

which is essentially an integral of the square-root process. This quantity has been studied extensively in the literatures as it is a popular model for interest rate in financial applications. Many attempts has been made to obtain analytical solutions to the statistical properties of L_t. [Dufresne, 2001] was the first to gives formulas for computing the statistical moments. The same results was later developed independently by [Dassios and Nagaradjasarma, 2006], but in a simpler form. [Dassios and Nagaradjasarma, 2006] also gives joint probability density function of the squared-root process and its integral, as well as the marginal probability density functions in analytical form. The key to finding the joints moment of order j for L_t and order k for r_t is to apply Ito's formula to the product $L_t^j r_t^k$

$$\mathrm{d}(L_t^j r_t^k) = r_t^k \,\mathrm{d}(L_t^j) + L_t^j \,\mathrm{d}(r_t^k) \tag{4.92}$$

where

$$\begin{aligned}
\mathrm{d}(L_t^j) &= jL_t^{j-1}\,\mathrm{d}L_t + \frac{1}{2}j(j-1)L_t^{j-2}(\,\mathrm{d}L_t)^2 && (4.93)\\
&= jL_t^{j-1} r_t\,\mathrm{d}t + \frac{1}{2}j(j-1)L_t^{j-2}(r_t\,\mathrm{d}t)^2 && (4.94)\\
&= jL_t^{j-1} r_t\,\mathrm{d}t && (4.95)
\end{aligned}$$

and

$$\begin{aligned}
\mathrm{d}(r_t^k) &= kr_t^{k-1}\,\mathrm{d}r_t + \frac{1}{2}k(k-1)r_t^{k-2}(\,\mathrm{d}r_t)^2 && (4.96)\\
&= kr_t^{k-1}\left[b(a-r_t)\,\mathrm{d}t + \sigma\sqrt{r_t}\,\mathrm{d}W_t\right] + \frac{1}{2}k(k-1)r_t^{k-2}\sigma^2 r_t\,\mathrm{d}t && (4.97)\\
&= \left[abk + \frac{1}{2}k(k-1)\sigma^2\right] r_t^{k-1}\,\mathrm{d}t + bkr_t^k\,\mathrm{d}t + kr_t^{k-1}\sqrt{r_t}\,\mathrm{d}W_t && (4.98)
\end{aligned}$$

Substituting Eq. (4.92) and Eq. (4.98) into Eq. (4.92) yields

$$\mathrm{d}(L_t^j r_t^k) = jL_t^{j-1} r_t^{k+1}\,\mathrm{d}t \tag{4.99}$$

$$+ \left[abk + \frac{1}{2}k(k-1)\sigma^2\right] L_t^j r_t^{k-1}\,\mathrm{d}t + bkL_t^j r_t^k\,\mathrm{d}t + kL_t^j r_t^{k-1}\sqrt{r_t}\,\mathrm{d}W_t \tag{4.100}$$

Take expectation on both side and define $M_{jk}(t) = \mathrm{E}[L_t^j r_t^k]$, and this yields the following ordinary differential equation on a discrete grid of $M_{jk}(t)$:

$$\frac{\mathrm{d}}{\mathrm{d}t}M_{jk}(t) = abkM_{jk}(t) + \left[abk + \frac{1}{2}k(k-1)\sigma^2\right] M_{j,k-1}(t) + jM_{j-1,k+1}(t) \tag{4.101}$$

This equation can be solved recursively, but derivation is quite lengthy and technical. See [Dufresne, 2001] and [Dassios and Nagaradjasarma, 2006] for a complete derivation. Here we states the results using the notations in [Dufresne, 2001]. These formulas will be used to estimate model parameters from observational data. The k-th moments of r_t is given by

$$\mathrm{E}[r_t^k] = \sum_{j=0}^{k} \theta_{kj} e^{-bjt}, \quad k = 0, 1, \ldots \tag{4.102}$$

where

$$\theta_{kj} = \sum_{i=0}^{j} r_0^i \frac{k!(-1)^{k-j}\bar{u}^{k-i}}{i!(j-i)!(k-j)!}\frac{(\bar{v})_k}{(\bar{v})_i}, \quad 0 \le j \le k \tag{4.103}$$

$$\bar{u} = -\frac{\sigma^2}{2b} \tag{4.104}$$

$$\bar{v} = \frac{2ab}{\sigma^2} \tag{4.105}$$

$$(y)_k = y(y+1)\cdots(y+k-1), \quad k \ge 1, (y)_0 = 1. \tag{4.106}$$

And then the J-th moments of L_t is computed using the following recursive formula:

$$\mathrm{E}[L_t^J] = M_{J0}(t) \tag{4.107}$$

$$M_{JK}(t) = \sum_{m=0}^{J+K} M_{JKm}(t)e^{-bmt} \tag{4.108}$$

$$M_{jkm}(t) = \sum_{n=0}^{\min(j,j+k-m)} M_{jkmn}t^n \tag{4.109}$$

$$M_{jkmn}(t) = \sum_{i=n}^{\min(j,j+k-m)} \frac{(n+1)_{i-n}}{[b(k-m)]^{i-n+1}} R_{jkmi}, \quad k \neq m \tag{4.110}$$

where

$$R_{jkmn} = \beta_k M_{j,k-1,m,n} + jM_{j-1,k+1,m,n} \tag{4.111}$$

$$\beta_k = abk + \frac{1}{2}\sigma^2 k(k-1) \tag{4.112}$$

and specially,

$$M_{jkkn} = \frac{1}{n} R_{j,k,k,n-1},^{4} \quad n = 1, \ldots, j \tag{4.113}$$

$$M_{jkk0} = -\sum_{m=0,\, m\neq k}^{j+k} M_{jkm0}, \quad j \geq 1 \tag{4.114}$$

$$M_{0km0} = \theta_{km} \tag{4.115}$$

$$M_{0kmn} = 0, \quad n \geq 1. \tag{4.116}$$

These formulas for computing moments of arbitrary order can be easily implemented numerically, or symbolically. See Appendix B for an implementation in

[4]There is a typo in the original paper.

Matlab®.

4.5.1.1 Model calibration by moment matching

In this section the state-independent model is calibrated to four datasets: artificially corroded wires in Carleton Lab, Severn Bridge wires, Forth Road Bridge wires and Williamsburg Bridge cables. Four model parameters are to be estimated, three of which are parameters of the dynamics of squared-root process: a, b, σ, and the fourth is the initial value r_0 of the squared-root process. These parameters are estimated by matching the first four statistical moments using the analytical formulas for computing moments of loss of wire strength L_t. In this definition of loss of strength, the initial wire strength S_0 of each data set is given in Table 3.7.

The moment matching problem can be formulated as a multi-objective optimization problem. To linearize the Feller's condition, define the following new variables:

$$\alpha = -b \tag{4.117}$$

$$\beta = ab \tag{4.118}$$

$$\gamma = \sigma^2 \tag{4.119}$$

And the state variable is represented by the new variables:

$$\boldsymbol{x} = \{\alpha, \beta, \gamma, r_0\} \tag{4.120}$$

The error measure of the goodness of match of moments is defined as the relative error as the following:

$$\varepsilon_i(\boldsymbol{x}) = [M_{i0}(t; \boldsymbol{x}) - \tilde{M}_i]/\tilde{M}_i \times 100\%, \quad i = 1, 2, \cdots \tag{4.121}$$

where $\tilde{M}_i$ is the i-th moment estimated from the data set. These error measurement can either be used as objective function for an approximate match, or used as constraints for an exact match. Depending on how the error measure is used, the optimization problem can be formulated in different variations. The model is first calibrated to the artificially corroded wires from the Carleton Lab as an example for comparing three different formulations.

The most straight-forward formulation of the optimization problem is to post all four error measures for the first four moments as objectives, which is given by

$$\max_{\boldsymbol{x}} \min_{i} \quad |\varepsilon_i(t;\boldsymbol{x})|, \quad i = 1,2,3,4 \tag{4.122}$$

$$\text{subject to} \quad \gamma - 2\beta < 0 \tag{4.123}$$

$$\alpha < 0,\ \beta > 0,\ \gamma > 0 \tag{4.124}$$

After solving this optimization problem[5], the results of moment matching for Carleton Lab wires are summarized in Table 4.2. The 2nd moment achieves a good match, but the 1st, 3rd and the 4th moment reach their minimum error uniformly, which is about 9.28% in relative value. This might not be a satisfactory result due to the error on the 1st moment. Figure 4.4 shows the probability plot of the original data set of loss of strength, and the samples of simulated L_t, as well as a gamma distribution fit to the original data set as a reference. The Euler scheme is used to simulated paths of r_t and then trapezoidal rule is used to compute L_t. A total number of 10,000 samples of L_t are generated. The results indicates a poor match between the simulated samples and the original samples.

To achieve a better match, or even exact match for the first two moments, the

[5]Using the Optimization Toolbox of Matlab®, for example.

optimization problem is formulated by using the first two moments as constraints, while the 3rd and 4th moments remains objectives. This yields:

$$\max_{\boldsymbol{x}} \min_{i} \quad |\varepsilon_i(t;\boldsymbol{x})|, \qquad i = 3,4 \tag{4.125}$$

$$\text{subject to} \quad \gamma - 2\beta < 0 \tag{4.126}$$

$$\alpha < 0,\ \beta > 0,\ \gamma > 0 \tag{4.127}$$

$$|\varepsilon_i(t;\boldsymbol{x})| = 0 \qquad i = 1,2 \tag{4.128}$$

This formulation is often favorable since matching the first two moments are far more important than matching any other higher order moment. This formulation requires that the feasible set defined by the equality constraints not be empty. However, compared to the previous formulation, exact match of the first two moment may come at a cost of less accurate matches of the other moments. Table 4.3 shows that applying this formulation to the Carleton Lab data set results in about 45% error for the 4th moment. Nevertheless, since exact match is achieved for the first two moments, the probability plot in Figure 4.5 shows a better match between the original data set and simulated samples, compared to the previous formulation.

The formulation with two equality constraint is also applied to the other three data sets: Severn Bridge, Forth Road Bridge and Williamsburg Bridge. The results are listed in Table 4.5, 4.6 and 4.7, and the probability plots of the original data set and simulated samples are in Figure 4.7, 4.8 and 4.9, respectively. Two of these three data sets, namely Severn Bridge and Williamsburg Bridge show good match for all four moments, while Forth Road Bridge, similar to Carleton Lab wires, shows poor match for the 4th moments.

Table 4.1 compares the estimated parameters among all four data sets by enforcing

exact match of the first two moments. The physical meaning of each parameter is also mentioned in the table. All four data sets show consistent pattern in terms of the physics of deterioration. Note that for the Severn Bridge data, the moment

Table 4.1: Comparison of estimated parameters for all data sets by enforce exact match of the first moments.

Parameter	Carleton Lab	Severn Bridge	Forth Road Bridge	Williamsburg Bridge
a (ultimate mean)	0.5775	0.4713	0.4894	0.5300
b (convergence speed)	0.4429	0.2054	0.1763	0.1498
σ (volatility)	0.7153	0.4081	0.4154	0.3149
r_0 (initial value)	2.2681	0.0000	0.1097	0.0036

matching method estimates $r_0 \approx 0.0$. Due to the mean-reversion property of the squared-root process, even though r_t starts from 0.0, it quickly drifts away from 0.0 and stays strictly positive since the Feller's condition is enforced as an constraint in the optimization problem.

Lastly, in case that in the previous formulation the feasible set defined by the two equality constraints is empty, or a balance of goodness of match is desired for all four moments in a controlled manner, a tolerance can be used to relax the equality constraints. As a result, the two constraints are written as $\varepsilon_i(t; \boldsymbol{x}) < \delta$, where δ is the desired level of tolerance. As a demonstration, this formulation is applied to Carleton Lab data set with 1% tolerance, and the results is listed in Table 4.4. And Figure 4.6 compares the original data set against the simulated samples.

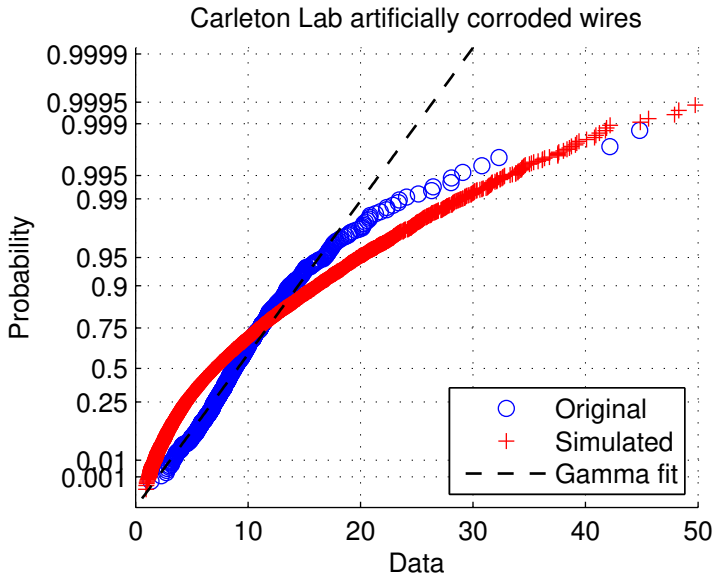

Figure 4.4: Probability plot of loss of strength of Carleton Lab artificially corroded wires and simulated samples by the state-independent corrosion model. Model parameters are estimated without contraints on any specific moment. A gamma distribution is fitted to the wire samples.

Table 4.2: Moment matching results for Carleton Lab artificially corroded wires. Model parameters are estimated without constraints on any specific moment.

a	1.3597
b	0.2475
σ	0.8204
r_0	0.0255

	Samples	Model	Rel. Err.
1st moment	9.55	8.66	-9.28%
2nd moment	110.07	109.66	-0.37%
3rd moment	1762.76	1926.39	9.28%
4th moment	48764.24	44237.64	-9.28%

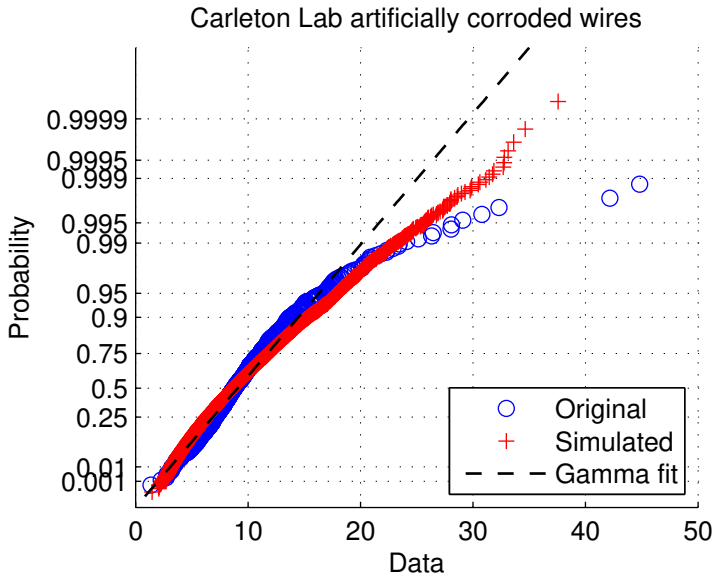

Figure 4.5: Probability plot of loss of strength of Carleton Lab artificially corroded wires and simulated samples by the state-independent corrosion model. Model parameters are estimated with equality constraints on first and second moment. A gamma distribution is fitted to the wire samples.

Table 4.3: Moment matching results for Carleton Lab artificially corroded wires. Model parameters are estimated with equality constraints on first and second moment.

a	0.5775
b	0.4429
σ	0.7153
r_0	2.2681

	Samples	Model	Rel. Err.
1st moment	9.55	9.55	0.00%
2nd moment	110.07	110.07	0.00%
3rd moment	1762.76	1518.89	-13.83%
4th moment	48764.24	24738.73	-49.27%

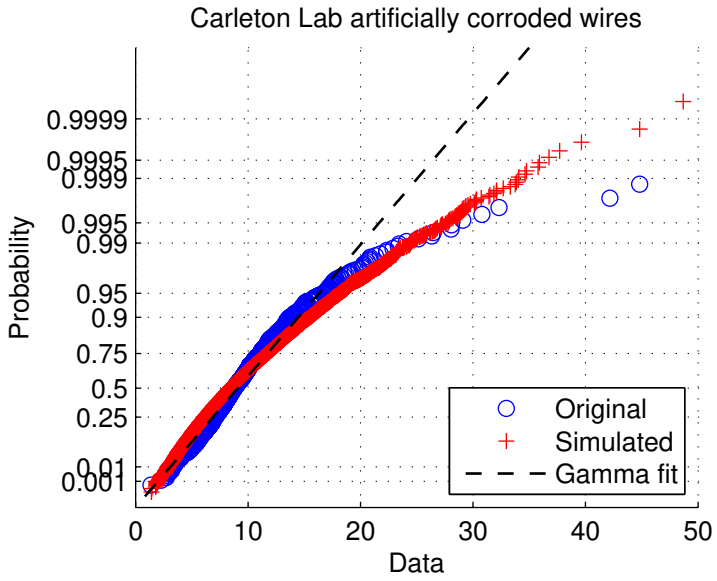

Figure 4.6: Probability plot of loss of strength of Carleton Lab artificially corroded wires and simulated samples by the state-independent corrosion model. Model parameters are estimated with constraints on first and second moment which allow 1% tolerence. A gamma distribution is fitted to the wire samples.

Table 4.4: Moment matching results for Carleton Lab artificially corroded wires. Model parameters are estimated with constraints on first and second moment which allow 1% tolerence.

a	1.0970
b	0.7216
σ	1.2582
r_0	0.0000

	Samples	Model	Rel. Err.
1st moment	9.55	9.45	-1.00%
2nd moment	110.07	111.17	1.00%
3rd moment	1762.76	1615.75	-8.34%
4th moment	48764.24	28613.10	-41.32%

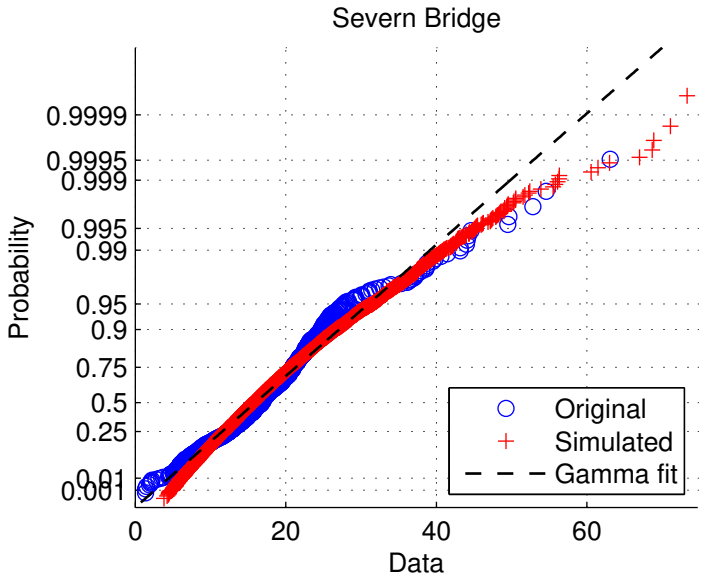

Figure 4.7: Probability plot of loss of strength of Severn Bridge wires and simulated samples by the state-independent corrosion model. Model parameters are estimated without constraints on any specific moment. A gamma distribution is fitted to the wire samples.

Table 4.5: Moment matching results for Severn Bridge wires. Model parameters are estimated with equality constraints on first and second moment.

a	0.4713
b	0.2054
σ	0.4081
r_0	0.0000

	Samples	Model	Rel. Err.
1st moment	17.03	17.03	0.00%
2nd moment	343.65	343.65	0.00%
3rd moment	8137.55	8193.08	0.68%
4th moment	228651.07	229196.00	0.24%

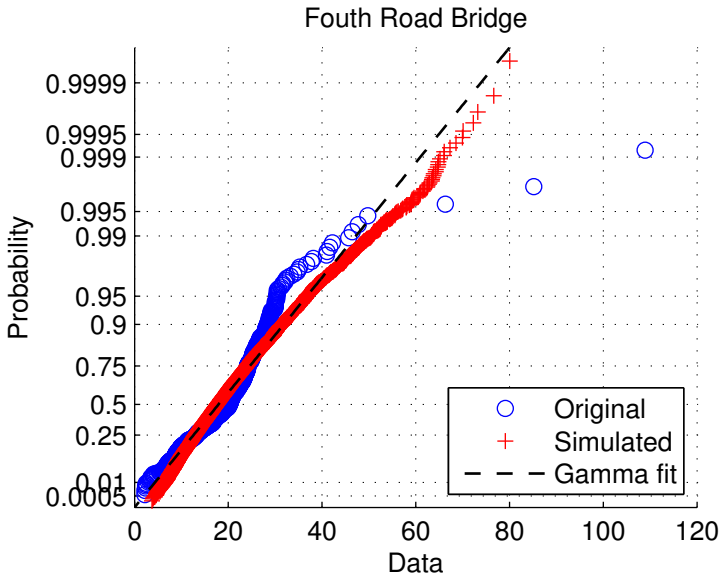

Figure 4.8: Probability plot of loss of strength of Fouth Road Bridge wires and simulated samples by the state-independent corrosion model. Model parameters are estimated without contraints on any specific moment. A gamma distribution is fitted to the wire samples.

Table 4.6: Moment matching results for Fouth Road Bridge wires. Model parameters are estimated with equality constraints on first and second moment.

a	0.4894
b	0.1763
σ	0.4154
r_0	0.1097

	Samples	Model	Rel. Err.
1st moment	19.38	19.38	0.00%
2nd moment	460.24	460.24	0.00%
3rd moment	14015.88	13314.49	-5.00%
4th moment	626898.71	464085.70	-25.97%

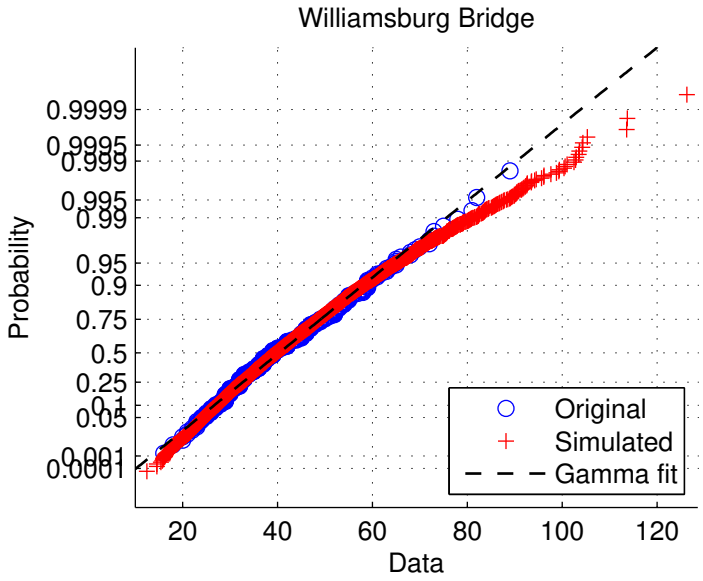

Figure 4.9: Probability plot of loss of strength of Williamsburg Bridge wires and simulated samples by the state-independent corrosion model. Model parameters are estimated without constraints on any specific moment. A gamma distribution is fitted to the wire samples.

Table 4.7: Moment matching results for Williamsburg Bridge wires. Model parameters are estimated with equality constraints on first and second moment.

a	0.5300
b	0.1498
σ	0.3149
r_0	0.0036

	Samples	Model	Rel. Err.
1st moment	41.53	41.53	0.00%
2nd moment	1885.10	1885.10	0.00%
3rd moment	93131.37	93472.01	0.37%
4th moment	4976931.02	5058848.86	1.65%

4.5.2 State-dependent model

Under the state-dependent model, the effective deterioration rate also depends on the current state of the wire strength:

$$g(t, r_t, S_t) = r_t \left(\frac{S_0}{S_t}\right)^p, \quad (p > 0) \tag{4.129}$$

where the ratio of initial wire strength S_0 over the current wire strength S_t represents the degree of deterioration. This forms a modulating function on the base deterioration rate, which makes the effective deterioration rate negatively correlated to the wire strength, as wires with lower strength will have a faster effective deterioration rate than those with high strength. Many factors may contribute to such phenomenon, including but not limited to the following:

1. Gradual loss of zinc protective coating;
2. Corroded wire surface may trap more moist;
3. Elevated strain due to loss of load bearing ability.

The exponential $p > 0$ adds more flexibility to the model for capturing the negative correlation. As a limiting case when $p = 0$ this model degenerates to the state-independent model.

The change of wire strength over time is given by

$$\mathrm{d}S_t = -r_t \left(\frac{S_0}{S_t}\right)^p \mathrm{d}t \tag{4.130}$$

whose solution is given by

$$S_t = S_0 \sqrt[p+1]{1 - \frac{p+1}{S_0} \int_0^t r_u \, \mathrm{d}u} \tag{4.131}$$

where r_t is a squared-root process as defined in Eq. (4.69). Compared with the state-independent model, statistical moments of wire strength S_t cannot be easily computed from the moment of the integral of r_t. Instead, we seek to directly estimate the probability distribution of S_t.

One approach for estimating the distribution of S_t is by solving for the joint distribution of S_t and r_t from Fokker-Planck equation, and then obtaining the marginal distribution of S_t by integration. Let $f_{r_t,S_t}(r,s)$ be the joint PDF of r_t and S_t. Then $f_{r_t,S_t}(r,s)$ satisfies the following two-dimensional Fokker-Planck forward equation:

$$\frac{\partial f}{\partial t} = r_t \left(\frac{S_0}{S_t}\right)^p \frac{\partial f}{\partial S_t} - b(a - r_t)\frac{\partial f}{\partial r_t} + \frac{1}{2}\sigma^2 r_t \frac{\partial^2 f}{\partial r_t^2} \tag{4.132}$$

which is a two-dimensional advection-diffusion time-dependent PDE. This equation is defined on an unbounded domain, but when applying numerically methods such as finite element method or finite difference method, solution is sought on a bounded domain

$$\Omega = [0, S_{\max}] \times [0, r_{\max}] \tag{4.133}$$

$S_{\max}$ is chosen to be S_0, as S_t must be strictly decreasing over time. $r_{\max}$ is so chosen that r_t never reaches $r_{\max}$, for $t \leq T$, where T is the maximum time horizon the solution is sought. The initial condition of f is given as a delta function located at (S_0, r_0). Boundary condition on $S = S_{\max}$ is no-flux, as the probability mass drifts away from the boundary, while all the other three boundaries are absorbing, assuming that the probability mass will not hit these three boundaries.

Alternative, the distribution of S_t can be estimated by Monte Carlo simulation. Realizations of deterioration rate process r_t can be generated using methods in Sec. 4.4.3.2, and then samples of S_t can be obtained by numerically integrating r_t in

Eq. (4.131).

4.5.2.1 Calibration of state-dependent model

Since analytical solutions to the statistical moments of wire strength are not readily available, moment matching method cannot be applied for estimating the parameters of the state-dependent model. Instead, model parameters are estimated by matching the probability distribution of simulated samples of wire strength to the data.

There are many distance/similarity measures between probability density functions in the literatures. A recent survey [Cha, 2007] listed and compared 45 different measures. The Kullback-Leibler divergence (KL divergence) is choosen as the measure for our application. Let P and Q be two discrete probabiltiy density functions, e.g. the empirical probability density function estimated from samples, the KL divergence of Q from P is defined as

$$D_{\mathrm{KL}}(P||Q) = \sum_{i \in \mathbb{Z}^+} P(i) \log \frac{P(i)}{Q(i)} \tag{4.134}$$

which is interpreted as relative entropy of P with respect to Q, or information deviation of Q from P. It is based on Shannon's information entropy measure defined as $H = -\sum_i P(i) \log P(i)$. Typically P represents the "true" distribution, or the target distribution, e.g., the distribution constructed from wire strength data, while Q represents the model distribution, e.g., the distribution estimated from samples of S_t generated by Monte Carlo simulation. However, the KL divergence is not a real distance metric as it is not symmetric. Therefore, a symmetric version of KL divergence defined as the following is used instead:

$$D_{\mathrm{KL}}^{\mathrm{sym}}(P||Q) = D_{\mathrm{KL}}(P||Q) + D_{\mathrm{KL}}(Q||P) \tag{4.135}$$

To calibrate the state-dependent model, five parameters need to be estimated, where four parameters $\boldsymbol{x} = \{\alpha, \beta, \gamma, r_0\}$ are related to the deterioration rate process, as defined in Eq. (4.120), plus the exponential p. These five parameters can be estimated by solving the following optimaztion problem:

$$\min_{\boldsymbol{x},p} \quad D_{\mathrm{KL}}^{\mathrm{sym}}(P||Q) \tag{4.136}$$

$$\text{subject to} \quad \gamma - 2\beta < 0 \tag{4.137}$$

$$\alpha < 0,\ \beta > 0,\ \gamma > 0 \tag{4.138}$$

$$p \geq 1 \tag{4.139}$$

Given p and $\boldsymbol{x}$, the probability density function Q is estimated by the following steps:

1. Generate realizations of r_t, starting with the same seed for the random number generator;

2. For each realization of r_t, compute a sample of S_t by Eq. (4.131);

3. Estimate Q from samples of S_t using the same rules for dividing bins as used for constructing P.

After solving the optimization problem, results indicate that $p = 0$ is the best fit for the three data sets obtained from real bridges: Forth Road Bridge, Severn Bridge and Williamsburg Bridge. In this case the model degenerates to the state-independent model and the values of the other four parameters stay the same. Results also indicate that $p = 4.9$ is the best fit for the artificially corroded wires from Carleton Lab. Figure 4.10 compares the probability plots of loss of strength between data of artificially corroded wires from Carleton Lab and the fitted state-dependent model. Table 4.8 lists the values of the calibrated model parameters, as well as comparison

of statistical moments between data and simulated samples. It shows that the state-dependent model calibrated based on KL divergence provides good fits for the first two moments, but less satisfactory fit for the 3rd and the 4th moments.

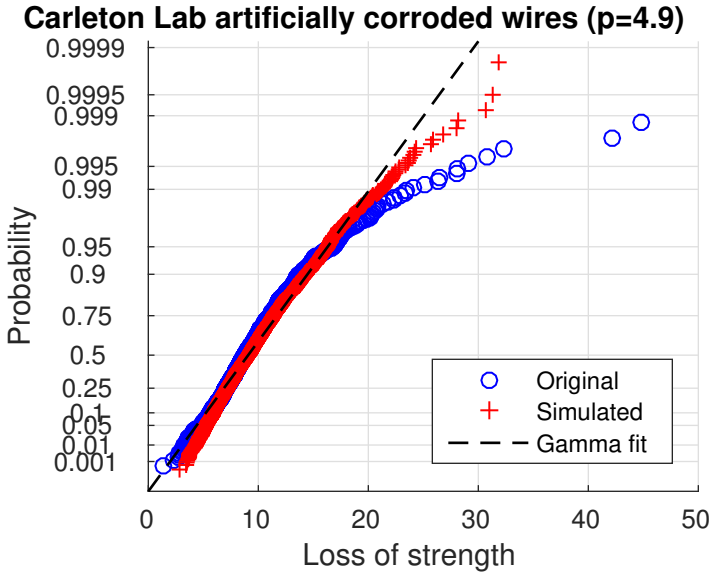

Figure 4.10: Probability plot of loss of strength of Carleton Lab artificially corroded wires and simulated samples by the state-dependent corrosion model with $p = 4.9$. A gamma distribution is fitted to the wire samples.

Table 4.8: Calibrated parameters of state-dependent model for Carleton Lab artificially corroded wires.

p	4.9
a	0.8347
b	0.5263
σ	0.5683
r_0	0.9950

	Samples	Model	Rel. Err.
1st moment	9.55	9.68	1.43%
2nd moment	110.07	106.08	-3.63%
3rd moment	1762.76	1322.29	-24.99%
4th moment	48764.24	18831.80	-61.38%

4.6 Proposed procedures for applying stochastic deterioration model

In this section a stochastic deterioration model of wire strength is developed. This model assumes the deterioration rate is a stochastic process which is non-negative and mean reversion. The wire strength is therefore a function of the cumulation of the deterioration rate over time. A major advantage is that this model can be calibration using only one set of observational data of wire strength samples. Below are the main step for applying this model to modeling wire strength of real bridges:

1. Collect samples of wire strength from suspension bridge cables;
2. Gather information of the initial wire strength when the bridge is built, and the current age of the bridge;
3. Select either O-U process or squared-root process for modeling deterioration rate process. The squared-root process is preferred, unless the distribution of wire strength can be approximated by Gaussian distribution, where O-U process may be used as quick approximation;
4. Select either state-independent or state-dependent model for the actual deterioration of wire strength. The state-indenpendent model should be tried first, as it is easier to calibrate, and provides good fit to real bridge data;
5. Calibrate model parameters. For state-independent model moment matching method is used, while for state-dependent model KL divergence based method is used;
6. Make prediction of the distribution of wire strength at any given time in the future using calibrated model.

Chapter 5

Discussion and conclusion

5.1 Quantify equivalent age of lab corroded wires

In Chapter 2 the artificially corroded wire from the Carleton Lab was assumed to have an equivalent age of 10 year as if the wires were taken from a real bridge. However, this judgment was purely empirical, as it was based on observing the corrosion stages of the wires. In this section the equivalent age of the lab corroded wires is estimated quantitatively using the stochastic deterioration model developed in Chapter 4.

The general idea is to apply parameters of the state-independent model, which is estimated using data from a real bridge, to generate wire strength samples for a given age. Then the equivalent age of the lab corroded wires is such an age that the KL divergence of the PDF's between the generated samples and the original strength data is minimized. Results shows that when using parameters of Forth Road Bridge, the equivalent age is 24.5; when using parameters of Severn Bridge, the equivalent age is 25.8; when using parameters of Williamsburg Bridge, the equivalent age is 25. Figure 5.2 compares the PDF of the wire strength of lab corroded wires with the PDF's of the generated samples using parameters from real bridges and estimated equivalent

ages. Table 5.1 compares statistical moments of loss of strength computed from data of lab corroded wires and from samples generated using real bridge parameters and estimated equivalent ages.

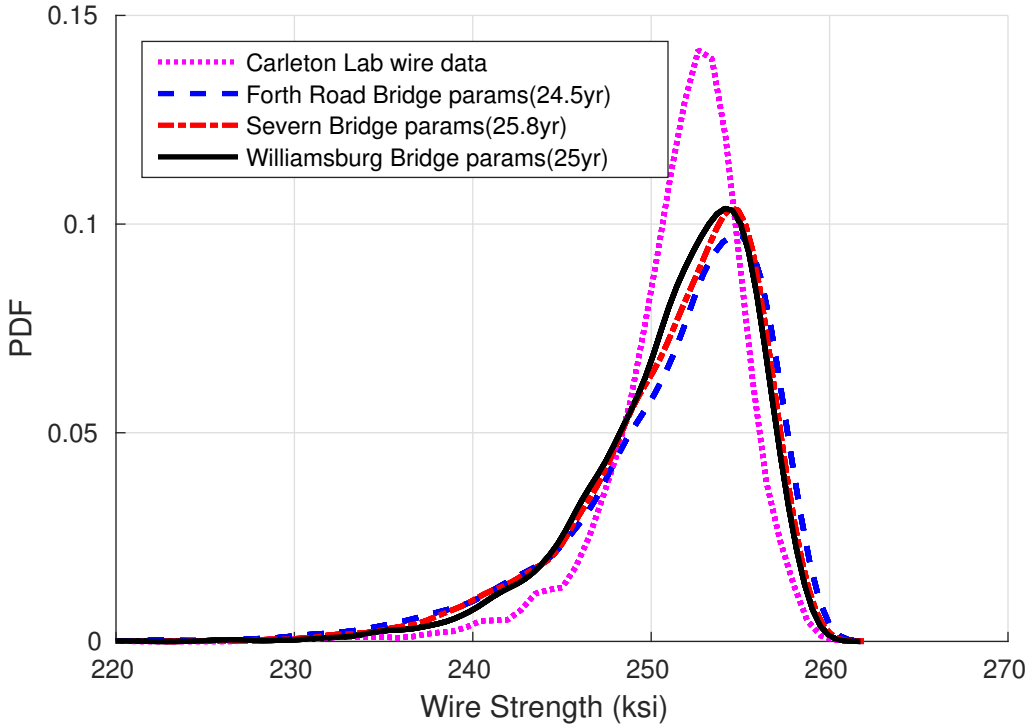

Figure 5.1: Comparison of PDF's of wire strength of lab corroded wires and generated samples with estimated equivalent ages.

Table 5.1: Comparison of statistical moments of loss of strength.

	Carleton Lab	Using Forth Road Bridge Parameters		Using Severn Bridge Parameters		Using Williamsburg Bridge Parameters	
Order	Moment	Moment	Error	Moment	Error	Moment	Error
1st	9.55	9.83	3.01%	9.80	2.69%	9.77	2.36%
2nd	110.07	128.43	16.68%	120.86	9.80%	117.68	6.91%
3rd	1762.76	2180.71	23.71%	1823.68	3.46%	1720.39	-2.40%
4th	48764.24	46739.32	-4.15%	32482.59	-33.39%	29949.85	-38.58%

5.2 Comparison between evolutionary distribution model and stochastic deterioration model

The evolutionary distribution model was developed in Chapter 3 and the stochastic deterioration model was developed in Chapter 4. Once calibrated, both models are able to predict the marginal probability distribution of wire strength at any given time. The similarities and differences between the two methods are compared from various aspects in this section.

Object of study

The evolutionary distribution model is based on descriptive statistics, and it directly studies the evolution of the distribution in time. The stochastic deterioration model 4 studies deterioration rate process, which is the source of uncertainty for the wire strength.

Assumptions

The evolutionary distribution model assumes that the wire strength follows the same probability distribution at all time, whose parameters can be expressed as functions of time. The stochastic deterioration model assumes that the wire strength is function of the cumulation of deterioration rate over time, and the parameters of the stochastic deteriorate process are constant at all time.

Model calibration

The evolutionary distribution model needs to observe multiple snapshots of probability distribution of wire strength in order to establish a reliable pattern of how the distribution evolves in time. The stochstic deterioration model needs only one snapshot for calibrating the deteriotion rate process. This advantage is due to the fact that the deterioration mechanism is relatively stable in time if the environment is not drastically changed.

Making prediction

Once calibrated, both models can predict the probability distribution at any given time. The evolutionary distribution model is relatively easy to use, since the analytical form of the distribution function is available. The stochastic deterioration model a few more steps for making predictions, as it needs to first generate realizations of the stochastic deterioration process and compute samples of wire strength, and then estimate the distribution from samples.

Example

For comparison, both models are used to estimate distribution of normalized wire strength at 20, 40, 80 and 120 years. The evolutionary distribution model assumes Weibull distribution for wire strength, with time-dependent parameters given in Eq. (3.32) and Eq. (3.33). The stochastic deterioration model assumes deterioration rate follows squared-root process with parameters calibrated for the Severn Bridge data, as listed Table 4.5. It also assumes the deterioration is independent of current wire strength. The estimated PDF's are shown in Figure 5.2 and statistics are listed in Table.5.2. Both models predicts comparable mean values, however, the evolutionary distribution model predicts larger variance than the stochastic deterioration model. The PDF plots also suggests that the evolutionary distribution model predicts a faster deterioration speed than the stochastic deterioration model.

Table 5.2: Comparison of statistics of normalized wire strength estimated by evolutionary distribution model (ED) and by stochastic deterioration model (SD).

	Mean		Variance	
	ED	SD	ED	SD
20yr	0.96028	0.97297	2.7342e-04	2.2668e-04
40yr	0.93632	0.93778	6.2643e-04	7.3129e-04
80yr	0.84966	0.86638	2.9394e-03	1.7791e-03
120yr	0.71048	0.79563	1.1195e-02	2.8086e-03

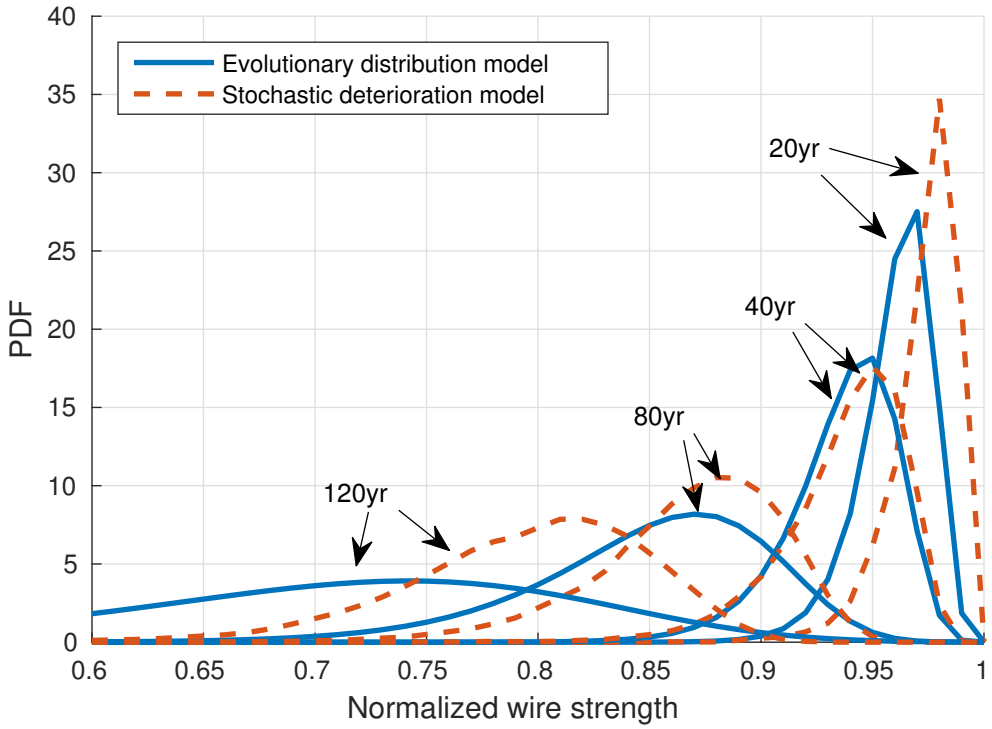

Figure 5.2: Comparison of PDF's of normalized wire strength estimated by evolutionary distribution model and by stochastic deterioration model.

5.3 Spatial correlation in stochastic deterioration model

The wire strength was modeled as a random process in Chapter 3 to account for the its spatial variation and correlation. However, this was not considered in the stochastic deterioration model developed in Chapter 4. This section extends the stochastic deterioration model to account for spatial correlation.

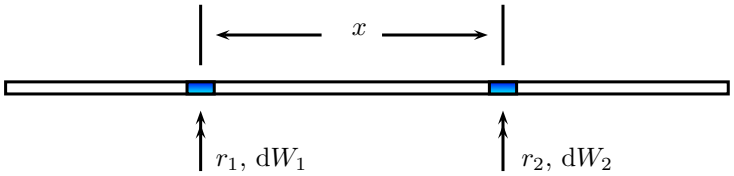

Figure 5.3: Wire segments that are x apart are subject to different deterioration rates r_1 and r_2.

As shown in Figure 5.2, consider two infinitesimal wire segments that are x apart, and are subject to deterioration rates r_1 and r_2. For demonstration purpose the deterioration rates are assumed to be both O-U processes with the same parameters but driven by different Brownian motions W_1 and W_2:

$$\begin{aligned} \mathrm{d}r_1 &= b(a - r_1)\,\mathrm{d}t + \sqrt{r_1}\sigma\,\mathrm{d}W_1, \\ \mathrm{d}r_2 &= b(a - r_2)\,\mathrm{d}t + \sqrt{r_2}\sigma\,\mathrm{d}W_2. \end{aligned} \tag{5.1}$$

Note that for square-root processes the following derivations would still apply, but not as easily tractable as the O-U process. Suppose that $\mathrm{d}W_1$ and $\mathrm{d}W_2$ are correlated and the correlation is time-invariant but depends on the spatial distance x:

$$\mathrm{E}[\,\mathrm{d}W_1\,\mathrm{d}W_2] = \rho(x) \tag{5.2}$$

Using the state-independent model, the loss of wire strength of the two wire segments are given by

$$L_1(t) = \int_0^t r_1(u)\,\mathrm{d}u, \quad L_2(t) = \int_0^t r_2(u)\,\mathrm{d}u \tag{5.3}$$

The goal the to find the spatial correlation $\rho_L(x)$ between L_1 and L_2, which is given by

$$\begin{aligned}\mathrm{E}[L_1(t)L_2(t)] &= \mathrm{E}\left[\left(\int_0^t r_1(u)\,\mathrm{d}u\right)\left(\int_0^t r_2(u)\,\mathrm{d}u\right)\right] \\ &= \int_0^t\int_0^t \mathrm{E}\left[r_1(u)r_2(v)\right]\,\mathrm{d}u\,\mathrm{d}v\end{aligned} \tag{5.4}$$

With the explicit solutions of r_1 and r_2 given by Eq. (4.66), the expectation $\mathrm{E}[r_1(u)r_2(v)]$ can be computed as

$$\begin{aligned}\mathrm{E}[r_1(u)r_2(v)] &= \mu_r(u)\mu_r(v) + \sigma^2 e^{-2b(u+v)}\mathrm{E}\left[\int_0^u e^{bs}\,\mathrm{d}W_1(s)\cdot\int_0^v e^{bs}\,\mathrm{d}W_2(s)\right] \\ &= \mu_r(u)\mu_r(v) + \sigma^2 e^{-2b(u+v)}\int_0^{u\wedge v} e^{2bs}\rho(x)\,\mathrm{d}s, \quad \text{(Ito isometry)} \\ &= \mu_r(u)\mu_r(v) + \sigma^2 e^{-2b(u+v)}\left[e^{2b(u\wedge v)}-1\right]\rho(x),\end{aligned} \tag{5.5}$$

where $u \wedge v = \min\{u, v\}$, $\mu_r(t)$ is the mean of r_1 and r_2 given by Eq. (4.67). Substituting Eq. (5.5) into Eq. (5.4) yields

$$\mathrm{E}[L_1(t)L_2(t)] = \left[\int_0^t \mu_r(u)\,\mathrm{d}u\right]^2 + \sigma^2\left[\frac{1}{4b^2}\left(1-e^{-4bt}\right) - \frac{t}{b}e^{-2bt}\right]\rho(x) \tag{5.6}$$

It can be verified that

$$\mathrm{E}[L_i(t)] = \int_0^t \mu_r(u)\,\mathrm{d}u \tag{5.7}$$

and therefore the correlation coefficient between $L_1(t)$ and $L_2(t)$ is given by

$$\rho_{LL}(x) = \frac{\mathrm{E}[L_1(t)L_2(t)] - \mathrm{E}[L_1(t)]\mathrm{E}[L_2(t)]}{\sqrt{\mathrm{Var}[L_1(t)]}\sqrt{\mathrm{Var}[L_2(t)]}} = \rho(x) \tag{5.8}$$

The result shows that if we view $L(t;x)$ as a random process in space than it has a time-invariance correlation structure determined by the correlation of the Brownian motions drivers in the deterioration rate process.

5.4 Conclusions and contributions

This research applied probabilistic methods to study the wire strength data collected from real bridges and artificially corroded wires. Two methods were developed for the purpose of estimating reliability of suspension cables at any given time. The first method developed in Chapter 3 models the wire strength as random process in space whose statistical properties evolves in time. The second method developed in Chapter 4 models the deterioration rate as stochastic process in time. This research has made the following significant and innovative contributions:

1. Recognized of the time-dependency of the marginal distribution and power spectral density of the random process representing wire strength, while at any given time the random process is considered as a stationary process in space. The evolution of both characteristics is due to constant corrosion and deterioration of wire strength. The evolutionary pattern is captured by fitting analytical function in time to the parameters of both distribution function and power spectral density.

2. Applied copula theory to explained the origin of the incompatibility issue of the first type between marginal distribution and power spectral density which

arises when simulating non-Gaussian random processes by translation process theory.

3. Proposed guidelines for fitting probability distribution and power spectral density to a data set of wire strength, avoiding the aforementioned incompatibility issue of the first type by requiring the corresponding correlation function to be within the attainable correlation bounds specified by the marginal distribution.

4. Identified the deterioration rate process as a square-root process under Ito's stochastic calculus theory. Subsequently the actual loss of strength is expressed in terms of the integral of the square-root process. A method of moments is proposed to estimate the model parameters from the observed probability distribution.

5. Proposed that the actual deterioration of strength may also depend on the state of the wire, as intuitively corroded wires are more prone to further corrosion. Such model is able to explain the tail distribution of the observed data.

5.5 Future works

5.5.1 Incompatibility issue in non-Gaussian process simulation

To completely avoid the incompatibility issue, one might directly construct the power spectral density function of the underlying Gaussian process by matching its corresponding non-Gaussian power spectral density with that estimated from data. Following this proposal, the Clough-Penzien spectrum would be directly constructed for the underlying Gaussian process.

5.5.2 Spatial correlation of the stochastic deterioration model

In Section 5.3 the stochastic deterioration model developed in Chapter 4 was extended to account for spatial correlation. The resulting wire strength can be viewed as a stationary random process in space at any given time. However, the derivation was done assuming the deterioration rate process takes a simpler form, i.e., the O-U process, instead of the previously suggested square-root process. The same derivation may be applied to square-root process but would be much labor-intensive.

Bibliography

[Abdel-Hameed, 1975] Mohamed Abdel-Hameed. A gamma wear process. *Reliability, IEEE Transactions on*, R-24(2):152–153, June 1975.

[Albanese and Campolieti, 2006] Claudio Albanese and Giuseppe Campolieti. *Advanced Derivatives Pricing and Risk Management: Theory, Tools and Hands-on Programming Application*. Academic Press, 2006.

[Barton *et al.*, 2000] Scott Calabrese Barton, Garry W Vermaas, Paul F Duby, Alan C West, and Raimondo Betti. Accelerated corrosion and embrittlement of high-strength bridge wire. *Journal of materials in civil engineering*, 12(1):33–38, 2000.

[Benowitz, 2013] Brett A Benowitz. *Modeling and Simulation of Random Processes and Fields in Civil Engineering and Engineering Mechanics*. PhD thesis, Columbia University, 2013.

[Betti *et al.*, 2005] Raimondo Betti, AC West, G Vermaas, and Y Cao. Corrosion and embrittlement in high-strength wires of suspension bridge cables. *Journal of Bridge Engineering*, 10(2):151–162, 2005.

[Björk, 2009] Tomas Björk. *Arbitrage Theory in Continuous Time (Oxford Finance Series)*. Oxford University Press, 3 edition edition, 4 October 2009.

[Bocchini and Deodatis, 2008] P. Bocchini and G. Deodatis. Critical review and latest developments of a class of simulation algorithms for strongly non-gaussian random fields. *Probabilistic Engineering Mechanics*, 23(4):393–407, 2008.

[Camo, 2003] S. Camo. Probabilistic strength estimates and reliability of damaged parallel wire cables. *Journal of Bridge Engineering*, 8(5):297–311, 2003.

[Cha, 2007] Sung-Hyuk Cha. Comprehensive survey on distance/similarity measures between probability density functions. *City*, 1(2):1, 2007.

[Cocksedge *et al.*, 2010] Charles Cocksedge, Tony Hudson, Beverley Urbans, and Stephen Baron. M48 severn bridge–main cable inspection and rehabilitation. *Proceedings of the ICE-Bridge Engineering*, 163(4):181–195, 2010.

[Dassios and Nagaradjasarma, 2006] A Dassios and J Nagaradjasarma. The square-root process and asian options. *Quant. Finance*, 2006.

[Deeble Sloane *et al.*, 2012] Matthew Jake Deeble Sloane, Raimondo Betti, Gioia Marconi, Ah Lum Hong, and Dyab Khazem. Experimental analysis of a nondestructive corrosion monitoring system for main cables of suspension bridges. *Journal of Bridge Engineering*, 18(7):653–662, 2012.

[Deeble Sloane *et al.*, 2013] M J Deeble Sloane, R Betti, G Marconi, and others. Experimental analysis of a nondestructive corrosion monitoring system for main cables of suspension bridges. *J. Bridge Eng.*, 18(7):653–662, 2013.

[Deodatis and Micaletti, 2001a] George Deodatis and Raymond C Micaletti. Simulation of highly skewed non-gaussian stochastic processes. *Journal of engineering mechanics*, 127(12):1284–1295, 2001.

[Deodatis and Micaletti, 2001b] George Deodatis and Raymond C Micaletti. Simulation of highly skewed Non-Gaussian stochastic processes. *J. Eng. Mech.*, 127(12):1284–1295, 2001.

[Deodatis, 1996a] G. Deodatis. Non-stationary stochastic vector processes: seismic ground motion applications. *Probabilistic Engineering Mechanics*, 11(3):149–167, 1996.

[Deodatis, 1996b] George Deodatis. Non-stationary stochastic vector processes: seismic ground motion applications. *Probab. Eng. Mech.*, 11(3):149–167, July 1996.

[Doane and Seward, 2011] David P Doane and Lori E Seward. Measuring skewness: a forgotten statistic. *Journal of statistics education: an international journal on the teaching and learning of statistics*, 19(2):118, 2011.

[Dufresne, 2001] Daniel Dufresne. *The Integrated Square-root Process.* Centre for Actuarial Studies, Department of Economics, University of Melbourne, 2001.

[Fisher and Lambert, 2011] Jeff Fisher and Paul Lambert. Severn bridge–recent assessment of main suspension cables. In *Taller, Longer, Lighter: IABSE–IASS London Symposium Report, UK*, 2011.

[Frangopol *et al.*, 2004] Dan M Frangopol, Maarten-Jan Kallen, and Jan M Van Noortwijk. Probabilistic models for life-cycle performance of deteriorating structures: review and future directions. *Prog. Struct. Eng. Mater.*, 6(4):197–212, 2004.

[Fu, 1995] Gongkang Fu. Seismic response statistics of sdof system to exponentially modulated coloured input: an explicit solution. *Earthquake engineering & structural dynamics*, 24(10):1355–1370, 1995.

[Gersch and Yonemoto, 1977] W Gersch and J Yonemoto. Synthesis of multivariate random vibration systems: a two-stage least squares ar-ma model approach. *Journal of sound and vibration*, 52(4):553–565, 1977.

[Grigoriu, 1995] Mircea Grigoriu. *Applied non-Gaussian processes: Examples, theory, simulation, linear random vibration, and MATLAB solutions*. Prentice Hall, 1995.

[Grigoriu, 1998] Mircea Grigoriu. Simulation of stationary non-gaussian translation processes. *Journal of engineering mechanics*, 124(2):121–126, 1998.

[Grigoriu, 2002] Mircea Grigoriu. *Stochastic calculus: applications in science and engineering*. Springer Science & Business Media, 2002.

[Grigoriu, 2009] M Grigoriu. Existence and construction of translation models for stationary non-gaussian processes. *Probab. Eng. Mech.*, 24(4):545–551, October 2009.

[Haight *et al.*, 1997] R.Q. Haight, D.P. Billington, and D. Khazem. Cable safety factors for four suspension bridge. *Journal of Bridge Engineering*, 2:157, 1997.

[Heutink *et al.*, 2004] A Heutink, A Van Beek, J M Van Noortwijk, H E Klatter, and A Barendregt. Environment-friendly maintenance of protective paint systems at lowest costs. In *XXVII FATIPEC Congress, 19-21 April 2004, Aix-en-Provence, France*, pages 351–364. progis.nl, 2004.

[Karhunen, 1947] Kari Karhunen. *Über lineare Methoden in der Wahrscheinlichkeitsrechnung*, volume 37. Universitat Helsinki, 1947.

[Kolmogorov and Fomin, 1975] Andrei Nikolaevich Kolmogorov and Sergeĭ Vasilevich Fomin. *Introductory real analysis*. Courier Dover Publications, 1975.

[Kung and Pecknold, 1982] Shyh-Yuan Kung and DA Pecknold. Effect of ground motion characteristics on the seismic response of torsionally coupled elastic systems. Technical report, University of Illinois Engineering Experiment Station. College of Engineering. University of Illinois at Urbana-Champaign., 1982.

[Loeve, 1978] Michel Loeve. Probability theory, vol. ii. *Graduate texts in mathematics*, 46:0–387, 1978.

[Mahmoud, 2006] Khaled Mahmoud. *Advances in Cable-Supported Bridges: Selected Papers, 5th International Cable-Supported Bridge Operator's Conference, New York City, 28-29 August, 2006*. CRC Press, 2006.

[Matteo, 1994] J. Matteo. Safety analysis of suspension-bridge cables: Williamsburg bridge. *Journal of Structural Engineering*, 120:3197, 1994.

[Montoya, 2012] Arturo Montoya. *A validated methodology to estimate the reliability and safety of suspension bridge cables*. PhD thesis, Columbia University, 2012.

[Nicolai *et al.*, 2007] Robin P Nicolai, Rommert Dekker, and Jan M van Noortwijk. A comparison of models for measurable deterioration: An application to coatings on steel structures. *Reliab. Eng. Syst. Saf.*, 92(12):1635–1650, December 2007.

[Øksendal, 2003] Bernt Øksendal. *Stochastic differential equations*. Springer, 2003.

[Perry, 1998] R.J. Perry. Estimating strength of the williamsburg bridge suspension cables. *The American Statistician*, 52(3):211–217, 1998.

[Price, 1958] R Price. A useful theorem for nonlinear devices having gaussian inputs. *IRE Transactions on Information Theory*, 4(2):69–72, June 1958.

[Santner *et al.*, 2013] Thomas J Santner, Brian J Williams, and William I Notz. *The design and analysis of computer experiments*. Springer Science & Business Media, 2013.

[Shi *et al.*, 2007] Y. Shi, G. Deodatis, and R. Betti. Random field-based approach for strength evaluation of suspension bridge cables. *Journal of Structural Engineering*, 133:1690, 2007.

[Shi, 2006] Y Shi. *Simulation of stationary non-Gaussian stochastic processes/fields with application in suspension bridge cable strength estimation*. PhD thesis, Ph. D. thesis, Columbia Univ., New York, 2006.

[Shields *et al.*, 2011] MD Shields, G Deodatis, and P Bocchini. A simple and efficient methodology to approximate a general non-gaussian stationary stochastic process by a translation process. *Probabilistic Engineering Mechanics*, 26(4):511–519, 2011.

[Shinozuka and Jan, 1972] Masanobu Shinozuka and C-M Jan. Digital simulation of random processes and its applications. *Journal of sound and vibration*, 25(1):111–128, 1972.

[Steinman *et al.*, 1988] Steinman, Boynton, Gronquist, and Birdsall. Williamsburg bridge cable investigation program: Final report. Technical report, Columbia University, New York, 1988.

[Stoica and Moses, 2005] Petre Stoica and Randolph L Moses. *Spectral analysis of signals*, volume 452. Pearson Prentice Hall Upper Saddle River, NJ, 2005.

[Tankov, 2003] Peter Tankov. *Financial modelling with jump processes*, volume 2. CRC press, 2003.

[van Noortwijk, 2009] J M van Noortwijk. A survey of the application of gamma processes in maintenance. *Reliab. Eng. Syst. Saf.*, 94(1):2–21, January 2009.

[Yamazaki and Shinozuka, 1988] Fumio Yamazaki and Masanobu Shinozuka. Digital generation of non-gaussian stochastic fields. *Journal of Engineering Mechanics*, 114(7):1183–1197, 1988.

Appendix A

Tensile testing results from Carleton Lab

Results of the tensile testing performed in the Carleton Lab as part of this research are presented in the following sections. Measurements include gross diameter, net diameter which is diameter after removing zinc coating on both ends of the wire specimen, and the diameter at the necking area. Test results include Young's moduli, maximum stress (engineering stress), yield stress, and stress at 2.5% strain.

A.1 New wires

A total of 5 new wires were tested and 65 test results were obtained, as presented in Table A.1.

Table A.1: Tensile testing results of new wires

Test	Wire	d_{gross}(in)	d_{net}(in)	d_{neck}(in)	E(psi)	$\sigma_{\max}$(ksi)	σ_{yield}(ksi)	$\sigma_{2.5\%}(ksi)$
1	1N	0.1955	0.1919	0.1565	28278	250.62	192.85	233.46
2	1N	0.1953	0.1919	0.1555	27499	251.68	190.16	233.46
3	1N	0.1951	0.1918	0.1548	26956	252.56	190.35	235.01
4	1N	0.1950	0.1919	0.1568	26963	253.88	189.18	234.93
5	1N	0.1953	0.1918	0.1573	26246	252.84	188.56	233.95
6	1N	0.1954	0.1918	0.1578	26584	251.93	187.30	233.28
7	1N	0.1954	0.1921	0.1545	26328	253.74	190.89	235.17
8	1N	0.1951	0.1918	0.1540	26644	255.74	191.82	236.99
9	1N	0.1950	0.1915	0.1525	27004	255.77	191.77	237.27
10	1N	0.1953	0.1918	0.1570	27259	252.49	190.08	234.70
11	1N	0.1950	0.1918	0.1565	27320	253.26	191.20	236.66
12	1N	0.1958	0.1918	0.1530	27127	254.02	190.76	235.26
13	1N	0.1956	0.1916	0.1525	26559	254.77	190.62	236.05
14	2N	0.1954	0.1915	0.1575	26295	252.29	186.29	232.81
15	2N	0.1955	0.1916	0.1570	26282	252.23	187.31	233.05
16	2N	0.1954	0.1918	0.1565	26920	254.33	190.01	235.39
17	2N	0.1954	0.1919	0.1550	26135	255.50	190.12	235.75
18	2N	0.1955	0.1919	0.1568	26533	254.77	189.05	235.11
19	2N	0.1959	0.1916	0.1605	25441	252.40	187.32	232.79
20	2N	0.1953	0.1915	0.1585	25703	253.81	188.05	234.18
21	2N	0.1953	0.1918	0.1588	26507	254.02	187.75	234.32
22	2N	0.1959	0.1919	0.1605	26173	252.47	187.13	233.22

Continued on next page...

Test	Wire	d_{gross}(in)	d_{net}(in)	d_{neck}(in)	E(psi)	$\sigma_{\max}$(ksi)	σ_{yield}(ksi)	$\sigma_{2.5\%}$(ksi)
23	2N	0.1955	0.1921	0.1645	25694	249.32	184.26	230.92
24	2N	0.1948	0.1915	0.1600	26868	255.68	189.16	235.90
25	2N	0.1955	0.1915	0.1608	25619	250.87	185.49	231.60
26	2N	0.1954	0.1915	0.1573	25647	255.57	188.90	235.63
27	3N	0.1945	0.1913	0.1543	26502	257.08	188.49	236.93
28	3N	0.1951	0.1913	0.1585	25833	253.27	185.42	233.25
29	3N	0.1945	0.1913	0.1580	25961	255.09	186.95	234.81
30	3N	0.1946	0.1913	0.1578	26219	255.12	187.11	234.98
31	3N	0.1951	0.1911	0.1583	26049	253.13	185.51	233.15
32	3N	0.1951	0.1913	0.1568	26824	253.11	186.52	233.37
33	3N	0.1949	0.1915	0.1543	27025	253.88	186.78	234.11
34	3N	0.1948	0.1911	0.1538	27161	254.29	187.52	234.43
35	3N	0.1949	0.1913	0.1560	26829	254.19	187.12	234.31
36	3N	0.1948	0.1911	0.1550	27190	253.60	186.28	233.76
37	3N	0.1945	0.1914	0.1560	27131	255.35	189.14	236.34
38	3N	0.1948	0.1913	0.1523	27218	256.35	189.52	236.60
39	3N	0.1945	0.1911	0.1513	27583	257.43	190.96	237.83
40	4N	0.1946	0.1911	0.1550	26608	255.94	188.53	236.21
41	4N	0.1948	0.1909	0.1553	26212	255.36	188.89	235.87
42	4N	0.1945	0.1910	0.1543	26739	258.04	190.77	238.44
43	4N	0.1955	0.1911	0.1540	26300	255.63	198.73	237.88
44	4N	0.1946	0.1914	0.1543	26634	258.12	191.40	238.45
45	4N	0.1944	0.1913	0.1603	26750	257.83	190.02	237.87

Continued on next page...

Test	Wire	d_{gross}(in)	d_{net}(in)	d_{neck}(in)	E(psi)	$\sigma_{\max}$(ksi)	σ_{yield}(ksi)	$\sigma_{2.5\%}$(ksi)
46	4N	0.1950	0.1914	0.1623	25946	252.79	186.02	233.35
47	4N	0.1948	0.1911	0.1558	26506	256.99	190.54	237.94
48	4N	0.1949	0.1911	0.1555	27015	257.79	190.99	238.51
49	4N	0.1948	0.1914	0.1560	26516	256.79	189.99	237.31
50	4N	0.1946	0.1909	0.1550	26188	255.87	189.06	236.12
51	4N	0.1949	0.1911	0.1545	26335	255.43	188.97	235.78
52	4N	0.1953	0.1910	0.1555	26169	254.99	188.34	235.21
53	5N	0.1951	0.1913	0.1550	25625	251.20	184.88	232.71
54	5N	0.1951	0.1914	0.1538	26159	255.87	188.64	236.47
55	5N	0.1946	0.1909	0.1540	26406	258.17	190.41	238.07
56	5N	0.1948	0.1910	0.1518	26015	257.04	189.74	237.26
57	5N	0.1944	0.1911	0.1558	26081	256.14	188.55	236.30
58	5N	0.1948	0.1914	0.1545	25980	255.62	187.81	235.68
59	5N	0.1946	0.1909	0.1545	26320	256.35	188.31	236.16
60	5N	0.1945	0.1914	0.1543	26627	256.37	188.91	236.53
61	5N	0.1949	0.1911	0.1550	26539	255.22	188.08	235.41
62	5N	0.1954	0.1911	0.1560	26688	254.00	186.93	234.35
63	5N	0.1951	0.1910	0.1568	26542	254.65	187.34	234.95
64	5N	0.1951	0.1911	0.1585	26959	254.56	187.53	234.95
65	5N	0.1948	0.1915	0.1613	26367	255.18	187.79	235.21

A.2 Artificially corroded wires

A total of 93 artificially corroded wires were tested and 1209 test results were obtained, as presented in Table A.2. The wires are labeled according to their location in the cable. There are 12 wires that were taken from the surface of the cable, which are labeled as 100 to 1200, as shown in Figure A.1. The remaining 81 wires were taken from the inside of the cable, and they are labeled in the following format, for example:

16R5

The first number is the strand number, as shown in Figure A.2. The letter indicates whether the strand is from the left or right part of the cable. The second number indicates the location of the wire within the strand, as shown in Figure A.3.

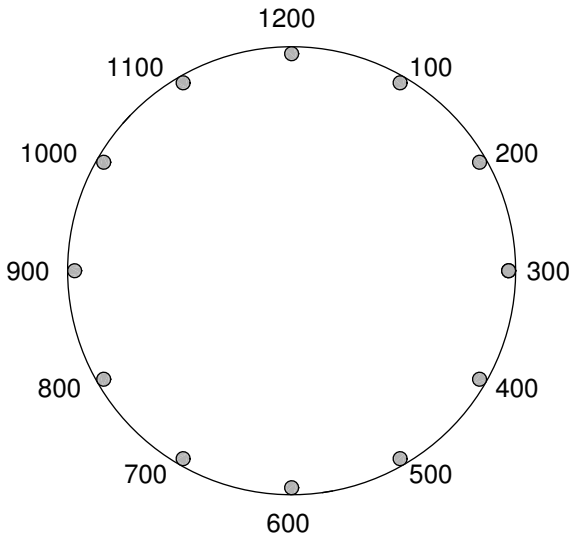

Figure A.1: Numbering of wires on the surface of the cable.

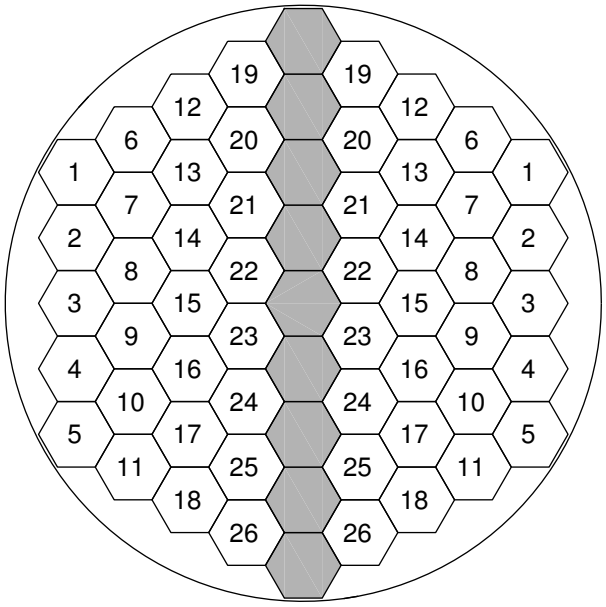

Figure A.2: Numbering of strands.

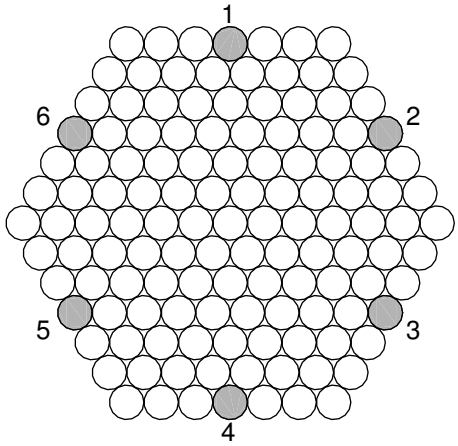

Figure A.3: Numbering of wires within a strand.

Table A.2: Tensile testing results of artifially corroded wires

Test	Wire	d_{gross}(in)	d_{net}(in)	d_{neck}(in)	E(psi)	$\sigma_{\max}$(ksi)	σ_{yield}(ksi)	$\sigma_{2.5\%}(ksi)$
1	100	0.1960	0.1918	0.1603	25484	251.72	184.96	231.79
2	100	0.1968	0.1921	0.1565	25518	251.44	185.99	232.22

Continued on next page...

Test	Wire	d_{gross}(in)	d_{net}(in)	d_{neck}(in)	E(psi)	$\sigma_{\max}$(ksi)	σ_{yield}(ksi)	$\sigma_{2.5\%}$(ksi)
3	100	0.1968	0.1916	0.1660	26270	251.90	187.44	232.60
4	100	0.1971	0.1918	0.1565	27139	249.91	189.57	232.37
5	100	0.1975	0.1918	0.1568	26948	249.52	188.29	231.13
6	100	0.1979	0.1918	0.1555	27237	247.90	189.83	230.07
7	100	0.1963	0.1920	0.1630	26997	251.48	189.25	232.91
8	100	0.1940	0.1911	0.1658	27266	241.46	190.42	233.38
9	100	0.1973	0.1909	0.1675	36028	234.53	187.36	234.41
10	100	0.1971	0.1916	0.1568	25669	249.05	185.51	230.22
11	100	0.1966	0.1918	0.1588	26059	251.24	185.61	231.47
12	100	0.1955	0.1914	0.1573	26621	254.26	188.08	234.69
13	100	0.1959	0.1918	0.1575	25902	251.78	184.96	232.00
14	200	0.1959	0.1918	0.1615	24882	254.69	186.18	233.39
15	200	0.1973	0.1920	0.1630	24250	250.32	184.05	229.81
16	200	0.1985	0.1920	0.1683	23778	243.89	180.05	224.71
17	200	0.1985	0.1921	0.1673	23967	243.80	180.86	226.05
18	200	0.1978	0.1920	0.1643	24300	246.22	183.07	227.96
19	200	0.1976	0.1919	0.1663	24720	248.48	184.03	228.60
20	200	0.1998	0.1919	0.1695	23627	242.99	180.10	223.38
21	200	0.1993	0.1911	0.1640	23913	240.73	180.83	224.48
22	200	0.1975	0.1918	0.1630	24913	249.93	184.94	230.63
23	200	0.1969	0.1920	0.1615	24807	252.55	185.38	231.88
24	200	0.1963	0.1919	0.1643	24865	252.65	184.36	231.84
25	200	0.1979	0.1919	0.1613	23890	247.95	181.04	227.16

Continued on next page...

Test	Wire	d_{gross}(in)	d_{net}(in)	d_{neck}(in)	E(psi)	$\sigma_{\max}$(ksi)	σ_{yield}(ksi)	$\sigma_{2.5\%}$(ksi)
26	200	0.1970	0.1920	0.1625	24115	250.51	183.30	229.62
27	300	0.1964	0.1919	0.1585	26292	251.83	186.65	232.48
28	300	0.1963	0.1918	0.1590	26964	251.41	187.65	232.80
29	300	0.1980	0.1918	0.1608	26296	246.95	185.30	228.93
30	300	0.1975	0.1916	0.1623	26249	249.84	187.17	231.66
31	300	0.1976	0.1919	0.1590	26732	250.82	187.99	232.13
32	300	0.1966	0.1919	0.1613	27230	252.88	190.95	234.43
33	300	0.1976	0.1916	0.1605	26678	247.58	187.07	229.89
34	300	0.1970	0.1916	0.1635	26469	246.48	184.89	229.27
35	300	0.1969	0.1919	0.1613	27086	248.26	188.20	231.34
36	300	0.1964	0.1916	0.1645	27443	250.19	188.46	231.68
37	300	0.1953	0.1920	0.1613	38994	254.57	201.94	237.22
38	300	0.1955	0.1919	0.1583	27128	256.01	190.75	236.60
39	300	0.1950	0.1919	0.1555	26968	257.61	191.08	238.07
40	400	0.1956	0.1919	0.1573	27240	252.60	188.37	234.08
41	400	0.1961	0.1915	0.1700	27700	250.34	191.16	232.91
42	400	0.1964	0.1914	0.1593	26943	249.80	188.19	231.72
43	400	0.1960	0.1916	0.1590	27709	250.64	190.73	232.99
44	400	0.1979	0.1951	0.1600	26505	246.54	185.20	228.61
45	400	0.1980	0.1919	0.1585	26085	246.14	184.98	228.10
46	400	0.1966	0.1915	0.1580	27156	249.47	188.75	231.82
47	400	0.1998	0.1916	0.1560	26449	243.16	186.91	226.53
48	400	0.1963	0.1919	0.1540	27254	253.44	191.13	235.14

Continued on next page...

Test	Wire	d_{gross}(in)	d_{net}(in)	d_{neck}(in)	E(psi)	$\sigma_{\max}$(ksi)	σ_{yield}(ksi)	$\sigma_{2.5\%}$(ksi)
49	400	0.1958	0.1916	0.1555	28101	254.36	193.83	236.07
50	400	0.1961	0.1918	0.1550	27124	251.36	190.30	234.30
51	400	0.1959	0.1921	0.1593	26865	250.53	187.60	241.62
52	400	0.1950	0.1913	0.1613	28020	253.90	190.87	235.69
53	500	0.1960	0.1919	0.1598	24986	249.97	180.98	228.89
54	500	0.1975	0.1918	0.1630	24177	245.41	178.58	224.69
55	500	0.1973	0.1920	0.1630	24578	246.22	180.84	226.67
56	500	0.1974	0.1918	0.1593	24809	248.86	181.76	228.20
57	500	0.1996	0.1915	0.1588	23595	242.82	178.39	222.54
58	500	0.1996	0.1914	0.1570	23410	238.67	176.23	220.19
59	500	0.1965	0.1919	0.1615	24648	246.33	180.03	227.07
60	500	0.1993	0.1920	0.1623	23617	240.16	175.82	220.85
61	500	0.1970	0.1919	0.1588	24947	248.71	181.10	227.95
62	500	0.1968	0.1916	0.1575	24586	249.42	181.99	228.45
63	500	0.1950	0.1918	0.1568	25629	254.17	184.59	232.86
64	500	0.1955	0.1919	0.1565	25566	254.20	185.16	232.99
65	500	0.1958	0.1914	0.1585	25445	254.07	185.26	232.71
66	600	0.1968	0.1920	0.1555	25956	250.60	184.16	229.42
67	600	0.2020	0.1920	0.1565	23802	237.56	175.02	217.23
68	600	0.1983	0.1918	0.1550	25846	245.90	181.43	225.65
69	600	0.2000	0.1920	0.1635	24317	240.19	176.32	220.06
70	600	0.1994	0.1923	0.1650	24573	241.75	178.70	221.98
71	600	0.1976	0.1920	0.1558	25329	246.17	180.62	225.64

Continued on next page...

Test	Wire	d_{gross}(in)	d_{net}(in)	d_{neck}(in)	E(psi)	σ_{max}(ksi)	σ_{yield}(ksi)	$\sigma_{2.5\%}$(ksi)
72	600	0.2011	0.1920	0.1633	24100	236.91	175.71	217.45
73	600	0.1984	0.1923	0.1575	25295	243.84	179.73	223.78
74	600	0.1983	0.1921	0.1580	25390	244.02	179.00	223.76
75	600	0.1969	0.1920	0.1658	25666	247.82	182.12	227.15
76	600	0.1974	0.1921	0.1565	25832	246.39	181.26	226.03
77	600	0.1968	0.1923	0.1600	25968	247.82	182.28	227.32
78	600	0.1971	0.1921	0.1550	26080	248.89	182.78	228.21
79	700	0.1968	0.1921	0.1580	26347	249.36	184.74	229.98
80	700	0.1956	0.1920	0.1590	27140	252.85	187.14	233.32
81	700	0.1963	0.1919	0.1588	26352	251.18	185.45	231.63
82	700	0.1960	0.1918	0.1583	26373	251.76	185.88	232.25
83	700	0.1983	0.1919	0.1553	26177	247.68	183.87	228.50
84	700	0.1960	0.1924	0.1550	27300	253.85	189.45	234.36
85	700	0.1953	0.1916	0.1605	27200	256.13	190.01	236.26
86	700	0.1956	0.1920	0.1575	26800	254.01	187.58	234.18
87	700	0.1950	0.1920	0.1663	27246	253.80	187.47	234.29
88	700	0.1964	0.1915	0.1668	26914	251.65	186.16	232.11
89	700	0.1963	0.1920	0.1670	26589	251.01	185.88	231.60
90	700	0.1950	0.1921	0.1575	27138	254.34	186.88	234.73
91	700	0.1959	0.1920	0.1605	26060	251.44	185.18	232.01
92	800	0.1955	0.1919	0.1800	26187	256.96	189.72	237.14
93	800	0.1964	0.1914	0.1543	25885	256.95	190.51	236.76
94	800	0.1969	0.1920	0.1538	25600	255.36	189.90	235.34

Continued on next page...

Test	Wire	d_{gross}(in)	d_{net}(in)	d_{neck}(in)	E(psi)	$\sigma_{\max}$(ksi)	σ_{yield}(ksi)	$\sigma_{2.5\%}$(ksi)
95	800	0.1975	0.1916	0.1580	26017	250.58	186.12	232.13
96	800	0.1976	0.1921	0.1573	26455	250.64	187.61	231.82
97	800	0.1968	0.1918	0.1543	25534	255.10	188.99	234.97
98	800	0.1963	0.1916	0.1553	25877	256.99	189.95	236.86
99	800	0.1969	0.1918	0.1550	25294	255.39	189.57	235.17
100	800	0.1955	0.1915	0.1530	26113	259.63	191.92	239.31
101	800	0.1964	0.1916	0.1600	25696	256.87	190.73	237.06
102	800	0.1961	0.1920	0.1525	25888	258.71	191.36	238.09
103	800	0.1963	0.1919	0.1528	25765	257.42	189.95	236.94
104	800	0.1954	0.1915	0.1543	25786	258.26	189.23	237.41
105	900	0.1956	0.1919	0.1535	26248	251.69	184.75	232.02
106	900	0.1971	0.1919	0.1545	24975	247.78	182.96	228.09
107	900	0.1979	0.1915	0.1578	24808	246.13	182.54	226.66
108	900	0.1996	0.1916	0.1565	24380	241.92	179.82	222.98
109	900	0.1989	0.1914	0.1545	24584	243.41	180.27	224.39
110	900	0.1980	0.1920	0.1558	24663	245.97	182.24	226.78
111	900	0.1979	0.1913	0.1535	24907	248.59	185.04	229.01
112	900	0.1980	0.1918	0.1560	25384	248.51	184.11	228.95
113	900	0.1969	0.1918	0.1630	25714	251.17	186.23	231.52
114	900	0.1966	0.1919	0.1560	25482	249.65	185.10	231.05
115	900	0.1969	0.1916	0.1553	25442	249.69	184.06	230.00
116	900	0.1984	0.1920	0.1615	24923	243.64	180.58	224.95
117	900	0.1968	0.1919	0.1540	26282	248.73	184.32	229.66

Continued on next page...

Test	Wire	d_{gross}(in)	d_{net}(in)	d_{neck}(in)	E(psi)	$\sigma_{\max}$(ksi)	σ_{yield}(ksi)	$\sigma_{2.5\%}$(ksi)
118	1100	0.1963	0.1920	0.1635	25339	250.52	182.62	229.95
119	1100	0.1963	0.1920	0.1598	24920	250.86	183.46	230.07
120	1100	0.1975	0.1919	0.1630	25514	247.65	184.22	228.03
121	1100	0.1975	0.1916	0.1615	25833	246.29	184.29	227.82
122	1100	0.1978	0.1920	0.1640	25936	246.58	183.95	227.38
123	1100	0.1988	0.1918	0.1605	27185	243.96	189.82	226.60
124	1100	0.1976	0.1919	0.1605	27059	244.92	186.72	227.74
125	1100	0.1944	0.1905	0.1650	28046	228.68	191.74	NaN
126	1100	0.1975	0.1891	0.1563	27173	232.91	187.55	225.34
127	1100	0.1980	0.1921	0.1590	27108	246.44	187.81	228.62
128	1100	0.1976	0.1919	0.1650	26213	249.09	184.39	229.45
129	1100	0.1968	0.1919	0.1615	24881	251.55	184.36	230.82
130	1100	0.1969	0.1916	0.1625	27861	247.33	198.71	230.79
131	1200	0.1971	0.1921	0.1588	25184	249.57	182.97	229.03
132	1200	0.1968	0.1919	0.1590	25112	250.48	183.74	229.99
133	1200	0.2001	0.1918	0.1600	25067	242.08	181.41	223.18
134	1200	0.1988	0.1919	0.1580	25823	243.98	184.81	226.31
135	1200	0.1990	0.1920	0.1588	25706	245.27	184.41	226.16
136	1200	0.1985	0.1919	0.1630	27778	244.24	201.37	229.35
137	1200	0.1980	0.1920	0.1580	25911	249.20	187.61	230.18
138	1200	0.1979	0.1921	0.1588	28073	244.31	210.35	234.31
139	1200	0.1968	0.1921	0.1623	27820	241.14	208.16	235.14
140	1200	0.1974	0.1921	0.1598	24918	250.35	185.43	230.78

Continued on next page...

Test	Wire	d_{gross}(in)	d_{net}(in)	d_{neck}(in)	E(psi)	σ_{max}(ksi)	σ_{yield}(ksi)	$\sigma_{2.5\%}$(ksi)
141	1200	0.1965	0.1920	0.1598	25674	254.69	187.25	234.22
142	1200	0.1960	0.1919	0.1575	25349	256.30	188.76	235.44
143	1200	0.1958	0.1918	0.1598	25397	256.18	188.09	235.28
144	16R5	0.1955	0.1920	0.1570	26057	251.71	184.10	231.36
145	16R5	0.1975	0.1916	0.1570	25988	249.31	185.16	229.51
146	16R5	0.1961	0.1925	0.1555	26505	254.82	189.00	234.80
147	16R5	0.1956	0.1920	0.1560	26292	256.38	188.84	235.83
148	16R5	0.1960	0.1920	0.1680	26774	253.44	187.52	233.64
149	16R5	0.1971	0.1919	0.1610	26785	248.93	186.60	229.74
150	16R5	0.1979	0.1918	0.1600	25834	248.94	184.92	229.42
151	16R5	0.1979	0.1915	0.1570	25025	249.25	183.66	229.11
152	16R5	0.1970	0.1913	0.1580	26210	251.04	185.75	231.13
153	16R5	0.1973	0.1915	0.1590	26346	250.29	185.38	230.45
154	16R5	0.1961	0.1920	0.1605	27322	253.83	188.70	234.05
155	16R5	0.1958	0.1918	0.1600	26460	255.50	188.00	234.99
156	16R5	0.1948	0.1914	0.1575	26741	257.77	188.27	236.85
157	13R1	0.1963	0.1920	0.1528	25343	253.22	184.83	232.23
158	13R1	0.1968	0.1925	0.1520	25440	253.98	186.80	233.14
159	13R1	0.1966	0.1919	0.1505	25872	255.72	189.35	234.99
160	13R1	0.1965	0.1911	0.1530	26565	256.40	190.03	235.74
161	13R1	0.1966	0.1950	0.1555	26598	255.85	189.86	235.48
162	13R1	0.1968	0.1915	0.1570	26517	253.08	189.30	233.51
163	13R1	0.1968	0.1918	0.1545	26477	253.14	188.50	233.67

Continued on next page...

Test	Wire	d_{gross}(in)	d_{net}(in)	d_{neck}(in)	E(psi)	$\sigma_{\max}$(ksi)	σ_{yield}(ksi)	$\sigma_{2.5\%}$(ksi)
164	13R1	0.1968	0.1918	0.1540	26277	253.84	188.38	234.00
165	13R1	0.2136	0.1918	0.1538	19128	216.19	164.11	198.58
166	13R1	0.1968	0.1920	0.1555	25910	256.14	188.46	235.23
167	13R1	0.1959	0.1925	0.1545	26023	254.83	186.93	233.74
168	13R1	0.1963	0.1920	0.1555	25152	252.75	185.25	231.75
169	13R1	0.1959	0.1920	0.1548	24932	252.71	184.35	231.43
170	11R4	0.1968	0.1919	0.1590	24742	247.59	180.75	227.42
171	11R4	0.1979	0.1919	0.1568	24521	247.71	183.17	228.30
172	11R4	0.1961	0.1923	0.1585	25439	253.30	185.62	232.62
173	11R4	0.1970	0.1919	0.1578	24877	252.26	185.55	231.55
174	11R4	0.1993	0.1919	0.1590	22926	245.84	182.42	225.45
175	11R4	0.1979	0.1915	0.1600	24079	247.23	181.96	227.08
176	11R4	0.1979	0.1923	0.1623	24118	247.51	182.22	227.44
177	11R4	0.1974	0.1920	0.1600	24105	248.97	183.33	228.64
178	11R4	0.1961	0.1918	0.1615	25010	252.09	184.43	231.35
179	11R4	0.1965	0.1919	0.1605	24744	251.56	184.45	230.82
180	11R4	0.1960	0.1921	0.1593	25254	253.02	185.47	232.19
181	11R4	0.1958	0.1919	0.1590	25034	254.06	186.11	233.17
182	11R4	0.1953	0.1918	0.1578	25147	254.65	186.41	233.94
183	26R3	0.1955	0.1916	0.1573	32896	253.46	195.45	239.13
184	26R3	0.1961	0.1919	0.1575	26320	251.84	187.33	232.05
185	26R3	0.1964	0.1916	0.1598	29265	251.01	183.57	231.41
186	26R3	0.1959	0.1919	0.1655	34961	251.94	171.00	233.17

Continued on next page...

Test	Wire	d_{gross}(in)	d_{net}(in)	d_{neck}(in)	E(psi)	$\sigma_{\max}$(ksi)	σ_{yield}(ksi)	$\sigma_{2.5\%}$(ksi)
187	26R3	0.1955	0.1919	0.1573	26712	253.52	187.20	234.13
188	26R3	0.1958	0.1921	0.1580	26299	255.23	188.57	235.09
189	26R3	0.1961	0.1920	0.1555	26638	254.15	188.17	234.57
190	26R3	0.1968	0.1920	0.1558	25787	251.58	186.80	232.40
191	26R3	0.1960	0.1918	0.1548	26421	252.92	187.76	233.41
192	26R3	0.1959	0.1918	0.1585	26426	252.60	187.23	233.10
193	26R3	0.1951	0.1915	0.1525	26583	256.81	189.49	236.60
194	26R3	0.1961	0.1919	0.1550	26294	253.63	186.56	233.49
195	26R3	0.1958	0.1915	0.1550	25696	253.44	186.42	233.59
196	10R5	0.1965	0.1920	0.1615	24767	252.67	184.47	231.52
197	10R5	0.1963	0.1916	0.1680	25043	253.09	185.01	232.14
198	10R5	0.1966	0.1918	0.1653	25308	252.22	183.96	231.36
199	10R5	0.1985	0.1918	0.1630	23945	247.22	181.14	226.65
200	10R5	0.1980	0.1919	0.1625	24514	188.46	181.61	NaN
201	10R5	0.1994	0.1919	0.1605	24139	246.46	181.38	226.02
202	10R5	0.1981	0.1920	0.1615	24483	249.56	183.84	229.22
203	10R5	0.1975	0.1918	0.1588	24761	250.48	183.39	230.03
204	10R5	0.1983	0.1919	0.1578	24330	249.50	183.12	228.84
205	10R5	0.1964	0.1923	0.1585	25060	254.02	185.57	232.94
206	10R5	0.1956	0.1919	0.1553	25454	256.23	187.23	234.89
207	10R5	0.1956	0.1919	0.1613	25097	253.32	185.13	232.87
208	10R5	0.1961	0.1920	0.1610	24779	253.25	184.75	232.12
209	1R3	0.1961	0.1920	0.1548	25545	253.01	185.31	232.47

Continued on next page...

Test	Wire	d_{gross}(in)	d_{net}(in)	d_{neck}(in)	E(psi)	σ_{max}(ksi)	σ_{yield}(ksi)	$\sigma_{2.5\%}$(ksi)
210	1R3	0.1995	0.1918	0.1608	24166	243.32	179.83	223.38
211	1R3	0.1973	0.1919	0.1563	24834	248.97	183.21	228.52
212	1R3	0.1986	0.1913	0.1588	25845	245.06	182.28	225.66
213	1R3	0.1966	0.1913	0.1580	26211	249.78	185.54	230.06
214	1R3	0.1974	0.1911	0.1555	26283	248.19	185.79	228.90
215	1R3	0.1965	0.1881	0.1585	26898	250.02	187.53	230.85
216	1R3	0.2014	0.1920	0.1580	24667	238.11	178.45	219.47
217	1R3	0.1976	0.1915	0.1580	25119	247.86	183.13	227.83
218	1R3	0.1980	0.1913	0.1550	24668	246.98	182.58	226.76
219	1R3	0.1968	0.1913	0.1545	25577	251.91	185.68	231.33
220	1R3	0.1968	0.1916	0.1553	25690	252.44	186.42	231.88
221	1R3	0.1976	0.1914	0.1593	25206	249.85	184.79	229.65
222	5R3	0.1953	0.1918	0.1535	23499	231.90	177.37	225.27
223	5R3	0.1969	0.1916	0.1728	25207	218.83	185.75	NaN
224	5R3	0.1974	0.1919	0.1545	25166	253.21	188.04	233.44
225	5R3	0.1968	0.1915	0.1580	25834	254.84	188.99	235.18
226	5R3	0.1970	0.1915	0.1593	25459	254.01	188.77	234.19
227	5R3	0.1968	0.1915	0.1580	25453	254.15	188.51	234.44
228	5R3	0.1964	0.1916	0.1570	25650	254.84	189.08	234.94
229	5R3	0.1970	0.1915	0.1618	25057	250.52	186.47	231.84
230	5R3	0.1950	0.1916	0.1613	25826	257.17	189.67	236.90
231	5R3	0.1955	0.1915	0.1615	25511	255.86	189.58	236.15
232	5R3	0.1954	0.1910	0.1603	26035	257.79	190.43	245.32

Continued on next page...

Test	Wire	d_{gross}(in)	d_{net}(in)	d_{neck}(in)	E(psi)	$\sigma_{\max}$(ksi)	σ_{yield}(ksi)	$\sigma_{2.5\%}$(ksi)
233	5R3	0.1960	0.1915	0.1585	25039	255.28	189.39	243.41
234	5R3	0.1955	0.1915	0.1670	25336	255.00	187.34	234.75
235	2R3	0.1951	0.1915	0.1593	26241	254.83	186.90	234.75
236	2R3	0.1956	0.1915	0.1595	25806	253.18	186.30	233.21
237	2R3	0.1973	0.1916	0.1605	25294	249.78	184.40	230.20
238	2R3	0.1966	0.1923	0.1610	25620	251.10	185.59	231.50
239	2R3	0.1971	0.1916	0.1648	25589	249.67	184.17	230.18
240	2R3	0.1955	0.1920	0.1600	25969	253.81	187.96	233.83
241	2R3	0.1968	0.1919	0.1598	25971	251.03	185.28	231.38
242	2R3	0.1963	0.1924	0.1623	21596	251.69	190.71	230.74
243	2R3	0.1978	0.1918	0.1685	25282	247.31	182.95	228.33
244	2R3	0.1958	0.1919	0.1583	26141	254.74	188.39	235.07
245	2R3	0.1956	0.1911	0.1603	26437	256.13	189.44	236.06
246	2R3	0.1951	0.1919	0.1595	26593	256.25	189.62	237.13
247	2R3	0.1963	0.1919	0.1598	26101	253.92	187.41	234.16
248	15R3	0.1986	0.1919	0.1635	24580	249.26	183.57	228.87
249	15R3	0.1980	0.1918	0.1605	24044	250.03	183.57	229.28
250	15R3	0.1978	0.1914	0.1675	24676	249.43	182.86	228.86
251	15R3	0.1978	0.1913	0.1648	24480	249.13	183.02	228.79
252	15R3	0.1973	0.1916	0.1648	24875	249.85	184.31	230.27
253	15R3	0.1976	0.1915	0.1635	24721	249.14	184.19	229.20
254	15R3	0.1979	0.1916	0.1623	24393	248.51	182.65	228.17
255	15R3	0.1988	0.1915	0.1618	24082	245.45	181.31	226.11

Continued on next page...

Test	Wire	d_{gross}(in)	d_{net}(in)	d_{neck}(in)	E(psi)	$\sigma_{\max}$(ksi)	σ_{yield}(ksi)	$\sigma_{2.5\%}$(ksi)
256	15R3	0.1969	0.1916	0.1638	24866	251.13	184.88	231.35
257	15R3	0.1968	0.1918	0.1603	24762	252.44	184.75	231.62
258	15R3	0.1980	0.1919	0.1588	24296	249.31	182.72	228.65
259	15R3	0.1958	0.1914	0.1863	25609	257.13	188.16	235.99
260	15R3	0.1973	0.1920	0.1583	24892	253.51	185.89	232.52
261	23R1	0.1953	0.1913	0.1568	26246	255.29	188.58	235.13
262	23R1	0.1958	0.1914	0.1603	25448	252.16	186.01	232.27
263	23R1	0.1963	0.1920	0.1565	25710	252.56	187.18	232.30
264	23R1	0.1961	0.1915	0.1548	26980	253.35	188.61	233.74
265	23R1	0.1979	0.1918	0.1565	25787	248.47	185.34	229.61
266	23R1	0.1983	0.1918	0.1578	25929	247.97	185.64	228.71
267	23R1	0.1968	0.1914	0.1555	25753	250.50	186.26	231.17
268	23R1	0.1995	0.1915	0.1588	25009	242.76	180.53	223.40
269	23R1	0.1978	0.1915	0.1583	25936	247.53	184.54	227.86
270	23R1	0.1976	0.1916	0.1580	25296	247.76	183.28	227.72
271	23R1	0.1968	0.1920	0.1545	25827	249.51	184.05	229.33
272	23R1	0.1963	0.1918	0.1590	26351	250.43	184.76	230.30
273	23R1	0.1955	0.1920	0.1630	26326	252.66	185.78	232.22
274	24R5	0.1964	0.1916	0.1540	26564	254.34	189.49	234.78
275	24R5	0.1954	0.1915	0.1593	26887	254.59	187.93	235.17
276	24R5	0.1968	0.1916	0.1573	26330	252.98	186.95	233.47
277	24R5	0.1968	0.1913	0.1563	26252	251.50	185.98	232.06
278	24R5	0.1963	0.1913	0.1573	26788	252.96	187.63	233.66

Continued on next page...

Test	Wire	d_{gross}(in)	d_{net}(in)	d_{neck}(in)	E(psi)	$\sigma_{\max}$(ksi)	σ_{yield}(ksi)	$\sigma_{2.5\%}$(ksi)
279	24R5	0.1959	0.1919	0.1595	26959	254.15	188.94	234.63
280	24R5	0.1954	0.1911	0.1565	26569	255.17	188.50	235.21
281	24R5	0.1961	0.1911	0.1555	26020	252.95	186.88	233.25
282	24R5	0.1964	0.1920	0.1540	26356	252.10	186.12	232.53
283	24R5	0.1956	0.1919	0.1568	26311	254.52	187.31	234.46
284	24R5	0.1958	0.1923	0.1608	26509	254.08	187.07	234.14
285	24R5	0.1969	0.1916	0.1548	25990	250.99	184.44	231.30
286	24R5	0.1954	0.1918	0.1545	26578	256.48	188.88	236.66
287	6R3	0.1948	0.1914	0.1603	25447	255.81	186.91	234.64
288	6R3	0.1958	0.1915	0.1585	25066	253.33	185.17	232.38
289	6R3	0.1954	0.1915	0.1630	25918	254.18	185.60	233.53
290	6R3	0.1961	0.1920	0.1583	32869	252.80	186.31	232.83
291	6R3	0.1960	0.1913	0.1615	25549	252.62	185.54	232.03
292	6R3	0.1966	0.1914	0.1595	25731	251.07	186.79	231.29
293	6R3	0.1975	0.1915	0.1568	25150	250.38	185.70	230.41
294	6R3	0.1978	0.1914	0.1628	25011	249.61	186.21	230.05
295	6R3	0.1973	0.1918	0.1565	25059	251.49	185.69	231.19
296	6R3	0.1961	0.1914	0.1598	25044	253.09	186.23	232.80
297	6R3	0.1961	0.1916	0.1603	24596	250.26	183.69	230.18
298	6R3	0.1961	0.1918	0.1623	24696	251.67	184.26	231.10
299	6R3	0.1956	0.1913	0.1655	24785	251.73	184.07	231.25
300	21R5	0.1954	0.1916	0.1580	26315	254.14	187.73	234.15
301	21R5	0.1950	0.1919	0.1605	26040	254.40	187.65	234.33

Continued on next page...

Test	Wire	d_{gross}(in)	d_{net}(in)	d_{neck}(in)	E(psi)	$\sigma_{\max}$(ksi)	σ_{yield}(ksi)	$\sigma_{2.5\%}$(ksi)
302	21R5	0.1959	0.1916	0.1573	26146	252.97	187.96	233.45
303	21R5	0.1960	0.1914	0.1563	26456	254.82	190.44	235.23
304	21R5	0.1959	0.1916	0.1563	26916	255.61	192.18	236.07
305	21R5	0.1949	0.1921	0.1575	26976	257.36	192.28	237.58
306	21R5	0.1954	0.1918	0.1618	26469	254.07	189.46	234.80
307	21R5	0.1963	0.1914	0.1610	26355	252.14	187.90	233.10
308	21R5	0.1974	0.1918	0.1668	25883	246.93	183.83	228.23
309	21R5	0.1956	0.1915	0.1585	26302	255.46	189.93	235.64
310	21R5	0.1950	0.1919	0.1605	26352	258.19	190.69	237.70
311	21R5	0.1954	0.1919	0.1558	25906	257.44	190.65	236.98
312	21R5	0.1950	0.1920	0.1568	26594	255.69	188.71	236.11
313	17R5	0.1964	0.1916	0.1615	25187	250.20	183.58	230.35
314	17R5	0.1958	0.1916	0.1568	25393	251.48	184.63	231.53
315	17R5	0.1955	0.1915	0.1638	25540	249.17	183.57	230.20
316	17R5	0.1970	0.1913	0.1565	25359	249.83	184.40	230.22
317	17R5	0.1971	0.1916	0.1565	25520	250.55	184.90	230.62
318	17R5	0.1964	0.1916	0.1558	26012	253.10	186.50	233.10
319	17R5	0.1975	0.1916	0.1568	25072	249.29	184.38	229.61
320	17R5	0.1965	0.1916	0.1638	25431	249.90	183.97	230.09
321	17R5	0.1971	0.1914	0.1600	25087	248.24	182.41	228.50
322	17R5	0.1949	0.1916	0.1568	26011	254.35	185.64	233.87
323	17R5	0.1951	0.1916	0.1590	25718	253.64	185.34	233.18
324	17R5	0.1959	0.1916	0.1570	25661	251.77	184.42	231.50

Continued on next page...

Test	Wire	d_{gross}(in)	d_{net}(in)	d_{neck}(in)	E(psi)	$\sigma_{\max}$(ksi)	σ_{yield}(ksi)	$\sigma_{2.5\%}$(ksi)
325	17R5	0.1953	0.1916	0.1575	25873	253.18	185.15	232.69
326	26R6	0.1950	0.1918	0.1573	26857	254.38	187.43	234.49
327	26R6	0.1950	0.1916	0.1550	26867	255.78	188.32	235.38
328	26R6	0.1951	0.1914	0.1608	26413	255.48	188.19	235.05
329	26R6	0.1958	0.1915	0.1595	25874	253.79	186.92	233.39
330	26R6	0.1965	0.1915	0.1570	25257	250.52	184.11	230.36
331	26R6	0.1954	0.1920	0.1605	25814	252.39	185.21	232.02
332	26R6	0.1971	0.1919	0.1595	25015	248.56	182.58	228.34
333	26R6	0.1965	0.1919	0.1615	25418	249.80	182.92	229.44
334	26R6	0.1953	0.1915	0.1578	25887	253.31	185.81	232.74
335	26R6	0.1949	0.1915	0.1595	25901	254.17	186.07	233.46
336	26R6	0.1961	0.1918	0.1575	25203	251.24	184.64	230.82
337	26R6	0.1948	0.1914	0.1563	25900	255.19	186.51	234.46
338	26R6	0.1955	0.1918	0.1615	25389	252.76	184.68	232.09
339	14R3	0.1963	0.1915	0.1545	26240	249.74	185.88	230.31
340	14R3	0.1961	0.1910	0.1550	26681	250.86	187.17	231.78
341	14R3	0.1960	0.1913	0.1550	26695	251.27	187.30	232.10
342	14R3	0.1985	0.1914	0.1538	25712	244.32	182.86	225.59
343	14R3	0.1986	0.1910	0.1540	25665	244.09	183.41	225.58
344	14R3	0.1963	0.1913	0.1543	26798	250.42	187.87	231.60
345	14R3	0.1971	0.1914	0.1545	26222	248.39	186.42	229.67
346	14R3	0.1991	0.1910	0.1560	26051	242.28	183.08	224.25
347	14R3	0.1979	0.1914	0.1545	25886	246.13	185.20	227.83

Continued on next page...

Test	Wire	d_{gross}(in)	d_{net}(in)	d_{neck}(in)	E(psi)	$\sigma_{\max}$(ksi)	σ_{yield}(ksi)	$\sigma_{2.5\%}$(ksi)
348	14R3	0.1983	0.1910	0.1530	25003	248.06	185.43	228.71
349	14R3	0.1953	0.1914	0.1550	26292	255.33	189.21	235.21
350	14R3	0.1961	0.1913	0.1578	24973	248.25	185.47	230.68
351	14R3	0.1953	0.1915	0.1528	26249	255.56	189.63	235.65
352	19R2	0.1961	0.1913	0.1593	25163	250.45	183.89	230.55
353	19R2	0.1964	0.1915	0.1573	24999	250.83	184.96	231.60
354	19R2	0.1955	0.1914	0.1548	26342	254.07	189.31	235.64
355	19R2	0.1969	0.1916	0.1520	25485	253.45	190.52	233.71
356	19R2	0.1969	0.1911	0.1518	26649	253.67	190.03	234.16
357	19R2	0.1951	0.1916	0.1543	28230	257.23	196.84	238.30
358	19R2	0.1960	0.1913	0.1543	26338	252.63	188.00	232.96
359	19R2	0.1984	0.1918	0.1560	25343	246.90	184.23	227.69
360	19R2	0.1980	0.1913	0.1555	25239	247.58	183.96	227.99
361	19R2	0.1963	0.1910	0.1603	25685	251.38	184.85	231.24
362	19R2	0.1963	0.1914	0.1555	24759	251.78	184.68	231.17
363	19R2	0.1964	0.1911	0.1545	24804	252.03	184.97	231.51
364	19R2	0.1956	0.1911	0.1558	25167	254.11	186.15	233.21
365	4R1	0.1948	0.1916	0.1583	26133	255.57	187.67	235.44
366	4R1	0.1963	0.1916	0.1623	25080	249.56	183.76	230.14
367	4R1	0.1960	0.1916	0.1565	25719	251.76	186.91	232.56
368	4R1	0.1960	0.1920	0.1555	25904	253.79	188.08	234.22
369	4R1	0.1973	0.1913	0.1560	25605	252.04	187.32	232.19
370	4R1	0.1965	0.1915	0.1568	25723	253.70	188.13	233.55

Continued on next page...

Test	Wire	d_{gross}(in)	d_{net}(in)	d_{neck}(in)	E(psi)	$\sigma_{\max}$(ksi)	σ_{yield}(ksi)	$\sigma_{2.5\%}$(ksi)
371	4R1	0.1955	0.1920	0.1555	25899	253.78	187.04	233.84
372	4R1	0.1963	0.1921	0.1555	25566	252.07	186.57	232.23
373	4R1	0.1961	0.1915	0.1590	25431	252.72	186.56	232.57
374	4R1	0.1966	0.1921	0.1548	25311	251.32	185.39	231.34
375	4R1	0.1960	0.1914	0.1538	25350	253.12	187.05	232.85
376	4R1	0.1943	0.1920	0.1555	26253	257.79	189.51	237.12
377	4R1	0.1951	0.1916	0.1573	25741	255.54	188.10	234.86
378	18L5	0.1964	0.1918	0.1533	24949	254.55	188.17	233.72
379	18L5	0.1958	0.1919	0.1568	25152	253.85	186.65	233.56
380	18L5	0.1958	0.1918	0.1585	25052	252.89	185.32	231.97
381	18L5	0.1963	0.1914	0.1553	24994	251.98	184.89	231.12
382	18L5	0.1966	0.1916	0.1560	25073	251.15	183.79	230.31
383	18L5	0.1963	0.1916	0.1615	24988	251.56	184.73	230.93
384	18L5	0.1953	0.1919	0.1588	25228	253.81	186.55	232.92
385	18L5	0.1954	0.1921	0.1590	25084	254.08	186.78	233.19
386	18L5	0.1963	0.1920	0.1568	24761	251.69	184.92	230.94
387	18L5	0.1968	0.1916	0.1613	24528	250.33	183.41	229.54
388	18L5	0.1964	0.1920	0.1558	25027	252.30	185.48	231.53
389	18L5	0.1954	0.1919	0.1543	25729	256.90	188.50	235.78
390	18L5	0.1958	0.1919	0.1525	25650	255.95	187.67	234.88
391	8L1	0.1954	0.1916	0.1600	25413	254.79	185.85	233.56
392	8L1	0.1959	0.1916	0.1595	24854	253.11	185.19	232.03
393	8L1	0.1965	0.1919	0.1623	24988	251.17	183.72	230.30

Continued on next page...

Test	Wire	d_{gross}(in)	d_{net}(in)	d_{neck}(in)	E(psi)	$\sigma_{\max}$(ksi)	σ_{yield}(ksi)	$\sigma_{2.5\%}$(ksi)
394	8L1	0.1960	0.1915	0.1583	25265	253.18	185.81	232.53
395	8L1	0.1963	0.1918	0.1565	25317	253.98	187.49	233.29
396	8L1	0.1963	0.1914	0.1580	25462	253.60	187.24	233.15
397	8L1	0.1968	0.1915	0.1605	25238	252.45	186.55	231.96
398	8L1	0.1971	0.1920	0.1600	24592	250.56	184.49	230.01
399	8L1	0.1961	0.1918	0.1598	25079	253.30	186.22	232.62
400	8L1	0.1963	0.1915	0.1610	25053	253.58	185.70	232.59
401	8L1	0.1956	0.1918	0.1613	24730	251.86	184.19	231.07
402	8L1	0.1969	0.1918	0.1618	24816	249.54	183.12	229.68
403	8L1	0.1959	0.1915	0.1565	25009	255.36	187.55	234.22
404	9L1	0.1949	0.1919	0.1568	25972	255.77	186.85	234.85
405	9L1	0.1953	0.1914	0.1578	25353	255.21	186.97	234.26
406	9L1	0.1965	0.1919	0.1593	25028	251.42	184.16	230.68
407	9L1	0.1964	0.1911	0.1568	24967	252.00	184.67	231.20
408	9L1	0.1956	0.1913	0.1578	25148	254.15	186.37	233.06
409	9L1	0.1961	0.1918	0.1590	25239	253.43	186.30	232.63
410	9L1	0.1958	0.1918	0.1630	25164	252.84	185.30	232.17
411	9L1	0.1961	0.1916	0.1593	25451	253.12	186.19	232.82
412	9L1	0.1965	0.1916	0.1565	24919	253.37	187.03	232.96
413	9L1	0.1955	0.1916	0.1618	25222	255.13	186.30	234.07
414	9L1	0.1966	0.1919	0.1553	25298	253.49	185.96	232.75
415	9L1	0.1956	0.1918	0.1593	25176	253.99	184.93	233.06
416	9L1	0.1953	0.1921	0.1558	25412	257.54	188.46	236.26

Continued on next page...

Test	Wire	d_{gross}(in)	d_{net}(in)	d_{neck}(in)	E(psi)	σ_{max}(ksi)	σ_{yield}(ksi)	$\sigma_{2.5\%}$(ksi)
417	2L1	0.1960	0.1919	0.1575	25549	253.10	185.83	232.25
418	2L1	0.1959	0.1919	0.1588	25529	254.15	187.69	233.51
419	2L1	0.1966	0.1916	0.1585	25451	252.41	186.28	231.86
420	2L1	0.1949	0.1918	0.1575	25958	256.48	189.44	235.83
421	2L1	0.1960	0.1918	0.1580	25720	251.81	185.59	231.83
422	2L1	0.1968	0.1914	0.1603	25208	249.17	184.01	229.11
423	2L1	0.1974	0.1918	0.1613	25060	248.44	183.52	228.34
424	2L1	0.1975	0.1920	0.1595	24357	246.02	182.54	226.95
425	2L1	0.1973	0.1919	0.1640	24624	248.24	182.91	228.14
426	2L1	0.1969	0.1920	0.1630	25353	249.22	184.01	229.13
427	2L1	0.1956	0.1918	0.1585	25652	252.97	186.42	232.47
428	2L1	0.1955	0.1920	0.1623	26256	252.52	185.84	232.13
429	2L1	0.1959	0.1921	0.1615	24834	251.29	184.21	230.68
430	1L5	0.1956	0.1921	0.1595	25553	253.91	186.07	233.12
431	1L5	0.1954	0.1919	0.1610	25976	254.43	186.65	233.79
432	1L5	0.1959	0.1920	0.1665	25547	252.39	186.04	232.11
433	1L5	0.1959	0.1920	0.1623	26139	253.74	187.60	233.77
434	1L5	0.1966	0.1916	0.1603	26008	253.04	187.36	232.93
435	1L5	0.1956	0.1920	0.1633	26558	252.76	189.17	235.13
436	1L5	0.1963	0.1918	0.1600	25932	252.94	188.14	233.17
437	1L5	0.1970	0.1921	0.1590	25693	251.73	187.13	231.96
438	1L5	0.1966	0.1919	0.1583	25727	250.88	186.46	231.80
439	1L5	0.1965	0.1923	0.1600	25155	250.81	186.15	231.64

Continued on next page...

Test	Wire	d_{gross}(in)	d_{net}(in)	d_{neck}(in)	E(psi)	σ_{max}(ksi)	σ_{yield}(ksi)	$\sigma_{2.5\%}$(ksi)
440	1L5	0.1964	0.1921	0.1613	25907	252.96	186.57	232.66
441	1L5	0.1966	0.1924	0.1580	25333	251.31	185.11	231.19
442	1L5	0.1951	0.1921	0.1590	25625	254.86	186.41	234.09
443	17L1	0.1951	0.1918	0.1568	26160	256.96	189.88	236.62
444	17L1	0.1953	0.1918	0.1565	25486	255.76	188.50	235.30
445	17L1	0.1961	0.1923	0.1605	24654	252.23	185.99	231.60
446	17L1	0.1968	0.1920	0.1560	25331	251.42	185.31	231.15
447	17L1	0.1968	0.1918	0.1578	25609	251.12	185.19	231.12
448	17L1	0.1969	0.1919	0.1585	25279	250.55	184.30	230.44
449	17L1	0.1958	0.1921	0.1553	25898	253.51	186.32	233.24
450	17L1	0.1973	0.1920	0.1613	25313	249.79	184.66	229.84
451	17L1	0.1960	0.1921	0.1603	25655	253.04	186.52	233.10
452	17L1	0.1954	0.1916	0.1593	26079	253.72	186.87	233.70
453	17L1	0.1956	0.1921	0.1550	25792	254.24	187.30	233.96
454	17L1	0.1956	0.1919	0.1558	25933	256.28	189.01	235.77
455	17L1	0.1960	0.1920	0.1555	25652	255.52	188.43	235.01
456	19L6	0.1966	0.1919	0.1555	24407	250.54	186.83	230.95
457	19L6	0.1973	0.1916	0.1548	24511	249.84	186.03	229.86
458	19L6	0.1974	0.1920	0.1560	25434	248.60	187.57	229.93
459	19L6	0.1975	0.1919	0.1563	25698	249.77	188.60	230.70
460	19L6	0.1984	0.1920	0.1558	24916	247.15	186.75	228.27
461	19L6	0.1983	0.1915	0.1555	26857	245.92	190.91	228.30
462	19L6	0.1975	0.1923	0.1550	25445	247.96	186.70	228.97

Continued on next page...

Test	Wire	d_{gross}(in)	d_{net}(in)	d_{neck}(in)	E(psi)	$\sigma_{\max}$(ksi)	σ_{yield}(ksi)	$\sigma_{2.5\%}$(ksi)
463	19L6	0.1981	0.1918	0.1710	25351	240.56	185.75	225.50
464	19L6	0.1981	0.1919	0.1645	25932	247.81	191.19	232.32
465	19L6	0.1973	0.1920	0.1588	24507	248.49	185.90	228.93
466	19L6	0.1971	0.1921	0.1553	24575	249.22	185.42	229.41
467	19L6	0.1959	0.1921	0.1548	24964	252.63	187.31	232.43
468	19L6	0.1963	0.1921	0.1565	24667	250.91	186.52	230.69
469	23L5	0.1968	0.1920	0.1615	25226	251.01	184.46	231.28
470	23L5	0.1978	0.1918	0.1578	25242	249.40	183.97	229.58
471	23L5	0.1971	0.1919	0.1623	25682	250.90	185.27	230.99
472	23L5	0.1965	0.1916	0.1618	25563	250.93	184.23	231.10
473	23L5	0.1968	0.1920	0.1610	25441	249.89	184.05	230.13
474	23L5	0.1964	0.1919	0.1635	25231	250.93	185.05	230.83
475	23L5	0.1964	0.1919	0.1660	25164	250.99	184.89	231.04
476	23L5	0.1975	0.1916	0.1625	25451	247.64	182.25	228.27
477	23L5	0.1973	0.1915	0.1678	25057	248.59	180.94	228.43
478	23L5	0.1971	0.1918	0.1638	24936	249.00	183.37	229.14
479	23L5	0.1973	0.1920	0.1618	24903	248.74	182.60	228.62
480	23L5	0.1960	0.1915	0.1665	25736	251.89	183.83	231.57
481	23L5	0.1969	0.1921	0.1635	25712	250.65	184.03	230.91
482	5L1	0.1963	0.1914	0.1535	25018	253.07	186.00	232.38
483	5L1	0.1951	0.1918	0.1523	25241	257.06	189.59	236.03
484	5L1	0.1951	0.1916	0.1530	25742	257.33	189.52	236.54
485	5L1	0.1970	0.1918	0.1505	24962	252.25	186.52	231.97

Continued on next page...

Test	Wire	d_{gross}(in)	d_{net}(in)	d_{neck}(in)	E(psi)	$\sigma_{\max}$(ksi)	σ_{yield}(ksi)	$\sigma_{2.5\%}$(ksi)
486	5L1	0.1964	0.1913	0.1508	25268	254.13	188.31	233.75
487	5L1	0.1959	0.1916	0.1548	24810	253.59	188.05	233.16
488	5L1	0.1974	0.1920	0.1583	24689	248.80	183.93	228.85
489	5L1	0.1966	0.1916	0.1543	25356	252.43	186.18	232.28
490	5L1	0.1964	0.1919	0.1540	25680	253.55	202.26	236.22
491	5L1	0.1969	0.1919	0.1550	24297	249.95	184.38	230.00
492	5L1	0.1961	0.1918	0.1553	24817	251.87	184.70	231.38
493	5L1	0.1956	0.1921	0.1528	14623	253.39	202.44	227.10
494	5L1	0.1955	0.1916	0.1543	19149	253.14	193.03	230.10
495	22L5	0.1956	0.1914	0.1578	24843	251.75	187.43	231.45
496	22L5	0.1959	0.1919	0.1565	16735	251.26	197.48	227.68
497	22L5	0.1956	0.1923	0.1563	22003	253.53	193.42	232.76
498	22L5	0.1974	0.1915	0.1550	25618	249.87	187.26	230.59
499	22L5	0.1975	0.1915	0.1570	25639	248.82	188.17	230.21
500	22L5	0.1964	0.1915	0.1608	26293	250.88	188.30	231.70
501	22L5	0.1951	0.1916	0.1628	19601	251.57	194.95	230.66
502	22L5	0.1964	0.1918	0.1570	25705	251.45	188.81	232.22
503	22L5	0.2005	0.1919	0.1558	23246	240.73	183.07	222.28
504	22L5	0.1956	0.1914	0.1570	23306	252.60	191.02	232.40
505	22L5	0.1961	0.1920	0.1555	20005	253.14	196.28	231.80
506	22L5	0.1979	0.1918	0.1553	23608	249.31	187.57	229.91
507	22L5	0.1975	0.1913	0.1570	26120	249.44	186.74	230.50
508	19L3	0.1964	0.1920	0.1540	26850	252.68	182.22	232.77

Continued on next page...

Test	Wire	d_{gross}(in)	d_{net}(in)	d_{neck}(in)	E(psi)	$\sigma_{\max}$(ksi)	σ_{yield}(ksi)	$\sigma_{2.5\%}$(ksi)
509	19L3	0.1961	0.1920	0.1540	25400	255.06	188.23	234.57
510	19L3	0.1980	0.1918	0.1630	25070	247.53	184.01	227.84
511	19L3	0.1969	0.1919	0.1545	25944	253.24	189.33	233.54
512	19L3	0.1975	0.1921	0.1548	16716	251.49	200.48	228.24
513	19L3	0.1966	0.1916	0.1575	28369	251.96	189.51	233.29
514	19L3	0.1968	0.1923	0.1608	21262	251.73	193.28	230.58
515	19L3	0.1971	0.1920	0.1568	21639	250.55	191.49	229.71
516	19L3	0.2001	0.1921	0.1633	25721	242.03	175.66	223.29
517	19L3	0.1971	0.1924	0.1560	24782	250.39	184.94	230.17
518	19L3	0.1979	0.1919	0.1570	21766	248.45	186.81	227.43
519	19L3	0.1960	0.1919	0.1545	25283	253.47	186.45	232.99
520	19L3	0.1963	0.1923	0.1575	24996	252.80	186.24	232.19
521	24L5	0.1965	0.1919	0.1550	25689	252.25	184.48	231.55
522	24L5	0.1964	0.1923	0.1560	25555	253.30	185.33	232.45
523	24L5	0.1966	0.1920	0.1595	26442	252.26	185.76	231.90
524	24L5	0.1961	0.1919	0.1583	26820	252.92	186.52	232.70
525	24L5	0.1979	0.1919	0.1583	26448	249.06	184.12	229.87
526	24L5	0.1971	0.1919	0.1573	26065	252.07	186.17	231.66
527	24L5	0.1963	0.1918	0.1565	26242	253.87	186.83	233.45
528	24L5	0.1958	0.1920	0.1588	25852	253.11	184.28	232.56
529	24L5	0.1968	0.1916	0.1605	26032	250.43	184.16	230.47
530	24L5	0.1963	0.1918	0.1598	25939	252.20	183.39	231.66
531	24L5	0.1974	0.1918	0.1593	25353	249.12	181.78	228.56

Continued on next page...

Test	Wire	d_{gross}(in)	d_{net}(in)	d_{neck}(in)	E(psi)	$\sigma_{\max}$(ksi)	σ_{yield}(ksi)	$\sigma_{2.5\%}$(ksi)
532	24L5	0.1958	0.1921	0.1565	25838	253.21	184.23	232.23
533	24L5	0.1960	0.1918	0.1573	25561	253.05	184.81	232.05
534	22L3	0.1966	0.1918	0.1593	26251	255.32	189.13	235.25
535	22L3	0.1956	0.1916	0.1535	26003	254.16	188.13	234.16
536	22L3	0.1960	0.1916	0.1513	26284	253.09	188.19	233.64
537	22L3	0.1963	0.1918	0.1498	25814	253.12	187.84	233.45
538	22L3	0.1973	0.1918	0.1518	26838	249.27	187.44	230.39
539	22L3	0.1973	0.1919	0.1523	27017	249.36	189.28	230.96
540	22L3	0.1985	0.1916	0.1530	26668	243.60	185.29	225.79
541	22L3	0.1970	0.1916	0.1538	26763	247.59	186.04	229.05
542	22L3	0.1978	0.1918	0.1545	25091	247.07	182.86	227.79
543	22L3	0.1973	0.1913	0.1590	27081	247.05	186.87	228.62
544	22L3	0.1975	0.1919	0.1540	26733	246.04	185.41	227.63
545	22L3	0.1956	0.1916	0.1528	25920	251.59	185.64	232.04
546	22L3	0.1966	0.1913	0.1510	26718	248.54	185.44	229.52
547	18L3	0.1958	0.1915	0.1545	25493	252.85	184.99	232.44
548	18L3	0.1966	0.1915	0.1528	24726	252.71	187.17	232.46
549	18L3	0.1966	0.1918	0.1545	25832	252.34	186.38	232.31
550	18L3	0.1955	0.1916	0.1513	26190	255.51	188.96	235.34
551	18L3	0.1958	0.1919	0.1563	25601	253.92	186.99	233.90
552	18L3	0.1963	0.1918	0.1560	25671	255.13	188.78	234.99
553	18L3	0.1958	0.1914	0.1550	25856	256.14	190.01	235.85
554	18L3	0.1958	0.1921	0.1538	25678	255.55	189.65	235.63

Continued on next page...

Test	Wire	d_{gross}(in)	d_{net}(in)	d_{neck}(in)	E(psi)	$\sigma_{\max}$(ksi)	σ_{yield}(ksi)	$\sigma_{2.5\%}$(ksi)
555	18L3	0.1964	0.1918	0.1598	25273	252.35	186.26	232.40
556	18L3	0.1960	0.1916	0.1540	25578	254.91	188.28	234.47
557	18L3	0.1963	0.1916	0.1533	25351	252.46	185.81	232.17
558	18L3	0.1958	0.1915	0.1530	25332	253.40	185.77	232.75
559	18L3	0.1951	0.1916	0.1558	25739	255.07	187.81	234.28
560	14L5	0.1954	0.1919	0.1498	25340	255.85	192.26	236.05
561	14L5	0.1950	0.1915	0.1500	25765	256.12	192.63	236.79
562	14L5	0.1958	0.1916	0.1530	25281	252.05	188.96	233.12
563	14L5	0.1959	0.1919	0.1570	25752	251.12	187.71	231.89
564	14L5	0.1961	0.1918	0.1533	25872	250.84	188.04	231.61
565	14L5	0.1958	0.1918	0.1525	25853	251.71	189.50	232.76
566	14L5	0.1976	0.1919	0.1533	25381	246.89	185.25	228.18
567	14L5	0.1961	0.1915	0.1623	25814	250.00	188.36	231.87
568	14L5	0.1958	0.1915	0.1533	25551	251.94	188.66	232.72
569	14L5	0.1985	0.1916	0.1530	24450	244.71	183.53	226.23
570	14L5	0.1970	0.1914	0.1553	25001	248.13	185.03	228.95
571	14L5	0.1964	0.1915	0.1563	25058	251.94	188.71	232.21
572	14L5	0.1958	0.1918	0.1538	25254	254.25	190.05	234.43
573	12L3	0.1973	0.1921	0.1553	24268	248.46	180.82	227.55
574	12L3	0.1968	0.1920	0.1560	25176	251.50	184.16	230.66
575	12L3	0.1973	0.1916	0.1585	25408	250.72	184.38	230.04
576	12L3	0.1960	0.1916	0.1573	26031	253.46	186.37	233.02
577	12L3	0.1966	0.1920	0.1583	25620	249.87	184.06	229.99

Continued on next page...

Test	Wire	d_{gross}(in)	d_{net}(in)	d_{neck}(in)	E(psi)	σ_{max}(ksi)	σ_{yield}(ksi)	$\sigma_{2.5\%}$(ksi)
578	12L3	0.1963	0.1918	0.1573	26610	250.46	185.79	230.97
579	12L3	0.1975	0.1920	0.1583	26270	246.80	184.93	228.30
580	12L3	0.1986	0.1918	0.1590	25916	243.51	182.52	224.75
581	12L3	0.1986	0.1915	0.1565	24564	244.07	180.39	224.85
582	12L3	0.1958	0.1919	0.1558	25167	252.11	184.61	231.69
583	12L3	0.1965	0.1918	0.1568	25139	250.42	182.88	230.13
584	12L3	0.1978	0.1915	0.1573	26511	245.48	183.74	226.74
585	12L3	0.1950	0.1918	0.1580	26190	253.13	184.20	232.48
586	18L1	0.1964	0.1916	0.1538	24511	249.23	181.91	228.35
587	18L1	0.1969	0.1916	0.1528	24118	248.29	181.66	227.38
588	18L1	0.1954	0.1918	0.1518	24084	252.05	185.17	230.71
589	18L1	0.1961	0.1915	0.1515	24599	250.41	183.36	229.38
590	18L1	0.1951	0.1915	0.1540	25452	252.82	184.53	231.90
591	18L1	0.1964	0.1918	0.1535	25431	249.47	182.53	229.45
592	18L1	0.1958	0.1914	0.1518	25895	253.09	185.45	232.25
593	18L1	0.1965	0.1919	0.1513	25534	251.26	184.48	230.51
594	18L1	0.1971	0.1919	0.1508	25126	249.15	182.97	228.50
595	18L1	0.1960	0.1921	0.1518	25645	251.83	184.91	231.05
596	18L1	0.1958	0.1918	0.1568	25818	252.96	185.07	231.98
597	18L1	0.1959	0.1918	0.1515	25177	251.52	184.40	230.77
598	18L1	0.1964	0.1918	0.1528	25222	249.85	182.85	229.60
599	4L5	0.1961	0.1916	0.1555	27737	252.03	186.07	232.69
600	4L5	0.1955	0.1921	0.1535	24974	253.60	186.30	232.62

Continued on next page...

Test	Wire	d_{gross}(in)	d_{net}(in)	d_{neck}(in)	E(psi)	σ_{max}(ksi)	σ_{yield}(ksi)	$\sigma_{2.5\%}$(ksi)
601	4L5	0.1961	0.1918	0.1538	24877	252.08	186.09	231.58
602	4L5	0.1960	0.1918	0.1560	22773	252.13	188.89	231.01
603	4L5	0.1965	0.1915	0.1535	25083	251.12	185.03	230.88
604	4L5	0.1958	0.1919	0.1525	25230	253.06	186.45	232.55
605	4L5	0.1970	0.1918	0.1538	24542	250.10	184.83	229.87
606	4L5	0.1963	0.1919	0.1543	24920	252.02	186.30	231.65
607	4L5	0.1953	0.1920	0.1523	25315	254.15	186.55	233.43
608	4L5	0.1964	0.1923	0.1513	25237	252.78	186.72	232.59
609	4L5	0.1956	0.1918	0.1503	25270	255.75	189.72	234.97
610	4L5	0.1955	0.1915	0.1520	25191	254.02	187.62	234.25
611	4L5	0.1955	0.1921	0.1538	24570	253.14	187.14	233.07
612	23L3	0.1953	0.1921	0.1538	25720	254.71	186.92	234.29
613	23L3	0.1960	0.1921	0.1568	26093	252.07	184.45	232.06
614	23L3	0.1959	0.1919	0.1568	25684	252.05	184.85	231.96
615	23L3	0.1951	0.1919	0.1550	26043	254.24	186.67	234.00
616	23L3	0.1965	0.1921	0.1570	25706	250.93	184.71	230.99
617	23L3	0.1981	0.1921	0.1560	25337	246.75	182.47	227.46
618	23L3	0.1956	0.1921	0.1568	26274	252.54	185.96	233.07
619	23L3	0.1969	0.1919	0.1528	26023	251.15	186.02	231.62
620	23L3	0.1965	0.1916	0.1523	26242	253.29	187.55	233.48
621	23L3	0.1963	0.1915	0.1595	26383	253.49	186.99	233.67
622	23L3	0.1958	0.1921	0.1588	26021	253.37	187.13	233.61
623	23L3	0.1953	0.1918	0.1653	26277	251.12	183.99	232.08

Continued on next page...

Test	Wire	d_{gross}(in)	d_{net}(in)	d_{neck}(in)	E(psi)	$\sigma_{\max}$(ksi)	σ_{yield}(ksi)	$\sigma_{2.5\%}$(ksi)
624	23L3	0.1955	0.1919	0.1573	26073	252.66	185.98	232.95
625	2L3	0.1954	0.1918	0.1575	25113	252.63	184.98	231.78
626	2L3	0.1956	0.1919	0.1563	25634	253.31	185.99	232.72
627	2L3	0.1953	0.1919	0.1575	26037	255.20	187.37	234.54
628	2L3	0.1963	0.1920	0.1558	25336	252.69	186.45	232.17
629	2L3	0.1954	0.1920	0.1570	25879	254.02	187.15	233.45
630	2L3	0.1961	0.1919	0.1578	25668	251.15	185.14	231.11
631	2L3	0.1954	0.1918	0.1580	25496	251.49	185.33	231.25
632	2L3	0.1954	0.1918	0.1678	24823	247.61	181.33	227.71
633	2L3	0.1955	0.1919	0.1578	25754	250.77	184.95	231.19
634	2L3	0.1960	0.1920	0.1600	26046	251.62	184.75	231.55
635	2L3	0.1949	0.1918	0.1575	26647	254.86	188.37	234.39
636	2L3	0.1951	0.1920	0.1605	25963	254.32	186.79	233.56
637	2L3	0.1948	0.1918	0.1595	25617	253.83	185.48	233.13
638	15L5	0.1963	0.1918	0.1543	25233	250.49	184.04	230.39
639	15L5	0.1958	0.1919	0.1548	25147	252.21	185.13	231.70
640	15L5	0.1963	0.1919	0.1578	25664	251.24	184.28	230.94
641	15L5	0.1948	0.1919	0.1555	26035	254.44	186.46	234.04
642	15L5	0.1963	0.1920	0.1545	25498	251.17	185.65	231.31
643	15L5	0.1961	0.1919	0.1540	26593	253.25	187.27	233.43
644	15L5	0.1954	0.1918	0.1570	26476	255.66	189.40	235.59
645	15L5	0.1965	0.1918	0.1630	25873	252.15	186.27	232.35
646	15L5	0.1971	0.1921	0.1533	25726	248.42	184.25	229.54

Continued on next page...

Test	Wire	d_{gross}(in)	d_{net}(in)	d_{neck}(in)	E(psi)	$\sigma_{\max}$(ksi)	σ_{yield}(ksi)	$\sigma_{2.5\%}$(ksi)
647	15L5	0.1966	0.1919	0.1610	25846	249.73	184.90	230.24
648	15L5	0.1960	0.1919	0.1585	26169	250.20	184.47	231.05
649	15L5	0.1955	0.1918	0.1585	26520	254.63	187.75	234.56
650	15L5	0.1960	0.1918	0.1533	26049	252.35	186.25	232.60
651	3L6	0.1955	0.1919	0.1590	25427	253.21	185.73	232.89
652	3L6	0.1953	0.1918	0.1565	25706	254.65	186.75	233.84
653	3L6	0.1948	0.1920	0.1600	25601	254.09	186.20	233.27
654	3L6	0.1959	0.1915	0.1600	25179	251.52	184.83	230.99
655	3L6	0.1964	0.1916	0.1610	25274	250.42	184.28	230.14
656	3L6	0.1963	0.1921	0.1588	25037	250.42	184.16	230.01
657	3L6	0.1964	0.1919	0.1590	25167	250.13	183.84	229.79
658	3L6	0.1961	0.1919	0.1588	24772	250.91	184.49	230.21
659	3L6	0.1961	0.1916	0.1568	25404	250.95	183.64	230.47
660	3L6	0.1951	0.1920	0.1603	25699	252.78	184.24	232.08
661	3L6	0.1959	0.1919	0.1565	25198	250.84	184.04	230.33
662	3L6	0.1958	0.1921	0.1550	25465	254.11	186.91	233.25
663	3L6	0.1956	0.1916	0.1545	25420	254.89	186.99	233.93
664	12L6	0.1961	0.1919	0.1528	25170	251.91	184.35	231.37
665	12L6	0.1961	0.1916	0.1570	25326	252.18	184.77	231.57
666	12L6	0.1966	0.1919	0.1543	25445	250.87	185.06	230.71
667	12L6	0.1964	0.1920	0.1573	25763	250.87	185.49	230.93
668	12L6	0.1958	0.1918	0.1528	26203	252.55	186.67	232.61
669	12L6	0.1960	0.1919	0.1513	26664	252.52	189.47	233.24

Continued on next page...

Test	Wire	d_{gross}(in)	d_{net}(in)	d_{neck}(in)	E(psi)	$\sigma_{\max}$(ksi)	σ_{yield}(ksi)	$\sigma_{2.5\%}$(ksi)
670	12L6	0.1970	0.1916	0.1525	26063	249.29	185.29	229.96
671	12L6	0.1985	0.1920	0.1540	25417	245.13	183.26	226.19
672	12L6	0.1974	0.1919	0.1528	26702	249.39	188.25	230.58
673	12L6	0.1974	0.1918	0.1563	27289	249.77	189.36	231.09
674	12L6	0.1964	0.1919	0.1530	26736	252.14	188.46	232.62
675	12L6	0.1958	0.1920	0.1545	26190	252.51	188.37	232.88
676	12L6	0.1956	0.1918	0.1523	27802	251.92	193.47	233.80
677	13L1	0.1959	0.1920	0.1553	26365	252.70	185.11	231.90
678	13L1	0.1956	0.1916	0.1558	26092	253.07	185.44	232.27
679	13L1	0.1963	0.1919	0.1545	26079	251.34	184.68	230.82
680	13L1	0.1963	0.1920	0.1523	26930	252.72	187.50	232.76
681	13L1	0.1961	0.1920	0.1555	27155	254.42	189.66	234.43
682	13L1	0.1960	0.1918	0.1530	27465	254.41	190.69	234.69
683	13L1	0.1966	0.1919	0.1570	26741	250.32	185.81	230.77
684	13L1	0.1973	0.1919	0.1585	26320	246.71	184.14	227.59
685	13L1	0.1964	0.1920	0.1510	26253	252.34	187.72	232.38
686	13L1	0.1963	0.1920	0.1503	26082	254.03	187.56	233.67
687	13L1	0.1960	0.1918	0.1538	25946	253.36	186.97	233.10
688	13L1	0.1969	0.1919	0.1575	25963	249.23	184.47	229.48
689	13L1	0.1955	0.1919	0.1535	25934	253.74	185.06	233.22
690	12L1	0.1966	0.1920	0.1618	24939	250.34	181.19	229.09
691	12L1	0.1978	0.1920	0.1603	24446	247.58	180.49	226.71
692	12L1	0.1964	0.1919	0.1650	24963	250.93	183.89	229.99

Continued on next page...

Test	Wire	d_{gross}(in)	d_{net}(in)	d_{neck}(in)	E(psi)	σ_{max}(ksi)	σ_{yield}(ksi)	$\sigma_{2.5\%}$(ksi)
693	12L1	0.1970	0.1920	0.1605	24923	249.93	184.24	229.31
694	12L1	0.1979	0.1921	0.1650	24884	247.46	181.79	227.18
695	12L1	0.1978	0.1920	0.1623	25692	247.38	185.18	227.98
696	12L1	0.1969	0.1918	0.1580	24953	251.96	187.45	231.61
697	12L1	0.1959	0.1920	0.1598	25805	250.14	186.30	232.00
698	12L1	0.1971	0.1915	0.1593	25614	247.86	185.44	230.27
699	12L1	0.1970	0.1916	0.1610	24759	250.90	184.37	230.40
700	12L1	0.1971	0.1918	0.1653	24783	249.25	182.08	228.96
701	12L1	0.1973	0.1918	0.1648	23848	248.15	180.96	227.43
702	12L1	0.1971	0.1919	0.1598	23823	247.93	180.84	227.23
703	26L4	0.1958	0.1919	0.1533	26313	255.45	185.72	234.50
704	26L4	0.1961	0.1920	0.1543	21200	254.41	193.97	232.12
705	26L4	0.1960	0.1920	0.1518	26196	254.35	188.00	233.85
706	26L4	0.1954	0.1916	0.1563	26088	255.21	188.26	234.85
707	26L4	0.1963	0.1919	0.1600	24869	254.10	188.83	233.29
708	26L4	0.1959	0.1919	0.1570	25639	253.42	187.15	232.99
709	26L4	0.1968	0.1919	0.1578	25671	250.80	184.35	230.51
710	26L4	0.1963	0.1915	0.1595	25265	251.83	184.32	231.13
711	26L4	0.1961	0.1920	0.1583	25211	252.44	185.42	231.69
712	26L4	0.1959	0.1918	0.1593	25334	252.66	184.36	231.65
713	26L4	0.1961	0.1920	0.1598	25271	251.96	185.04	231.19
714	26L4	0.1954	0.1920	0.1585	26112	254.11	186.20	233.26
715	26L4	0.1955	0.1919	0.1560	25658	253.89	185.62	232.91

Continued on next page...

Test	Wire	d_{gross}(in)	d_{net}(in)	d_{neck}(in)	E(psi)	σ_{max}(ksi)	σ_{yield}(ksi)	$\sigma_{2.5\%}$(ksi)
716	14L1	0.1973	0.1919	0.1558	25239	252.80	189.43	233.62
717	14L1	0.1971	0.1919	0.1523	22429	253.55	193.32	233.32
718	14L1	0.1988	0.1920	0.1553	24767	249.17	187.55	230.43
719	14L1	0.1963	0.1918	0.1610	25576	253.82	189.75	234.48
720	14L1	0.1965	0.1914	0.1548	25799	253.20	189.74	234.21
721	14L1	0.1970	0.1914	0.1550	25972	253.67	191.30	234.66
722	14L1	0.1984	0.1910	0.1570	25089	247.57	186.19	229.53
723	14L1	0.1995	0.1916	0.1578	24281	243.84	182.34	225.15
724	14L1	0.1959	0.1913	0.1558	25743	253.64	189.03	234.49
725	14L1	0.1974	0.1918	0.1560	24928	250.28	186.78	231.32
726	14L1	0.1961	0.1910	0.1570	25449	252.37	187.62	233.22
727	14L1	0.1981	0.1913	0.1573	24596	247.32	184.05	228.18
728	14L1	0.1963	0.1918	0.1560	24841	252.36	187.88	232.67
729	10L3	0.1963	0.1918	0.1600	28827	252.05	193.45	234.78
730	10L3	0.1953	0.1923	0.1613	28564	253.13	191.96	235.45
731	10L3	0.1951	0.1920	0.1545	28498	256.01	193.16	237.39
732	10L3	0.1958	0.1918	0.1543	28688	254.13	195.68	236.34
733	10L3	0.1954	0.1918	0.1563	28497	256.01	197.73	237.97
734	10L3	0.1953	0.1914	0.1563	29039	254.70	192.89	237.05
735	10L3	0.1953	0.1913	0.1605	29203	253.45	192.26	235.74
736	10L3	0.1961	0.1918	0.1555	28196	252.02	193.65	234.21
737	10L3	0.1956	0.1918	0.1588	27774	253.29	192.12	234.92
738	10L3	0.1949	0.1918	0.1578	28465	254.73	194.57	236.78

Continued on next page...

Test	Wire	d_{gross}(in)	d_{net}(in)	d_{neck}(in)	E(psi)	$\sigma_{\max}$(ksi)	σ_{yield}(ksi)	$\sigma_{2.5\%}$(ksi)
739	10L3	0.1954	0.1916	0.1558	27931	253.76	193.81	235.84
740	10L3	0.1954	0.1918	0.1550	27971	253.83	193.85	235.67
741	10L3	0.1951	0.1918	0.1570	28288	254.28	193.33	236.11
742	20L3	0.1955	0.1923	0.1538	25639	255.32	189.01	235.34
743	20L3	0.1958	0.1918	0.1578	26303	255.68	189.87	235.58
744	20L3	0.1951	0.1919	0.1545	26492	256.04	188.75	236.12
745	20L3	0.1963	0.1920	0.1578	26699	254.13	188.17	234.42
746	20L3	0.1959	0.1916	0.1573	22956	253.99	191.75	233.10
747	20L3	0.1955	0.1919	0.1538	26992	256.89	194.53	237.44
748	20L3	0.1965	0.1915	0.1520	28009	254.16	185.89	234.55
749	20L3	0.1973	0.1914	0.1543	26135	250.26	186.30	230.87
750	20L3	0.1970	0.1920	0.1553	25494	250.58	185.65	230.69
751	20L3	0.1959	0.1920	0.1548	25832	253.85	186.93	233.52
752	20L3	0.1961	0.1916	0.1553	25959	252.81	186.04	232.51
753	20L3	0.1963	0.1921	0.1553	25608	252.41	184.83	231.89
754	20L3	0.1951	0.1916	0.1550	25874	255.50	186.94	234.73
755	11L5	0.1961	0.1918	0.1558	25227	252.08	184.84	231.89
756	11L5	0.1964	0.1920	0.1575	19812	250.89	190.79	229.02
757	11L5	0.1963	0.1919	0.1588	26037	252.81	186.84	233.04
758	11L5	0.1951	0.1914	0.1523	26770	256.76	188.02	236.65
759	11L5	0.1955	0.1914	0.1540	27306	254.78	185.61	235.31
760	11L5	0.1954	0.1919	0.1603	25854	253.09	186.09	232.80
761	11L5	0.1955	0.1914	0.1598	25943	252.85	186.10	233.41

Continued on next page...

Test	Wire	d_{gross}(in)	d_{net}(in)	d_{neck}(in)	E(psi)	$\sigma_{\max}$(ksi)	σ_{yield}(ksi)	$\sigma_{2.5\%}$(ksi)
762	11L5	0.1961	0.1919	0.1530	25585	252.69	185.89	232.34
763	11L5	0.1964	0.1916	0.1555	25897	251.00	184.30	231.67
764	11L5	0.1964	0.1920	0.1545	25494	251.19	185.24	231.18
765	11L5	0.1971	0.1918	0.1523	25549	251.54	185.04	231.66
766	11L5	0.1959	0.1918	0.1510	26266	255.35	186.91	235.12
767	11L5	0.1960	0.1915	0.1518	27118	254.65	183.64	234.47
768	25L2	0.1964	0.1921	0.1595	24394	249.79	183.80	229.71
769	25L2	0.1963	0.1921	0.1600	23847	248.16	182.00	227.91
770	25L2	0.1963	0.1919	0.1593	24831	250.53	184.59	230.91
771	25L2	0.1966	0.1916	0.1548	24823	252.69	186.18	232.04
772	25L2	0.1968	0.1916	0.1518	24727	252.99	187.51	232.29
773	25L2	0.1966	0.1919	0.1538	24670	252.66	186.61	231.82
774	25L2	0.1974	0.1918	0.1575	24022	248.80	182.77	228.12
775	25L2	0.1974	0.1920	0.1558	24227	248.84	183.36	228.29
776	25L2	0.1985	0.1920	0.1535	23562	246.47	181.71	225.86
777	25L2	0.1973	0.1916	0.1533	23811	249.25	183.74	227.62
778	25L2	0.1964	0.1920	0.1530	24262	251.45	184.62	229.51
779	25L2	0.1963	0.1920	0.1558	24360	252.17	184.92	231.06
780	25L2	0.1961	0.1918	0.1520	24627	252.70	185.18	231.53
781	4L3	0.1958	0.1918	0.1540	25265	253.14	185.45	232.20
782	4L3	0.1963	0.1914	0.1505	25065	253.42	186.11	232.34
783	4L3	0.1961	0.1919	0.1563	25098	251.96	185.04	231.41
784	4L3	0.1958	0.1916	0.1525	25587	255.19	188.16	234.13

Continued on next page...

Test	Wire	d_{gross}(in)	d_{net}(in)	d_{neck}(in)	E(psi)	$\sigma_{\max}$(ksi)	σ_{yield}(ksi)	$\sigma_{2.5\%}$(ksi)
785	4L3	0.1963	0.1918	0.1518	25263	253.16	186.86	232.28
786	4L3	0.1964	0.1918	0.1565	25177	250.91	184.43	230.29
787	4L3	0.1956	0.1919	0.1525	25607	252.38	185.41	231.84
788	4L3	0.1963	0.1916	0.1545	25358	251.38	184.34	230.66
789	4L3	0.1963	0.1915	0.1535	25123	250.95	183.89	230.10
790	4L3	0.1956	0.1915	0.1568	25065	252.29	184.60	231.25
791	4L3	0.1960	0.1916	0.1568	25198	251.47	183.83	230.51
792	4L3	0.1964	0.1919	0.1525	24906	251.01	183.44	229.91
793	4L3	0.1948	0.1915	0.1525	25369	255.01	186.08	233.68
794	1L3	0.1963	0.1918	0.1570	24965	251.54	184.47	229.13
795	1L3	0.1964	0.1915	0.1553	25230	251.49	184.52	231.09
796	1L3	0.1956	0.1918	0.1550	25590	253.87	187.08	233.48
797	1L3	0.1960	0.1918	0.1563	25732	252.67	186.41	232.53
798	1L3	0.1958	0.1921	0.1573	25990	252.46	185.99	232.35
799	1L3	0.1953	0.1918	0.1568	26580	254.47	188.44	234.93
800	1L3	0.1965	0.1923	0.1550	25902	253.32	187.95	233.24
801	1L3	0.1970	0.1916	0.1585	26089	250.15	186.66	231.35
802	1L3	0.1975	0.1919	0.1563	25412	250.34	185.78	231.03
803	1L3	0.1961	0.1915	0.1558	25629	253.03	188.21	234.51
804	1L3	0.1958	0.1920	0.1543	25721	255.92	189.45	235.65
805	1L3	0.1966	0.1913	0.1553	24957	253.47	187.54	233.17
806	1L3	0.1958	0.1918	0.1565	25396	254.88	187.64	234.82
807	18L4	0.1956	0.1918	0.1550	24853	251.33	183.77	230.48

Continued on next page...

Test	Wire	d_{gross}(in)	d_{net}(in)	d_{neck}(in)	E(psi)	$\sigma_{\max}$(ksi)	σ_{yield}(ksi)	$\sigma_{2.5\%}$(ksi)
808	18L4	0.1948	0.1915	0.1563	25219	254.22	185.81	233.14
809	18L4	0.1956	0.1918	0.1560	25122	251.73	184.72	230.86
810	18L4	0.1953	0.1914	0.1540	25447	252.81	185.39	232.17
811	18L4	0.1951	0.1921	0.1553	25268	253.07	184.93	232.16
812	18L4	0.1961	0.1918	0.1538	24748	250.54	184.37	229.93
813	18L4	0.1953	0.1915	0.1563	25310	252.85	185.55	232.01
814	18L4	0.1959	0.1920	0.1563	25238	250.95	183.98	230.46
815	18L4	0.1959	0.1919	0.1563	25602	252.24	185.27	232.12
816	18L4	0.1956	0.1919	0.1585	25386	253.88	186.48	232.92
817	18L4	0.1958	0.1914	0.1558	25424	254.27	186.80	233.32
818	18L4	0.1959	0.1915	0.1558	25280	253.34	186.03	232.27
819	18L4	0.1955	0.1916	0.1523	25724	254.80	186.40	233.73
820	18L4	0.1948	0.1916	0.1553	25865	254.69	185.16	233.25
821	18L4	0.1954	0.1919	0.1568	25713	252.94	184.52	231.78
822	18L4	0.1953	0.1921	0.1548	26202	253.12	185.31	232.25
823	18L4	0.1961	0.1919	0.1575	25505	251.11	183.76	230.09
824	18L4	0.1958	0.1919	0.1575	25780	252.24	184.99	231.32
825	18L4	0.1966	0.1920	0.1558	25658	249.85	183.42	229.34
826	18L4	0.1960	0.1920	0.1608	26132	251.25	184.31	230.71
827	18L4	0.1954	0.1918	0.1560	26109	254.73	187.11	233.79
828	18L4	0.1961	0.1918	0.1555	25841	252.61	185.77	232.13
829	18L4	0.1956	0.1920	0.1623	25891	252.29	184.15	231.42
830	18L4	0.1956	0.1920	0.1563	26281	254.67	186.36	233.44

Continued on next page...

Test	Wire	d_{gross}(in)	d_{net}(in)	d_{neck}(in)	E(psi)	$\sigma_{\max}$(ksi)	σ_{yield}(ksi)	$\sigma_{2.5\%}$(ksi)
831	18L4	0.1956	0.1918	0.1550	26026	254.45	186.39	233.50
832	18L4	0.1958	0.1919	0.1623	25607	252.55	184.86	231.82
833	22L1	0.1966	0.1915	0.1533	25492	253.93	187.82	233.70
834	22L1	0.1953	0.1918	0.1593	26057	257.23	190.04	236.73
835	22L1	0.1960	0.1916	0.1533	25810	255.48	189.57	235.36
836	22L1	0.1963	0.1918	0.1585	25491	251.32	186.08	232.13
837	22L1	0.1963	0.1919	0.1578	25577	252.14	188.00	233.05
838	22L1	0.1970	0.1918	0.1610	25233	248.78	185.78	230.18
839	22L1	0.1986	0.1916	0.1520	25149	247.36	184.49	228.11
840	22L1	0.1968	0.1920	0.1590	25792	250.84	186.31	231.35
841	22L1	0.1995	0.1916	0.1528	24753	245.35	183.27	226.05
842	22L1	0.1965	0.1915	0.1558	25692	251.94	187.60	232.52
843	22L1	0.1960	0.1918	0.1583	25586	252.38	186.20	232.02
844	22L1	0.1961	0.1916	0.1580	25382	252.76	186.69	232.64
845	22L1	0.1955	0.1914	0.1538	25923	254.51	187.98	234.12
846	26L2	0.1956	0.1920	0.1600	25144	252.36	185.25	231.66
847	26L2	0.1955	0.1920	0.1605	24932	253.03	185.48	232.14
848	26L2	0.1955	0.1920	0.1635	25142	252.85	185.00	232.11
849	26L2	0.1958	0.1916	0.1603	24961	252.13	184.81	231.71
850	26L2	0.1960	0.1919	0.1598	24987	251.70	184.79	231.32
851	26L2	0.1956	0.1920	0.1610	25000	253.08	186.18	232.49
852	26L2	0.1963	0.1919	0.1600	24771	250.93	184.25	230.41
853	26L2	0.1958	0.1919	0.1608	25059	252.46	185.02	232.03

Continued on next page...

Test	Wire	d_{gross}(in)	d_{net}(in)	d_{neck}(in)	E(psi)	$\sigma_{\max}$(ksi)	σ_{yield}(ksi)	$\sigma_{2.5\%}$(ksi)
854	26L2	0.1960	0.1918	0.1585	25739	253.71	187.05	233.49
855	26L2	0.1959	0.1916	0.1585	25417	254.37	187.41	233.62
856	26L2	0.1955	0.1919	0.1595	25471	254.93	187.14	233.94
857	26L2	0.1953	0.1915	0.1618	24892	253.74	185.62	232.77
858	26L2	0.1956	0.1920	0.1583	25213	253.82	186.08	232.78
859	19L2	0.1963	0.1918	0.1595	24868	252.87	186.01	232.39
860	19L2	0.1986	0.1918	0.1585	23953	246.85	182.21	226.67
861	19L2	0.1978	0.1916	0.1595	25131	248.99	184.56	229.21
862	19L2	0.1994	0.1916	0.1583	24995	244.82	183.81	226.02
863	19L2	0.2013	0.1921	0.1593	24213	240.38	180.23	221.57
864	19L2	0.2039	0.1919	0.1580	25202	234.67	182.33	217.56
865	19L2	0.2009	0.1921	0.1600	23943	240.83	180.38	221.92
866	19L2	0.2025	0.1921	0.1595	24957	237.64	182.35	220.79
867	19L2	0.1984	0.1918	0.1673	25537	238.69	185.82	226.48
868	19L2	0.1981	0.1920	0.1608	24287	247.83	183.13	227.93
869	19L2	0.1978	0.1919	0.1580	24559	250.56	184.63	230.22
870	19L2	0.1971	0.1921	0.1530	25083	253.74	187.39	233.24
871	19L2	0.1986	0.1921	0.1538	24409	249.90	184.88	229.57
872	5L5	0.1963	0.1920	0.1565	24657	252.82	186.49	232.15
873	5L5	0.1968	0.1913	0.1538	24666	251.84	185.36	231.19
874	5L5	0.1955	0.1918	0.1560	25184	254.92	187.57	234.26
875	5L5	0.1966	0.1918	0.1543	24754	251.97	185.76	231.35
876	5L5	0.1970	0.1914	0.1590	24904	250.86	184.91	230.59

Continued on next page...

Test	Wire	d_{gross}(in)	d_{net}(in)	d_{neck}(in)	E(psi)	$\sigma_{\max}$(ksi)	σ_{yield}(ksi)	$\sigma_{2.5\%}$(ksi)
877	5L5	0.1976	0.1918	0.1585	24438	249.85	184.73	229.64
878	5L5	0.1954	0.1916	0.1545	25461	255.16	188.48	234.71
879	5L5	0.1976	0.1915	0.1553	24666	249.31	184.05	229.34
880	5L5	0.1969	0.1918	0.1555	24962	253.00	187.87	232.77
881	5L5	0.1971	0.1920	0.1535	24681	252.10	187.13	232.22
882	5L5	0.1959	0.1921	0.1593	25010	252.85	186.71	232.73
883	5L5	0.1961	0.1918	0.1560	24983	252.96	188.35	234.10
884	5L5	0.1958	0.1920	0.1543	25292	255.15	188.79	235.12
885	25R5	0.1954	0.1919	0.1573	25806	256.01	188.80	235.15
886	25R5	0.1951	0.1914	0.1585	26286	255.28	188.48	234.76
887	25R5	0.1956	0.1918	0.1590	25614	253.54	187.51	233.32
888	25R5	0.1956	0.1915	0.1583	25495	254.49	188.53	234.27
889	25R5	0.1959	0.1916	0.1558	25785	254.93	188.57	234.47
890	25R5	0.1958	0.1918	0.1600	26382	254.04	188.12	233.97
891	25R5	0.1963	0.1915	0.1590	25799	254.39	188.29	234.04
892	25R5	0.1965	0.1915	0.1568	25588	253.69	188.04	233.28
893	25R5	0.1954	0.1918	0.1580	25537	254.79	187.95	234.35
894	25R5	0.1960	0.1915	0.1605	25720	252.33	186.00	231.84
895	25R5	0.1959	0.1916	0.1565	25178	253.36	186.44	232.59
896	25R5	0.1955	0.1918	0.1583	25368	254.19	187.01	233.32
897	25R5	0.1956	0.1918	0.1598	25202	253.55	186.51	232.77
898	5R5	0.1965	0.1916	0.1550	26115	254.68	189.25	234.75
899	5R5	0.1961	0.1913	0.1550	26439	256.38	190.03	236.29

Continued on next page...

Test	Wire	d_{gross}(in)	d_{net}(in)	d_{neck}(in)	E(psi)	$\sigma_{\max}$(ksi)	σ_{yield}(ksi)	$\sigma_{2.5\%}$(ksi)
900	5R5	0.1964	0.1915	0.1543	26347	255.57	189.89	235.60
901	5R5	0.1975	0.1914	0.1525	26028	252.69	188.11	232.90
902	5R5	0.1953	0.1915	0.1555	26934	258.23	192.00	238.26
903	5R5	0.1969	0.1918	0.1568	26114	249.26	187.23	232.16
904	5R5	0.1968	0.1914	0.1593	27106	253.94	189.78	234.51
905	5R5	0.1965	0.1916	0.1580	26322	254.58	189.20	234.72
906	5R5	0.1959	0.1918	0.1530	25907	256.04	190.21	236.28
907	5R5	0.1963	0.1919	0.1570	25415	253.82	187.69	233.70
908	5R5	0.1949	0.1918	0.1560	26408	257.80	190.21	237.38
909	5R5	0.1973	0.1919	0.1535	25160	252.39	186.97	232.31
910	5R5	0.1961	0.1915	0.1553	25661	254.83	188.26	234.68
911	5R1	0.1958	0.1918	0.1570	25206	253.59	185.75	233.15
912	5R1	0.1968	0.1915	0.1568	24910	252.07	186.34	232.40
913	5R1	0.1955	0.1919	0.1538	25690	257.41	189.67	236.96
914	5R1	0.1958	0.1916	0.1555	25737	256.69	189.78	236.41
915	5R1	0.1959	0.1915	0.1548	25780	255.40	188.57	235.19
916	5R1	0.1965	0.1918	0.1593	25233	251.29	185.17	231.59
917	5R1	0.1983	0.1916	0.1580	24594	248.06	183.75	228.32
918	5R1	0.1964	0.1918	0.1565	25458	253.68	186.73	233.25
919	5R1	0.1969	0.1918	0.1555	25416	252.48	185.73	232.58
920	5R1	0.1955	0.1916	0.1553	25961	256.89	188.60	236.20
921	5R1	0.1964	0.1919	0.1583	25678	254.48	186.85	233.82
922	5R1	0.1963	0.1916	0.1568	25479	253.26	185.57	233.28

Continued on next page...

Test	Wire	d_{gross}(in)	d_{net}(in)	d_{neck}(in)	E(psi)	$\sigma_{\max}$(ksi)	σ_{yield}(ksi)	$\sigma_{2.5\%}$(ksi)
923	5R1	0.1954	0.1916	0.1573	25349	255.05	187.21	234.39
924	8R3	0.1960	0.1915	0.1613	25107	252.41	183.27	231.35
925	8R3	0.1965	0.1916	0.1575	25330	251.27	183.01	230.49
926	8R3	0.1974	0.1918	0.1578	24855	248.99	182.30	228.49
927	8R3	0.1969	0.1918	0.1590	24522	245.97	181.49	227.39
928	8R3	0.1971	0.1914	0.1605	24040	243.41	180.01	224.99
929	8R3	0.1980	0.1915	0.1585	24722	244.60	182.07	226.41
930	8R3	0.1965	0.1916	0.1610	24688	247.44	183.74	228.26
931	8R3	0.1978	0.1909	0.1625	24288	243.18	181.42	226.55
932	8R3	0.1978	0.1914	0.1540	24978	249.61	183.03	228.96
933	8R3	0.1983	0.1915	0.1585	24490	247.99	182.04	226.88
934	8R3	0.1965	0.1916	0.1565	24905	249.53	183.73	229.85
935	8R3	0.1978	0.1916	0.1545	24679	247.94	181.01	227.50
936	8R3	0.1970	0.1918	0.1553	24971	250.34	183.02	229.71
937	18R4	0.1956	0.1919	0.1533	25219	253.19	185.36	232.35
938	18R4	0.1959	0.1918	0.1590	25248	252.26	184.48	231.53
939	18R4	0.1964	0.1920	0.1588	25028	250.69	184.49	230.32
940	18R4	0.1951	0.1918	0.1535	26472	255.95	189.36	235.66
941	18R4	0.1964	0.1915	0.1563	25567	253.60	187.09	233.16
942	18R4	0.1989	0.1921	0.1573	23964	244.78	180.23	224.74
943	18R4	0.1966	0.1920	0.1555	24858	250.42	184.05	230.15
944	18R4	0.1984	0.1916	0.1528	24766	247.75	183.33	227.86
945	18R4	0.1956	0.1916	0.1520	25764	255.30	187.98	234.65

Continued on next page...

Test	Wire	d_{gross}(in)	d_{net}(in)	d_{neck}(in)	E(psi)	$\sigma_{\max}$(ksi)	σ_{yield}(ksi)	$\sigma_{2.5\%}$(ksi)
946	18R4	0.1954	0.1914	0.1520	25834	255.58	188.42	235.10
947	18R4	0.1950	0.1919	0.1555	25928	256.90	188.94	235.97
948	18R4	0.1948	0.1918	0.1603	25731	257.81	189.67	236.78
949	18R4	0.1950	0.1916	0.1545	25985	255.19	186.75	234.53
950	21R1	0.1959	0.1916	0.1548	25107	252.60	188.36	232.85
951	21R1	0.1960	0.1918	0.1565	24921	251.33	187.03	231.54
952	21R1	0.1971	0.1916	0.1558	25682	248.55	184.86	229.35
953	21R1	0.1969	0.1916	0.1568	25961	248.96	186.77	230.05
954	21R1	0.1965	0.1914	0.1593	25833	250.28	186.97	230.89
955	21R1	0.1963	0.1916	0.1555	26301	251.35	188.80	232.22
956	21R1	0.1978	0.1915	0.1568	25397	247.52	186.10	228.69
957	21R1	0.2008	0.1914	0.1560	24854	240.24	181.13	222.00
958	21R1	0.1970	0.1915	0.1560	25439	249.25	186.57	230.15
959	21R1	0.1984	0.1918	0.1558	24217	246.15	184.04	226.90
960	21R1	0.1964	0.1918	0.1525	25864	252.48	188.11	233.04
961	21R1	0.1968	0.1915	0.1568	26276	250.15	188.20	231.61
962	21R1	0.1953	0.1915	0.1563	25607	254.35	190.35	235.24
963	12R5	0.1951	0.1915	0.1583	25565	252.44	184.38	231.78
964	12R5	0.1958	0.1915	0.1568	25719	252.27	185.28	231.95
965	12R5	0.1954	0.1919	0.1578	26194	251.95	186.21	232.75
966	12R5	0.1959	0.1918	0.1588	26226	252.95	187.16	232.63
967	12R5	0.1966	0.1918	0.1558	26228	252.22	187.62	232.30
968	12R5	0.1960	0.1919	0.1555	27390	254.36	191.45	234.50

Continued on next page...

Test	Wire	d_{gross}(in)	d_{net}(in)	d_{neck}(in)	E(psi)	$\sigma_{\max}$(ksi)	σ_{yield}(ksi)	$\sigma_{2.5\%}$(ksi)
969	12R5	0.1964	0.1916	0.1568	26536	251.07	186.57	231.80
970	12R5	0.1960	0.1916	0.1593	25832	251.34	185.36	231.08
971	12R5	0.1963	0.1916	0.1583	25811	251.44	185.28	231.13
972	12R5	0.1955	0.1919	0.1593	25815	253.58	186.47	232.87
973	12R5	0.1954	0.1915	0.1570	25758	253.67	186.13	232.87
974	12R5	0.1949	0.1915	0.1570	25917	254.93	186.32	233.94
975	12R5	0.1955	0.1916	0.1563	25502	253.61	185.48	232.65
976	4R3	0.1964	0.1918	0.1530	25422	250.32	185.07	230.41
977	4R3	0.1960	0.1914	0.1528	25863	251.24	185.91	231.42
978	4R3	0.1968	0.1915	0.1560	25880	249.13	184.25	229.51
979	4R3	0.1974	0.1918	0.1533	25307	247.81	184.01	228.39
980	4R3	0.1960	0.1914	0.1538	26066	251.37	186.38	231.73
981	4R3	0.1974	0.1914	0.1563	25367	247.71	183.77	228.19
982	4R3	0.1975	0.1918	0.1535	25575	249.37	186.22	229.94
983	4R3	0.1968	0.1913	0.1545	25869	251.35	186.90	231.96
984	4R3	0.1963	0.1918	0.1523	26100	253.15	188.24	233.50
985	4R3	0.1964	0.1919	0.1515	25878	251.70	187.26	232.19
986	4R3	0.1960	0.1914	0.1543	25703	251.55	185.94	231.72
987	4R3	0.1963	0.1916	0.1523	25878	251.59	186.35	231.86
988	4R3	0.1956	0.1916	0.1615	25379	248.50	182.71	229.34
989	6R1	0.1958	0.1920	0.1585	25045	254.50	185.92	233.66
990	6R1	0.1960	0.1920	0.1603	25339	254.05	185.40	233.30
991	6R1	0.1968	0.1918	0.1628	25274	251.94	185.21	231.48

Continued on next page...

Test	Wire	d_{gross}(in)	d_{net}(in)	d_{neck}(in)	E(psi)	σ_{max}(ksi)	σ_{yield}(ksi)	$\sigma_{2.5\%}$(ksi)
992	6R1	0.1956	0.1916	0.1560	26046	255.27	188.05	234.78
993	6R1	0.1969	0.1920	0.1575	25554	251.20	185.39	231.21
994	6R1	0.1964	0.1915	0.1588	26523	252.73	188.69	233.24
995	6R1	0.1963	0.1915	0.1570	26229	254.72	189.18	234.57
996	6R1	0.1986	0.1916	0.1568	24890	247.38	183.25	227.89
997	6R1	0.1974	0.1919	0.1605	25197	249.35	183.64	229.30
998	6R1	0.1958	0.1915	0.1598	25588	254.77	186.48	234.00
999	6R1	0.1958	0.1918	0.1578	25535	255.07	186.77	234.38
1000	6R1	0.1965	0.1918	0.1660	24243	248.47	181.54	228.86
1001	6R1	0.1951	0.1920	0.1585	25660	256.87	187.63	236.10
1002	3R1	0.1949	0.1914	0.1578	25811	254.68	187.01	234.22
1003	3R1	0.1971	0.1918	0.1530	24655	249.15	183.92	229.15
1004	3R1	0.1970	0.1919	0.1533	25019	249.66	184.56	229.67
1005	3R1	0.1959	0.1918	0.1540	25676	252.65	186.41	232.48
1006	3R1	0.1960	0.1914	0.1563	25940	251.75	186.34	232.04
1007	3R1	0.1958	0.1915	0.1550	26308	252.81	188.04	233.33
1008	3R1	0.1965	0.1915	0.1510	26410	253.43	188.78	233.78
1009	3R1	0.1963	0.1916	0.1560	25978	253.77	188.66	233.75
1010	3R1	0.1954	0.1916	0.1593	26316	255.21	189.15	235.29
1011	3R1	0.1954	0.1916	0.1573	26477	254.39	188.34	234.45
1012	3R1	0.1968	0.1913	0.1600	25791	250.17	184.82	230.39
1013	3R1	0.1953	0.1913	0.1538	26167	255.76	188.61	235.37
1014	3R1	0.1950	0.1913	0.1565	25359	253.93	188.41	234.51

Continued on next page...

Test	Wire	d_{gross}(in)	d_{net}(in)	d_{neck}(in)	E(psi)	$\sigma_{\max}$(ksi)	σ_{yield}(ksi)	$\sigma_{2.5\%}$(ksi)
1015	7R3	0.1954	0.1918	0.1625	26530	254.81	189.01	234.92
1016	7R3	0.1959	0.1919	0.1610	26241	253.31	186.94	233.50
1017	7R3	0.1946	0.1916	0.1603	27129	255.93	190.66	236.60
1018	7R3	0.1953	0.1920	0.1575	28088	255.51	193.17	236.30
1019	7R3	0.1973	0.1918	0.1655	27993	250.10	194.14	232.45
1020	7R3	0.1949	0.1916	0.1583	27734	256.80	193.70	237.70
1021	7R3	0.1956	0.1919	0.1580	27117	255.39	192.14	236.65
1022	7R3	0.1978	0.1913	0.1580	27241	249.95	190.49	231.65
1023	7R3	0.1971	0.1916	0.1580	27691	251.10	190.42	232.99
1024	7R3	0.1973	0.1918	0.1578	26823	252.43	190.20	233.45
1025	7R3	0.1963	0.1918	0.1588	26780	255.06	189.96	235.40
1026	7R3	0.1948	0.1918	0.1613	26921	257.96	191.43	238.22
1027	7R3	0.1956	0.1915	0.1625	26876	253.94	188.21	234.18
1028	12R2	0.1964	0.1918	0.1553	25150	250.88	183.03	230.12
1029	12R2	0.1965	0.1916	0.1578	25035	250.18	182.77	229.33
1030	12R2	0.1960	0.1916	0.1583	25723	252.48	185.83	232.23
1031	12R2	0.1961	0.1915	0.1598	26102	253.45	187.48	232.98
1032	12R2	0.1955	0.1916	0.1585	26409	254.75	188.68	234.40
1033	12R2	0.1965	0.1920	0.1568	25652	252.21	184.74	231.29
1034	12R2	0.1963	0.1916	0.1620	26787	250.72	187.38	231.41
1035	12R2	0.1959	0.1916	0.1653	26230	252.48	186.97	232.26
1036	12R2	0.1969	0.1915	0.1640	25849	247.62	184.31	229.48
1037	12R2	0.1979	0.1918	0.1630	24425	243.74	179.75	224.37

Continued on next page...

Test	Wire	d_{gross}(in)	d_{net}(in)	d_{neck}(in)	E(psi)	$\sigma_{\max}$(ksi)	σ_{yield}(ksi)	$\sigma_{2.5\%}$(ksi)
1038	12R2	0.1966	0.1918	0.1583	25465	249.93	183.65	230.42
1039	12R2	0.1961	0.1914	0.1580	25507	253.78	186.04	232.81
1040	12R2	0.1956	0.1918	0.1548	25449	254.09	185.75	233.10
1041	14R1	0.1953	0.1918	0.1568	25964	253.91	187.67	233.70
1042	14R1	0.1956	0.1914	0.1593	25543	253.11	186.91	232.99
1043	14R1	0.1960	0.1916	0.1608	25673	251.69	186.35	231.91
1044	14R1	0.1966	0.1914	0.1618	26932	249.27	187.91	230.98
1045	14R1	0.1951	0.1913	0.1573	26421	254.44	188.98	234.76
1046	14R1	0.1959	0.1918	0.1583	25691	252.22	188.04	232.69
1047	14R1	0.1954	0.1915	0.1590	25599	254.20	189.77	234.67
1048	14R1	0.1971	0.1920	0.1570	24978	251.42	187.88	231.73
1049	14R1	0.1966	0.1918	0.1578	25056	252.81	188.59	232.97
1050	14R1	0.1950	0.1915	0.1595	25441	256.08	190.00	236.08
1051	14R1	0.1948	0.1914	0.1618	25477	254.18	186.94	234.03
1052	14R1	0.1951	0.1914	0.1620	24968	252.64	185.93	232.72
1053	14R1	0.1964	0.1915	0.1598	24887	253.13	187.47	232.68
1054	3R3	0.1956	0.1914	0.1570	25478	255.34	188.33	234.92
1055	3R3	0.1955	0.1916	0.1548	25807	255.18	188.00	234.80
1056	3R3	0.1958	0.1915	0.1568	25587	254.53	188.78	234.59
1057	3R3	0.1963	0.1916	0.1550	25938	255.17	189.81	235.47
1058	3R3	0.1961	0.1916	0.1533	26127	256.04	190.22	236.15
1059	3R3	0.1950	0.1914	0.1533	26386	258.01	191.73	238.24
1060	3R3	0.1956	0.1920	0.1548	25761	254.30	188.99	234.79

Continued on next page...

Test	Wire	d_{gross}(in)	d_{net}(in)	d_{neck}(in)	E(psi)	$\sigma_{\max}$(ksi)	σ_{yield}(ksi)	$\sigma_{2.5\%}$(ksi)
1061	3R3	0.1964	0.1918	0.1563	25680	252.85	188.45	233.93
1062	3R3	0.1961	0.1916	0.1543	25830	255.05	189.33	235.29
1063	3R3	0.1954	0.1918	0.1555	25912	257.57	190.85	237.30
1064	3R3	0.1950	0.1916	0.1580	26187	257.49	190.61	237.34
1065	3R3	0.1959	0.1918	0.1538	25184	253.55	186.69	233.26
1066	3R3	0.1953	0.1915	0.1550	25823	255.46	188.55	235.52
1067	24R6	0.1964	0.1919	0.1583	25513	252.62	186.55	233.08
1068	24R6	0.1956	0.1918	0.1593	25434	253.60	186.93	233.93
1069	24R6	0.1954	0.1919	0.1583	25554	256.38	189.03	235.79
1070	24R6	0.1955	0.1919	0.1590	25592	254.53	187.81	234.37
1071	24R6	0.1956	0.1914	0.1605	25721	253.75	186.52	233.62
1072	24R6	0.1973	0.1918	0.1615	25352	250.06	184.42	230.27
1073	24R6	0.1955	0.1915	0.1605	25737	254.10	186.93	233.96
1074	24R6	0.1960	0.1914	0.1640	25875	252.47	185.92	232.25
1075	24R6	0.1956	0.1916	0.1590	26280	253.46	187.05	233.68
1076	24R6	0.1948	0.1919	0.1615	26046	256.19	188.21	235.71
1077	24R6	0.1955	0.1918	0.1608	25782	254.09	185.78	233.40
1078	24R6	0.1960	0.1918	0.1620	26085	252.20	184.96	231.74
1079	24R6	0.1950	0.1918	0.1583	26981	255.76	189.15	235.66
1080	26R5	0.1949	0.1915	0.1545	26086	252.75	184.66	232.33
1081	26R5	0.1950	0.1918	0.1530	26624	254.25	186.60	234.05
1082	26R5	0.1955	0.1914	0.1540	26469	253.38	187.02	233.22
1083	26R5	0.1950	0.1916	0.1580	26592	254.50	188.12	234.38

Continued on next page...

Test	Wire	d_{gross}(in)	d_{net}(in)	d_{neck}(in)	E(psi)	$\sigma_{\max}$(ksi)	σ_{yield}(ksi)	$\sigma_{2.5\%}$(ksi)
1084	26R5	0.1965	0.1915	0.1610	25934	248.22	184.31	229.84
1085	26R5	0.1959	0.1919	0.1580	25329	248.35	182.68	229.30
1086	26R5	0.1959	0.1916	0.1608	25571	251.28	184.96	231.35
1087	26R5	0.1955	0.1913	0.1598	25573	252.50	185.65	232.25
1088	26R5	0.1956	0.1915	0.1593	25823	252.21	185.23	232.20
1089	26R5	0.1950	0.1915	0.1578	26013	255.42	187.45	234.75
1090	26R5	0.1954	0.1916	0.1613	26067	254.59	187.14	234.04
1091	26R5	0.1949	0.1915	0.1580	26240	255.17	186.80	234.53
1092	26R5	0.1960	0.1918	0.1598	25334	250.57	184.04	230.54
1093	17R1	0.1949	0.1913	0.1565	26252	255.13	187.42	234.78
1094	17R1	0.1959	0.1914	0.1588	25763	252.44	186.50	232.44
1095	17R1	0.1951	0.1916	0.1573	26732	254.34	187.80	234.36
1096	17R1	0.1966	0.1915	0.1585	25651	249.97	184.56	230.26
1097	17R1	0.1961	0.1914	0.1578	25951	251.66	185.79	232.15
1098	17R1	0.1963	0.1916	0.1548	26032	253.61	188.17	233.70
1099	17R1	0.1970	0.1915	0.1560	25714	249.88	186.86	231.47
1100	17R1	0.1949	0.1915	0.1538	26578	256.99	190.73	236.85
1101	17R1	0.1963	0.1916	0.1590	25816	249.58	185.38	231.23
1102	17R1	0.1953	0.1913	0.1598	25793	251.29	185.21	232.61
1103	17R1	0.1948	0.1915	0.1560	26644	256.81	189.06	236.70
1104	17R1	0.1948	0.1914	0.1558	26622	256.71	189.13	236.42
1105	17R1	0.1948	0.1916	0.1543	26854	257.41	189.58	237.37
1106	22R3	0.1949	0.1916	0.1560	26323	257.39	190.12	236.75

Continued on next page...

Test	Wire	d_{gross}(in)	d_{net}(in)	d_{neck}(in)	E(psi)	$\sigma_{\max}$(ksi)	σ_{yield}(ksi)	$\sigma_{2.5\%}$(ksi)
1107	22R3	0.1951	0.1916	0.1568	25792	255.79	189.38	235.57
1108	22R3	0.1964	0.1916	0.1588	25285	250.67	184.86	230.45
1109	22R3	0.1960	0.1914	0.1605	25333	251.52	185.75	231.41
1110	22R3	0.1956	0.1914	0.1583	26018	252.58	187.36	232.62
1111	22R3	0.1951	0.1915	0.1575	26096	253.95	188.18	233.99
1112	22R3	0.1963	0.1913	0.1583	25478	250.97	185.89	231.05
1113	22R3	0.1964	0.1915	0.1578	25539	250.71	185.81	230.90
1114	22R3	0.1959	0.1916	0.1588	25737	252.27	186.73	232.23
1115	22R3	0.1953	0.1916	0.1600	25361	253.48	187.51	233.11
1116	22R3	0.1950	0.1916	0.1573	25447	254.27	187.53	234.09
1117	22R3	0.1953	0.1918	0.1560	25651	255.57	189.98	235.46
1118	22R3	0.1953	0.1918	0.1540	25861	256.03	189.53	235.50
1119	10R1	0.1965	0.1916	0.1635	25293	250.74	182.33	229.80
1120	10R1	0.1968	0.1918	0.1625	24934	249.92	182.46	229.17
1121	10R1	0.1989	0.1919	0.1638	24543	244.21	179.03	224.03
1122	10R1	0.1983	0.1915	0.1608	24299	243.61	179.82	224.84
1123	10R1	0.1966	0.1913	0.1645	24911	246.25	180.55	226.96
1124	10R1	0.2000	0.1916	0.1625	23898	239.23	176.60	220.53
1125	10R1	0.1956	0.1911	0.1633	25483	247.62	183.41	230.01
1126	10R1	0.1963	0.1911	0.1585	25541	246.87	183.52	229.89
1127	10R1	0.2001	0.1916	0.1640	23837	242.50	178.99	222.76
1128	10R1	0.1985	0.1914	0.1640	23932	245.19	179.36	224.73
1129	10R1	0.1966	0.1911	0.1615	25119	250.90	183.98	230.85

Continued on next page...

Test	Wire	d_{gross}(in)	d_{net}(in)	d_{neck}(in)	E(psi)	$\sigma_{\max}$(ksi)	σ_{yield}(ksi)	$\sigma_{2.5\%}$(ksi)
1130	10R1	0.1961	0.1914	0.1635	25443	252.49	183.95	231.97
1131	10R1	0.1978	0.1916	0.1865	24610	248.39	182.22	228.37
1132	19R3	0.1951	0.1918	0.1550	25694	254.18	187.67	233.72
1133	19R3	0.1959	0.1916	0.1563	25194	252.36	186.62	232.11
1134	19R3	0.1958	0.1914	0.1553	25809	253.05	187.34	232.90
1135	19R3	0.1951	0.1918	0.1583	26087	254.09	188.67	234.01
1136	19R3	0.1954	0.1916	0.1575	26475	253.69	190.37	234.38
1137	19R3	0.1960	0.1916	0.1548	26667	254.13	193.99	235.33
1138	19R3	0.1961	0.1915	0.1560	26532	254.24	190.66	234.69
1139	19R3	0.1968	0.1916	0.1583	25445	249.72	186.33	230.16
1140	19R3	0.1965	0.1915	0.1545	26255	253.69	190.00	234.12
1141	19R3	0.1961	0.1915	0.1525	25774	255.00	189.51	234.68
1142	19R3	0.1960	0.1915	0.1543	25466	254.19	188.35	234.30
1143	19R3	0.1951	0.1915	0.1590	26071	257.48	190.30	236.74
1144	19R3	0.1950	0.1915	0.1513	26141	257.65	190.30	237.06
1145	23L1	0.1949	0.1919	0.1625	26454	255.40	187.35	234.94
1146	23L1	0.1954	0.1916	0.1700	25967	252.26	184.80	231.98
1147	23L1	0.1956	0.1916	0.1645	25638	250.97	184.12	230.75
1148	23L1	0.1956	0.1911	0.1715	25853	251.74	184.97	231.42
1149	23L1	0.1959	0.1915	0.1650	25655	250.98	184.44	230.86
1150	23L1	0.1960	0.1916	0.1680	25756	250.51	184.53	230.59
1151	23L1	0.1953	0.1918	0.1683	26077	252.54	185.75	232.75
1152	23L1	0.1968	0.1915	0.1650	25360	249.15	183.87	229.35

Continued on next page...

Test	Wire	d_{gross}(in)	d_{net}(in)	d_{neck}(in)	E(psi)	$\sigma_{\max}$(ksi)	σ_{yield}(ksi)	$\sigma_{2.5\%}$(ksi)
1153	23L1	0.1949	0.1911	0.1655	26415	253.94	186.81	233.94
1154	23L1	0.1950	0.1919	0.1658	25877	253.14	185.43	232.82
1155	23L1	0.1950	0.1918	0.1610	26194	254.36	186.67	234.21
1156	23L1	0.1951	0.1919	0.1605	26021	255.37	187.62	234.85
1157	23L1	0.1955	0.1919	0.1583	26017	253.38	186.31	233.07
1158	10L1	0.1955	0.1916	0.1558	25739	255.36	188.78	235.10
1159	10L1	0.1960	0.1919	0.1593	25729	253.10	187.04	233.34
1160	10L1	0.1970	0.1914	0.1588	25406	249.41	183.93	229.71
1161	10L1	0.1953	0.1915	0.1590	26815	253.99	189.20	235.29
1162	10L1	0.1963	0.1916	0.1588	26222	252.61	187.15	232.77
1163	10L1	0.1980	0.1914	0.1645	25098	246.99	182.91	227.38
1164	10L1	0.1966	0.1918	0.1625	25760	251.11	185.42	231.06
1165	10L1	0.1979	0.1919	0.1650	25353	247.42	183.26	227.66
1166	10L1	0.1958	0.1914	0.1625	26605	252.15	186.29	232.31
1167	10L1	0.1953	0.1915	0.1615	26288	253.56	186.65	233.50
1168	10L1	0.1963	0.1919	0.1595	25918	251.06	184.78	230.97
1169	10L1	0.1964	0.1916	0.1593	25943	251.26	185.54	231.36
1170	10L1	0.1960	0.1920	0.1575	25957	251.85	184.88	231.64
1171	21L5	0.1954	0.1916	0.1550	25402	255.61	186.94	234.44
1172	21L5	0.1958	0.1916	0.1578	25637	255.21	187.44	234.24
1173	21L5	0.1959	0.1919	0.1595	25792	254.48	187.15	233.70
1174	21L5	0.1964	0.1915	0.1570	25309	252.01	185.80	231.69
1175	21L5	0.1964	0.1915	0.1575	25204	251.34	184.90	230.80

Continued on next page...

Test	Wire	d_{gross}(in)	d_{net}(in)	d_{neck}(in)	E(psi)	$\sigma_{\max}$(ksi)	σ_{yield}(ksi)	$\sigma_{2.5\%}$(ksi)
1176	21L5	0.1954	0.1919	0.1583	25963	251.32	185.23	231.68
1177	21L5	0.1961	0.1915	0.1588	25901	249.61	185.39	231.54
1178	21L5	0.1960	0.1916	0.1555	25812	253.64	187.24	233.23
1179	21L5	0.1958	0.1914	0.1600	25563	254.79	188.01	233.92
1180	21L5	0.1961	0.1916	0.1600	25438	253.55	186.08	232.71
1181	21L5	0.1965	0.1915	0.1570	24917	251.06	184.09	230.58
1182	21L5	0.1954	0.1914	0.1595	24937	252.63	184.09	231.43
1183	21L5	0.1955	0.1913	0.1560	24953	252.79	184.46	231.59
1184	8R5	0.1983	0.1913	0.1553	24014	245.91	180.22	225.28
1185	8R5	0.1985	0.1915	0.1578	24037	245.97	179.98	224.88
1186	8R5	0.2005	0.1913	0.1550	23570	240.86	177.28	220.40
1187	8R5	0.1965	0.1914	0.1580	25121	249.33	182.54	228.68
1188	8R5	0.1965	0.1911	0.1568	24834	246.39	179.98	226.13
1189	8R5	0.1993	0.1914	0.1630	23753	239.67	177.53	221.26
1190	8R5	0.1999	0.1918	0.1628	22948	235.87	174.31	218.12
1191	8R5	0.2044	0.1915	0.1575	21713	230.21	169.99	210.68
1192	8R5	0.2038	0.1918	0.1588	22118	232.96	171.46	212.74
1193	8R5	0.1979	0.1914	0.1570	24663	247.88	181.77	227.07
1194	8R5	0.1998	0.1915	0.1568	23795	243.49	178.39	222.87
1195	8R5	0.1988	0.1916	0.1580	24131	245.14	179.49	224.43
1196	8R5	0.1979	0.1915	0.1590	23909	245.79	179.51	224.89
1197	10L5	0.1946	0.1918	0.1555	26334	255.15	187.17	234.57
1198	10L5	0.1955	0.1919	0.1570	26010	252.68	186.06	232.26

Continued on next page...

Test	Wire	d_{gross}(in)	d_{net}(in)	d_{neck}(in)	E(psi)	$\sigma_{\max}$(ksi)	σ_{yield}(ksi)	$\sigma_{2.5\%}$(ksi)
1199	10L5	0.1963	0.1918	0.1560	26091	250.96	184.80	231.06
1200	10L5	0.1960	0.1918	0.1603	25973	251.14	185.27	231.27
1201	10L5	0.1969	0.1918	0.1583	26120	249.51	185.27	230.18
1202	10L5	0.1959	0.1916	0.1613	27373	252.91	189.85	233.70
1203	10L5	0.1958	0.1916	0.1580	27008	254.29	188.95	234.54
1204	10L5	0.1968	0.1918	0.1590	26332	251.13	186.62	231.35
1205	10L5	0.1961	0.1919	0.1570	26382	252.18	186.96	232.30
1206	10L5	0.1960	0.1918	0.1608	25817	252.70	185.58	232.37
1207	10L5	0.1955	0.1916	0.1610	26414	251.69	185.73	231.85
1208	10L5	0.1956	0.1916	0.1650	26377	249.96	184.14	230.37
1209	10L5	0.1960	0.1918	0.1605	25612	250.87	184.50	230.75

Appendix B

Statistical moments of integral of squared-root process

The squared-root process and its integral are defined as

$$\mathrm{d}r_t = b(a - r_t)\,\mathrm{d}t + \sqrt{r_t}\sigma\,\mathrm{d}W_t, a, b > 0 \tag{B.1}$$

$$L_t = \int_0^t r_s\,\mathrm{d}s \tag{B.2}$$

Given a, b, σ and r_0, the recursive formula for computing the k-th moment of L_t is given Sec. 4.5.1. An implementation in Matlab® is given below.

Listing B.1: Matlab code for computing moments of integral of squared-root process.

```
function [ m ] = Moment(t, k, a, b, sigma, r0)
% Compute the k-th moment of integral of squared-root
% process from 0 to t, with parameters a, b, sigma
% and initial value r0.
params.alpha = -a;
params.beta = a * b;
```

```
7  params.gamma = sigma;
8  params.xb = r0;
9
10 m = M2(k, 0, t, params);
11 end
12
13 function [ res ] = theta( k, j, params )
14 ub = params.gamma^2 / 2 / params.alpha;
15 vb = 2 * params.beta / params.gamma^2;
16 res = 0;
17 for i = 0 : j
18     nom = factorial(k) * (-1)^(k-j) * ub^(k - i);
19     den = factorial(i) * factorial(j - i) ...
20         * factorial(k - j);
21     res = res + params.xb^i * nom / den ...
22         * fac(vb, k) / fac(vb, i);
23 end
24 end
25
26 function [ res ] = ak( k, params )
27 res = params.alpha * k;
28 end
29
30 function [ res ] = bk( k, params )
31 res = params.beta * k + 0.5 * params.gamma^2 ...
```

```
32      * k * (k - 1);
33  end
34
35  function [ res ] = fac( y, k )
36  if (k == 0)
37      res = 1;
38  else
39      res = prod(y + [0 : k - 1]);
40  end
41  end
42
43  function [ res ] = M2( j, k, t, params )
44  res = 0;
45  for m = 0 : (j + k)
46      res = res + M3(j, k, m, t, params) ...
47          * exp(params.alpha * m * t);
48  end
49  end
50
51  function [ res ] = M3( j, k, m, t, params )
52  res = 0.0;
53  for n = 0 : min(j, j + k - m)
54      res = res + M4(j, k, m, n, params) * t^n;
55  end
56  end
```

```
57
58 function [ res ] = M4( j, k, m, n, params )
59 % 0kmn
60 if (j == 0 && n >= 1)
61     res = 0;
62     return;
63 end
64
65 % 0km0
66 if (j == 0 && n == 0)
67     res = theta(k, m, params);
68     return;
69 end
70
71 % jkmn, k!=m
72 if ( k ~= m)
73     res = 0;
74     for i = n : min(j, j + k - m)
75         res = res + fac(n + 1, i - n) ...
76             / (params.alpha * (k - m))^(i - n + 1) ...
77             * R4(j, k, m, i, params);
78     end
79     res = -res;
80     return;
81 else
```

```
82      % jkkn, n=1,2,...
83      if (n > 0)
84          % Maybe here
85          res = 1.0 / n * R4(j, k, k, n - 1, params);
86          return;
87      else
88          % jkk0
89          res = 0;
90          for m = 0 : j + k
91              if (m == k)
92                  continue;
93              end
94              res = res + M4(j, k, m, 0, params);
95          end
96          res = - res;
97      end
98  end
99
100 end
101
102 function [ res ] = R4( j, k, m, n, params )
103 res = bk(k, params) * M4(j, k - 1, m, n, params) ...
104     + j * M4(j - 1, k + 1, m, n, params);
105 end
```

Appendix C

Coefficients of Clough-Penzien correlation function

$$C_{a1} = -\frac{\omega_g^6}{D}\left[(1+8\zeta_g^2-16\zeta_g^4)\left(1-\frac{\omega_g^4}{\omega_f^4}\right)-8\zeta_g^2\frac{\omega_g^2}{\omega_f^2}\left(1-2\zeta_f^2-\frac{\omega_g^2}{\omega_f^2}+2\zeta_g^2\frac{\omega_g^2}{\omega_f^2}\right)\right] \quad \text{(C.1)}$$

$$C_{b1} = \frac{2\omega_g^6}{D}\left[(1+8\zeta_g^2-16\zeta_g^4)\left(1-2\zeta_g^2-\frac{\omega_g^2}{\omega_f^2}+2\zeta_f^2\frac{\omega_g^2}{\omega_f^2}\right)-2\zeta_g^2\left(1-\frac{\omega_g^4}{\omega_f^4}\right)\right] \quad \text{(C.2)}$$

$$C_{a2} = \frac{\omega_g^4\omega_f^2}{D}\left[(1+8\zeta_g^2-16\zeta_g^4)\left(1-\frac{\omega_g^4}{\omega_f^4}\right)-8\zeta_g^2\frac{\omega_g^2}{\omega_f^2}\left(1-2\zeta_f^2-\frac{\omega_g^2}{\omega_f^2}+2\zeta_g^2\frac{\omega_g^2}{\omega_f^2}\right)\right] \quad \text{(C.3)}$$

$$C_{b2} = \frac{2\omega_g^2\omega_f^4}{D}\left[\frac{\omega_g^2}{\omega_f^2}\left(-\frac{\omega_g^2}{\omega_f^2}+8\zeta_g^2-16\zeta_g^2\zeta_f^2\right)\left(1-2\zeta_g^2-\frac{\omega_g^2}{\omega_f^2}+2\zeta_f^2\frac{\omega_g^2}{\omega_f^2}\right)+2\zeta_g^2\left(1-\frac{\omega_g^4}{\omega_f^4}\right)\right] \quad \text{(C.4)}$$

$$D = -4\omega_g^2\omega_f^2\left(1-2\zeta_g^2-\frac{\omega_g^2}{\omega_f^2}+2\zeta_f^2\frac{\omega_g^2}{\omega_f^2}\right)\left(1-2\zeta_f^2-\frac{\omega_g^2}{\omega_f^2}+2\zeta_g^2\frac{\omega_g^2}{\omega_f^2}\right)+4\omega_f^2\left(1-\frac{\omega_g^4}{\omega_f^4}\right) \quad \text{(C.5)}$$